# Following Motion of Early Heart Development at the Cellular Level Using Confocal Microscopy in Transgenic Quail Embryos

**Thesis by**
**Jennifer C. Yang**

**In Partial Fulfillment of the Requirements**
**For the Degree of**
**Doctor of Philosophy in**
**Biochemistry & Molecular Biophysics**

**California Institute of Technology**
**Pasadena, CA**
**2010**

**(Defended June 1, 2010)**

Acknowledgments

I would like to thank my advisor Scott Fraser for providing such a great work environment in Fraserland. Also of equal importance is the Quail Group, without which I would not have had a project. Yuki Sato taught me the lessons of working "karoshi" style while Dave Huss ensured I had my transgenic eggs every week for many nights of fun on the microscopes.

I would also like to thank Andres Collazo and the House Ear Institute for allowing me to use the high-speed Leica microscope, and to Langer's Deli for providing the lunch that sustained me on those days I had to commute to downtown Los Angeles for imaging.

Many thanks to the individuals in the Fraser and Gharib Labs that have crossed my path during my graduate career. Your insight and support were informative and necessary while I defined my project and continued onto the analysis.

And lastly but not least, I thank my SURF student Jason Lunn who did more research than I could have ever expected from a full-time undergraduate at Caltech.

The QH1 and MF20 antibodies developed by F. Dieterlen and D. Fischman, respectively, were obtained from the Developmental Studies Hybridoma Bank developed under the auspices of the NICHD and maintained by The University of Iowa, Department of Biology, Iowa City, IA 52242.

Abstract

The heart has fascinated scientists for centuries, from the days of Leonardo da Vinci to the modern scientist. As tools have developed over the years, we have begun to create a different perspective of how the heart develops and functions from original ideas. Genetics, molecular biology, and microscopes have allowed us to examine the heart with a level of detail that could not have been imagined by da Vinci.

The heart is a complex organ to study due to its innate nature of contracting and relaxing for the entire life of an organism. The motions of systole and diastole complicate any measurements and analysis that can be done. In general, most research has been done in either fixed tissue or dead organisms, neither being ideal for studying a live heart. But current research aims to change our knowledge of cardiogenesis through dynamic imaging of live tissue. With the progress made in the last few years, we have had to revise many of our assumptions about heart development and pumping mechanics. Now, we are at a new stage of research that requires the quantification of cardiogenesis to understand the requirements of heart development to prevent future diseases from occurring.

The following work divides the heart into three areas: 1-dimensional dynamic imaging and analysis of contractions and relaxation to achieve temporal resolution, 4-dimensional modeling of a beating heart during tube formation and early looping to observe individual cellular motion, and 4-dimensional fate mapping of the developing

heart tube to visualize development with cellular resolution. With these three perspectives, we are able to quantify the movements of the myocardium and endocardium during development while the heart is beating. This novel approach will give us a wealth of information never seen before.

We use transgenic Japanese quail to highlight the nuclei of individual endothelial cells in the vasculature to analyze the inner tube of the heart, and another transgenic with a ubiquitous marker that fluoresces in every cell of the embryo. The quail heart is comparable to the human heart in that both have 4-chambered hearts, yet the quail is a much easier organism to study. The embryo is transparent and develops outside the mother. The quail embryo can be imaged *ex ovo* on inverted microscopes, allowing for ease of setup in a controlled environment.

With the use of dynamic imaging and innovative computer software, we were able to reconstruct the live heart while it is beating and developing. By dynamically imaging the endocardium and myocardium, we were able to study the interactions between the two layers by offering unsurpassed visual access to the morphogenetic events of cardiogenesis. Questions that have remained elusive are now being answered with extensive analysis from the data collected. Quantification of cardiogenesis is possible and a detailed fate-map has been produced from this research.

# Table of Contents

# Chapter 1

# Introduction

## 1.1 Introduction

The heart is the first organ to form and function in the developing vertebrate embryo (Harvey and Rosenthal, 1999). It is a muscle that pumps blood every day, every hour, and every second. It is our body's way of moving blood through our system, from our brain to our feet, our lungs to our skin. We need the heart to pump the blood that carries oxygen and nutrients to the cells of our body, and remove the waste from cells in our body.

For centuries, scientists and medical doctors have been studying the heart. As early as the 15$^{th}$ century, detailed studies of the structure and function of the heart had already begun. One of the pioneers was famed artist Leonardo da Vinci (1452-1519) who made a glass model of the heart such that the flow of millet seeds in clear water so that flow patterns can be traced. (Keele, 1979) As the centuries passed, science and medicine eventually separated anatomy from physiology in heart-related studies. But in the last few decades, scientists have combined structure and function to provide a better understanding of how the heart moves blood and nutrients through the body.

The cells that will form the heart begin as the progenitor cardiac mesoderm on opposite sides of the primitive streak in forming blastulae. The progenitor cells are located in two bilaterally symmetrical regions of anterior lateral plate mesoderm, and come together at the midline to form a linear heart tube (Stalsberg & DeHaan, 1969).

The tube lengthens until it loops to the right to form a c-loop, then s-loop. Then septation and valve formation occur to form the adult heart (Manner, 2000; Martinsen, 2005). The looping process is integral to proper formation of the mature heart; unfortunately, the process is not foolproof. Approximately 1% of the human population is born with a congenital heart defect (reviewed by Srivastava, 2006). Conceptually, the embryonic heart tube begins in serial alignment of the forming primitive chambers, which then rearrange to form parallel atria and ventricles (reviewed by Moorman and Christoffels, 2003). The process of this realignment from serial to parallel has eluded scientists for decades.

The heart is a difficult organ to study due to its function: it pulses blood through the body. This extra dimension, the beating, is difficult to capture with live imaging techniques. With the advent of new technologies and theories, researchers are beginning to understand the mechanism underlying development of the embryonic heart. Transgenic animals, molecular biology, advanced microscopy techniques, and modern computer power provide new tools for further research into the detailed workings of this fascinating organ that supplies life to each cell of the body. Originally, scientists thought the embryonic heart tube functioned as a peristaltic pump but recent discoveries in zebrafish have shown it behaves more as an impedance pump (Forouhar *et al.*, 2006). In addition, new algorithmic theories have evolved to give a four-dimensional perspective of the beating, embryonic heart to create a new, dynamic model of the organ (Liebling *et al.*, 2006).

## 1.2 Previous Research in Zebrafish

The zebrafish (Danio rerio) is an ideal model for studying heart development in vertebrates. They are easy and inexpensive to maintain and reach sexual maturity within three months (Harvey and Rosenthal, 1999). The development of the heart is quite rapid, with beating occurring at approximately 22 hours post fertilization (hpf) and looping and chamber formation completed by 35 hpf (Stainier and Fishman, 1994). Protocols have been established to produce a variety of mutations, making it an excellent animal for studying genetics (Mullins and Nusslein-Volhard, 1993; Walker and Streisinger, 1983; Gaiano *et al.*, 1996). Large-scale mutant screens of zebrafish have yielded hundreds of mutations with various cardiac phenotypes, many of which resemble cardiac malformations observed in humans (Stainier *et al.*, 1996; Chen *et al.*, 1996). The transparent properties of the zebrafish embryo make advanced microscopy possible.

The morphology of the zebrafish heart consists of one heart tube that develops into two chambers while the human heart consists of two heart tubes that form four chambers, but the process of cardiogenesis is conserved between the two species. The heart tube begins as myocardial precursors that converge at the midline and fuse to form a cone by 21 somites (19.5 hpf) (Yelon *et al.*, 1999; Stainier, 1993). The cone transforms into the linear heart tube by forming concentric rings of endocardial and myocardial tissue separated by cardiac jelly, moving from the dorsal –ventral axis to the anterior-posterior axis along the ventral midline (Trinh and

Stainier, 2004). At 22 hpf, the myocardial contractions are sporadic, but by 24 hpf the tube has begun periodic contractions to begin moving blood through the heart. The heart tube then loops to the right to form an intermediate “C” shape at 31 hpf. By 36 hpf, distinct chambers within the looped heart have emerged.

Since the era of Leonardo da Vinci, researchers have been curious about how form and function influence the heart during development. Over time, the study of the heart became focused on genetics and anatomy. Only recently has a ground-breaking study been able to incorporate function into cardiac morphogenesis. In 2003, Hove and his colleagues implanted glass beads into zebrafish to disrupt the blood flow into and out of primitive stage hearts. They found that occlusion of flow resulted in improper looping, malformed chambers, and lack of valve formation (Hove *et al.*, 2003). The study signified that proper function is required for precise heart morphogenesis to occur.

Another recent key study in cardiogenesis occurred in 2006. With the advent of new microscopy techniques and transgenic fish, dynamic imaging of the zebrafish heart became possible. The transgenic line Tg(gata1:GFP) expresses GFP in blood cells, the endocardium (inner lining of the heart) and myocardium (cardiac muscles), allowing for innovative imaging with cellular resolution on modern confocal microscopes (Long *et al.*, 1997). Liebling and his colleagues developed an algorithm to reconstruct a three-dimensional time-series of a live zebrafish heart on the Zeiss LSM 5 LIVE confocal microscope. They acquired sequential time-series of

two-dimensional slices at increasing depths over several time periods at 150 frames per second, manipulated the data using gating signals to process the reconstruction (see figure 1) (Liebling *et al.*, 2005). The result is a novel and dynamic in vivo model of the beating zebrafish heart.

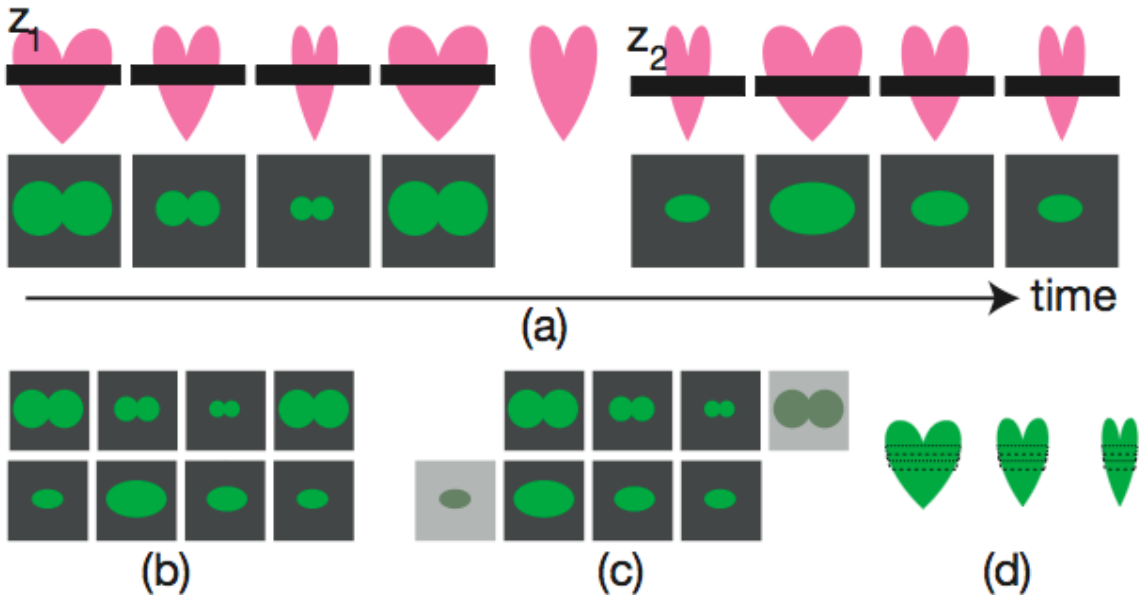


**Figure 1** Four-dimensional imaging: acquisition and reconstruction procedure. a) Sequential acquisition of two-dimensional slices (confocal microscopy) as a time-series at increasing depths of the beating heart. b) Direct reconstruction is not possible from the nongated data. c) Temporal alignment procedure d) Reconstruction.

Originally the embryonic vertebrate heart was thought to function as a peristaltic pump, propagating compression that pushes fluid through the length of the tube (see figure 2) (Fishman and Chien, 1997; Hickerson, 2005). By creating a computerized model of the beating zebrafish heart, Forouhar and colleagues were able to follow the blood cells, contractile wave, and pressure gradient to discover the heart tube behaves more like an impedance pump (Forouhar *et al.*, 2006). This type of pump

functions by an elastic wave propagation and reflection, which create suction within the heart tube in order to move blood through the organ (Hickerson *et al.*, 2005).

With these new technological and biological advances leading to new observations and discoveries, it only makes sense to apply this research to higher order taxa such as bird or mammal.

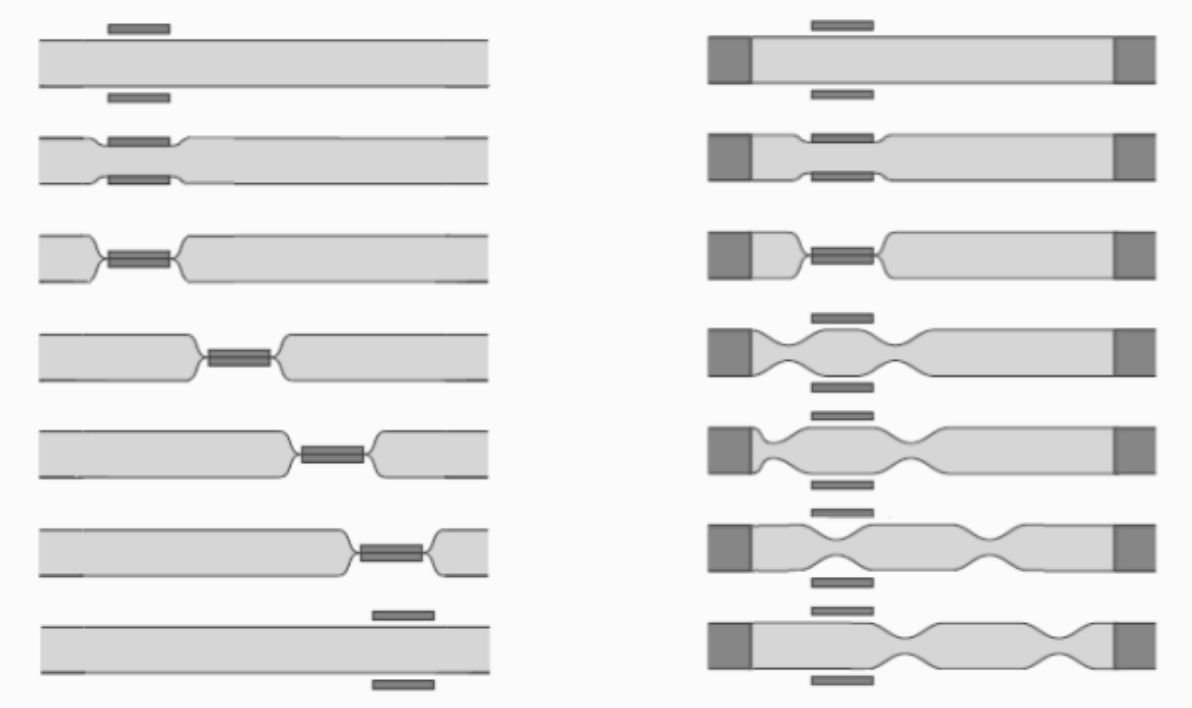

**Figure 2** (Left) Schematic of a peristaltic pump. The pump functions by a propagating compression zone pushing the fluid along the tube. (Right) Schematic of an impedance pump. The pump functions by an elastic wave propagation and reflection. The dark colored edges represent a mismatch of impedance.
(adapted from Hickerson thesis)

## 1.3 Quail as a Model Organism

The Japanese quail (Coturnix coturnix japonica) is an ideal system to study the pumping mechanics of the developing heart because it is a warm-blooded vertebrate with easily accessible embryos. It has been shown to be a useful research model (Padgett and Ivey, 1960) and experiments on quail easily complement the standard avian model, the white leghorn chicken (Gallus gallus domesticus).

While the zebrafish is an established model for heart development, most of the research on it uses genetics (Fishman & Chien, 1997). A few papers have recently come out showing the biomechanical advantages of using zebrafish to image due to its small size and available transgenics, allowing for updated conclusions about pump mechanics and fluid dynamics involved in chamber and valve formation (Forouhar *et al.*, 2006; Hove *et al.*, 2003). Also, the zebrafish has been used to develop a new method of visualizing 4D datasets to give a new perspective to modern imaging technology (Liebling *et al.*, 2005; Liebling *et al.*, 2006). Though the zebrafish has been a beneficial model for studying heart development, its main limitation is that it is a cold-blooded vertebrate with only a two-chambered heart. The quail is a much more comparable model to humans since it is a warm-blooded vertebrate with a four-chambered heart.

Consideration should also be given to the mouse as a model organism since it is a mammal like humans. The gestation period of mice is 20 days and they reach

sexual maturity within two months (Hetherington et al, 2000). They are easy and inexpensive to maintain, and the creation of transgenics is an established protocol (Hofker and Deursen, 2002). However, the limitations with mice are great considering their embryos can not be imaged easily through the mother due to placental growth. This requires the removal of embryos from the womb and creating an *ex ovo* environment to culture them for imaging (Jones *et al.*, 2002). This is a tedious and not well-established process that requires more development. Future technology might improve access to the developing mammalian embryo, but until it does, embryos that develop outside the mother have clear advantages as models for studying heart development.

The chicken is a possible model system in which much cardiac developmental research has already been completed (Fishman and Chien, 1997; Martinsen, 2005). One limitation in using the chicken to study genetics has been removed with the establishment of protocols for creating transgenics (Mozdziak *et al.*, 2003). The incubation time of the egg is 21 days, and the chick reaches sexual maturity in four to five months (Grandin and Johnson, 2005). Combining the growth period with the space required for maintaining transgenic lines makes the chicken a time-consuming and expensive model organism.

The quail is an ideal compromise between the mouse and chicken. The incubation period of an egg is 16 days, and the quail chick reaches sexual maturity in approximately six weeks (Woodward *et al.*, 1973), resulting in short production

cycles between generations. The size of the quail makes maintenance easy and keeps costs low. Recent advances have created transgenic quail, allowing it to be considered as a genetic model system only previously applied to other species such as the zebrafish and mice (Poynter and Lansford, 2008). Since the quail is an avian system, the developmental knowledge obtained from the chicken in cardiogenesis can easily be transferred.

All stages of the developing heart, including looping and chamber formation are accessible *in ovo* and *ex ovo* (Manner, 2000), allowing for easy manipulation of the embryo for dynamic imaging. Knowledge obtained from a quail four-chambered heart can then be applied to the less accessible mammalian and human hearts. For the stages before heart looping, *ex ovo* culturing is possible on semi-solid agarose plates (Chapman *et al.*, 2001), allowing for easy imaging of developing embryos.

Current experiments using transgenic quail to express fluorescent protein in endothelial cells using the tissue specific promoter Tie1 (Sato *et al.*, submitted). The resulting data produced an impressive fate map of cellular movements in the 2-day old quail embryo during early vasculature formation. By following these endothelial cells during cardiogenesis, a detailed fate map of the heart will provide a clear picture of cellular dynamics during tube formation, looping, and heartbeat contractions never seen before.

## 1.4 Quail Heart Morphogenesis

Recently, it has been shown that the quail embryo and chicken embryo are comparable in anatomy and development up to HH28, making it possible to use the Hamburger and Hamilton staging system for young quail embryos (Hamburger & Hamilton, 1951; Ainsworth *et al.*, 2010). During amniote cardiogenesis, epiblast cells ingress through the primitive streak to form the mesoderm. The mesodermal cells then move cranio-laterally and separate into the splanchnic mesoderm and the somatic mesoderm. About HH6, as the quail anterior endoderm folds, heart progenitor cells in the splanchnic mesoderm translocate to the midline and fuse to form a tubular heart. The primitive heart fold forms as the anterior intestinal portal regresses caudally (Moreno-Rodriguez *et al.*, 2006; Stalsberg and DeHaan, 1969). The quail heart morphologically appears as a cardiogenic crescent in which the lateral progenitor cells begin to fuse at the midline just below the head folds (Stalsberg & Dehaan, 1969). The anterior and posterior portions of the dorsal roof of the trough continue to close, and the tube elongates bidirectionally forming a linear heart tube between HH stages 9 and 11 (Moreno-Rodriguez *et al.*, 2006). It is located ventrally to the foregut, and is attached to the embryo and membrane through the dorsal and ventral mesocardium (Manner, 2000). The tubular heart contains a single atrium and a single ventricle and soon begins to undergo contractions (Stalsberg and DeHaan, 1969).

As the tube lengthens along the craniocaudal axis and begins to loop dextrally at

HH10, the heart begins to form a “c”-shape, which coincides with cranial flexure, but is independent of blood flow (Manner *et al.*, 1993; Patten, 1922). At HH11, the c-loop continues extending dextrally and at this point, the heartbeats are strong and consistent. At HH12, the beating heart has finished forming the c-loop and is comprised of a proximal primitive outlet, which connects to the ventral aortae cephalically, the apical portion of both ventricles, a primitive atrium and a primitive inlet (de la Cruz *et al.*, 1989). Laminar blood flow starts at HH12 and is maintained past HH18 (Yoshida *et al.*, 1983). The c-shaped heart loop transforms into the s-shaped heart loop from HH12-18 (Manner, 2000). By HH 14-15 the heart is a smooth-walled, single-chambered, looped tube composed of three layers: a thin compact outer mantle of myocardium with a basal membrane, an acellular extracellular matrix, and a single cell layer thick endocardium.

Numerous researchers have proposed positional fate maps of the heart forming regions by observing the location of heart precursor cells at progressive developmental stages (Dehaan, 1963; Garcia-Martinez and Schoenwolf, 1993; Rawles, 1943; Stalsberg & DeHaan, 1969). These studies generated a wide range of hypotheses regarding the spatial and temporal boundaries of the heart-forming region of amniotes. While valuable, this literature is difficult to reconcile and underscores the critical need for unbiased, dynamic cell and tissue positional fate maps.

Of significance are two research studies that try to elucidate the mechanism of heart tube formation and primitive looping from stages HH8 to 11. These experiments range from following dyes in the primary heart fields as the tube forms to highly detailed computational reconstructions of fixed sections of heart tube at different developmental stages (Moreno-Rodriguez *et al.*, 2006; Abu-Issa and Kirby, 2008). This has created similar yet competing theories for the formation of the heart tube, showing that cells migrate from one region to another and fusion of the heart tube occurs in a longitudinal manner, but differing in the specific regions of cell migration and fusion. The cause of this confusion is due to the lack of spatial and temporal resolution in the dye experiments used to analyze cellular movements.

Another area of controversy in embryonic heart morphogenesis is the basis of dextral looping in the heart beginning at HH10 and continuing through many stages of development, resulting in the formation of four chambers. We are discovering now that the initial looping process is composed of two components: looping to the right and torsional rotation (reviewed by Taber *et al.*, 2006). Voronov *et al.* (2002; 2004) discovered that removing the splanchnopleure (inflow tracts) still allows for looping but decreases the rotation during looping. Modeling of the chick heart has shown that looping is not a simple process (Manner, 2004) and much research still needs to be done to understand these early stages of development and prevent congenital heart defects from appearing.

## 1.5 Research Goals

With the development of new technological and biological tools over the last few decades, many advances have been made in understanding the structure and function of the heart. By focusing on the early stages of the quail heart, it is hoped that we will understand enough to prevent congenital heart defects from forming in newborns so they may lead a long and healthy life without cardiac abnormalities. In order to do this, we need to determine a system for understanding and measuring early heart development.

Cardiogenesis is a complex process. Current focus has been on the genetics and anatomy, so other aspects such as tube formation and cellular motion are still unknown. While the heart is developing it is also beating, and this mechanical process has stumped scientists trying to study the live beating heart due to the intrinsic motion involved. Finally, the quantification of organ development is not established and needs to be devised.

Quantification of cardiogenesis involves many aspects due to the complex nature of the heart. Not only is the organ growing in size, but it is also functioning during development. This requires multiple types of experiments to provide us an overall picture of cardiogenesis. Currently, we have the technology to begin the visualization of heart contractions and heart development to quantify cardiogenesis at the early stages of embryo development. Confocal laser scanning microscopy

combined with molecular biology give us the tools to visualize individual cells in the embryonic heart. High-speed confocal imaging provides the temporal resolution required to capture the heart beating during each contraction. Combined with new advances in theoretical computer algorithms, four-dimensional reconstruction of the beating heart is now possible and can show cellular movements not seen before.

Our results provide insight into heart tube formation and dextral bending from HH8 to HH12. Our imaging techniques give us a wealth of information to analyze and lay out a strategy for further studies into cardiogenesis. Our experiments interrogate cardiac development using the following three methods:

1) One-dimensional line scans of the developing three-dimensional heart tube to follow tissue motion of the heart walls with high temporal resolution for determination of the contraction and relaxation parameters that comprise a heartbeat (HH10-12).

2) Four-dimensional high-speed reconstructions of the beating heart to create dynamic models for an in-depth study of individual cellular motion during contraction in the forming and looping heart tube (HH9-12).

3) Three-dimensional timelapse of the heart developing from the cardiogenic crescent through dextral looping to determine the cellular migration patterns involved in tube formation, elongation, and primitive stages of looping (HH8-12).

Through this research, we are finding that many of the tools needed to analyze the data have not been created yet. Collaborations with other laboratories and scientists of other disciplines are a necessity to study all aspects of heart development. We require the expertise of molecular biologists, geneticists, computer scientists, mathematicians, imaging specialists and biophysicists.

The avian heart has already provided a strong platform to study the anatomy of heart development. With the combination of advanced imaging techniques and molecular biology, the quail will strengthen its role as a model organism for studying cardiogenesis, paving new paths for science and medicine to analyze the structure and function of the heart.

We hope that by being able to reconstruct the heart with detailed quantitative knowledge of cellular motions involved in contraction and development, we will be able to create a dynamic model of cardiogenesis that has never existed before. This research shows the first ever images of the early stages of a developing amniote heart tube with cellular resolution. Eventually, we hope this detailed mapping of cardiac beating during development can be used as an assay for developing new tools and drugs to prevent congenital heart disease in humans.

## 1.6 References

Abu-Issa, R. and Kirby, M.L., 2008. Patterning of the heart field in the chick. Dev. Biol. 319(2), 223-233.

Ainsworth S.J., Stanley, R.L. and Evans, D.J.R., 2010. Developmental stages of the Japanese quail. J. Anat. 216, 3-15.

Chapman, S.C., Collignon, J., Schoenwolf, G.C. and Lumsden, A., 2001. Improved method for chick whole-embryo culture using a filter paper carrier. Dev. Dyn. 220, 284-289.

Chen, J.-N., Haffter, P., Odenthal, J., Vogelsang, E., Brand, M., van Eeden, F.J., Furutani-Seiki, M., Granato, M., Hammerschmidt, M., Heisenberg, C.P., Jiang, Y.-J. Kane, D.A., Kelsh, R.N., Mullins, M.C. and Nusslein-Volhard, C., 1996. Mutations affecting the cardiovascular system and other internal organs in zebrafish. Development (Cambridge, UK 123, 293-302.

Dehaan, R.L., 1963. Migration patterns of the precardiac mesoderm in the early chick embryo. Exp Cell Res 29, 544-560.

De la Cruz, M.V., Sanchez-Gomez, C., Palo-Mino, M.A., 1989. The primitive cardiac regions in the straight tube heart (Stage 9-) and their anatomical expression in the mature heart: an experimental study in the chick embryo. J. Anat. 165,121–131.

Fishman, M.C. and Chien, K.R., 1997. Fashioning the vertebrate heart: earliest embryonic decisions. Development 124, 2099-2117.

Forouhar, A. S., Liebling, M., Hickerson, A., Nasiraei-Moghaddam, A., Tsai, H., Hove, J. R., Fraser, S. E., Dickson, M. E. and Gharib, M., 2006. The embryonic vertebrate heart tube is a dynamic suction pump. Science 312, 751-753.

Gaiano, N., Amsterdam, A., Kawakami, K., Allende, M., Becker, T., and Hopkins, N., 1996. Insertional mutagenesis and rapid cloning of essential genes in zebrafish. Nature (London) 376, 66-70.

Garcia-Martinez, V. and Schoenwolf, G.C., 1993. Primitive-streak origin of the cardiovascular system in avian embryos. Developmental Biology 159, 706-719.

Grandin, T. and Johnson, C. Animals in Translation. New York, New York: Scribner, 2005.

Hamburger, V. and Hamilton, H.L., 1951. A series of normal stages in the development of the chick embryo. J. Morph. 88, 49-92.

Harvey, R.P. and Rosenthal, N., Heart Development. San Diego: Academic Press, 1999.

Hetherington, M., Doe, B. and Hay, D. Mouse care and husbandry. In: Mouse Genetics and Transgenics: A Practical Approach. Jackson, I. J. and Abbott, C. M. editors. Oxford University Press, 2000.

Hickerson, A.I. An Experimental Analysis of the Characteristic Behaviors of an Impedance Pump, Dissertation, California Institute of Technology, 2005.

Hickerson, A.I., Rinderknecht, D. and Gharib, M., 2005. Experimental study of the behavior of a valveless impedance pump. Exper. Fluids, 38(4), 534-540.

Hofker, M.H. and Deursen, J. Transgenic Mouse: Methods and Protocols. In: Methods and Molecular Biology, vol. 209. Springer Protocols: Humana Press, 2003.

Hove, J.R., Reinhard, W.K., Forouhar, A.S., Acevedo-Bolton, G., Fraser, S.E. and Gharib, M., 2003. Intracardiac fluid forces are an essential epigenetic factor for embryonic cardiogenesis. Nature 421(6919), 172-7.

Jones, E. A. V., Crotty D., Kulesa P.M., Waters C.W., Baron M.H., Fraser S.E. and Dickinson, M.E., 2002. Dynamic in vivo imaging of postimplantation mammalian embryos using whole embryo culture. Genesis 34(4), 228-35.

Keele, K.D., 1979. Leonardo da Vinci's 'Anatomia naturale'. Yale journal of biology and medicine 52, 363-409.

Liebling, M., Forouhar, A.S., Gharib, M., Fraser, S.E., Dickinson, M.E., 2005. Four-dimensional cardiac imaging in living embryos via postacquisition synchronization of nongated slice sequences. J. Biomed. Opt. 10(5), 054001-10.

Liebling, M., Forouhar, A.S., Wooleschensky., R., Zimmermann., B., Ankerhold., R., Fraser., S.E., Gharib., M., Dickinson., M.E., 2006. Rapid three-dimensional imaging and analysis of the beating embryonic heart reveals functional changes during development. Dev. Dyn. 235(11), 2940-2948.

Long, Q., Meng, A., Wang, H., Jessen, J. R., Farrell, M. J. and Lin, S., 1997. GATA-1 expression pattern can be recapitulated in living transgenic zebrafish using GFP reporter gene. Development 124(20), 4105-4111.

Manner, J., 2000. Cardiac looping in the chick embryo: A morphological review with special reference to terminological and biomechanical aspects of the looping process. The Anatomical Record 259(3), 248-262.

Manner, J., 2004. On rotation, torsion, lateralization, and handedness of the embryonic heart loop: new insights from a simulation model for the heart loop of chick embryos. The Anatomical Record 278A, 481-492.

Manner, J., Seidl, W. and Steding, G., 1993. Correlation between the embryonic head flexures and cardiac development. An experimental study in chick embryos. Anat Embryol (Berl) 188, 269-285.

Martinsen, B.J., 2005. Reference guide to the stages of chick heart embryology. Dev. Dyn. 233, 1217-1237.

Moorman A.F. and Christoffels, V.M., 2003. Cardiac chamber formation: development, genes and evolution. Physiol. Rev. 83, 1223-1267.

Moreno-Rodriguez, R.A., Krug, E.L., Reyes, L., Villavicencio, L. Mjaatvedt, C.H. and Markwald, R.R., 2006. Bidirectional fusion of the heart-forming fields in the developing chick embryo. Dev. Dyn. 235, 191-202.

Mozdziak, P.E., Borwornpinyo, S., McCoy, D.W. and Petitte, J.N., 2003. Development of transgenic chickens expressing bacterial beta-galactosidase. Dev. Dyn. 226(3), 439-445.

Mullins, M.C. and Nusslein-Volhard, C., 1993. Mutational approaches to studying embryonic pattern formation in the zebrafish. Curr. Opin. Genet.Dev. 3, 648-654.

Padgett, C.S. and Ivey, W.D., 1960. The normal embryology of the Coturnix quail. The Anatomical Record 137, 1-11.

Patten, B.M., 1922. The formation of the cardiac loop in the chick. Am. J. Anat. 30, 373-397 .

Poynter, G. and Lansford, R., Avian Embryology. Methods in Cell Biology, 2nd edition. San Diego: Academic Press, 2008, pp. 281-293.

Rawles, M.E., 1943. The heart forming areas of the early chick blastoderm. Physiol. Zool. 16, 22-42.

Sato, Y., Poynter, G., Huss, D., Filla, M., Czirok, A., Rongish, B., Little, C., Fraser, S., and Lansford, R., Dynamic analysis of vascular morphogenesis using transgenic quail embryos. Submitted.

Srivastava, D., 2006. Making or breaking the heart: from lineage determination to morphogenesis. Cell 26, 1037-1048.

Stainier, D.Y., Lee, R.K., and Fishman, M.C., 1993. Cardiovascular development in the zebrafish. I. Myocardial fate map and heart tube formation. Development 119, 31-40.

Stainier, D.Y.R. and Fishman, M.C., 1994. The zebrafish as a model system to study cardiovascular development. Trends Cardiovasc. Med. 4, 207-212.

Stainier, D.Y.R., Fouquet, B., Chen, J.N., Warren, K.S., Weinstein, B.M., Meiler, S.E., Mohideen, M.A., Neuhauss, S.C., Solnica-Krezel, L., Schier, A.F., Zwartkruis, F., Stemple, D.L., Malicki, J., Driever, W., and Fishman, M.C., 1996. Mutations affecting the formation and function of the cardiovascular system in the zebrafish embryo. Development (Cambridge, UK) 123, 285-292.

Stalsberg, H. and DeHaan, R.L., 1969. The precardiac areas and formation of the tubular heart in the chick embryo. Dev. Biol. 19, 128-59.

Taber, L.A., 2006. Biophysical mechanisms of cardiac looping. Int. J. Dev. Biol. 50, 323-332.

Trinh, L.A. and Stainier, D.Y., 2004. Cardiac development. Methods Cell Biology 76, 455-473.

Voronov,D.A., Alford, P.W., Xu, G., and Taber, L.A., 2004. The role of mechanical forces in dextral rotation during cardiac looping in the chick embryo. Dev. Biol. 272, 339-350.

Voronov, D.A. and Taber, L.A., 2002. Cardiac looping in experimental conditions: the effects of extraembryonic forces. Dev. Dyn. 224, 413-421.

Walker, C. and Streisinger, G., 1983. Induction of mutations by gamma-rays in pregonial germ cells of zebrafish embryos. Genetics 103, 125-136.

Woodward, A.E., Abplanalp, H., Wilson, W.O. and Vohra, P., 1973. Japanese Quail Husbandry in the Laboratory. Department of Avian Sciences, University of California, Davis, CA 95616.

Yelon, D., Horne, S.A., and Stainier, D.Y., 1999. Restricted expression of cardiac myosin genes reveals regulated aspects of heart tube assembly in zebrafish. Dev Biol. 214, 23-27.

Yoshida, H., Manasek, F. and Arcilla, R.A., 1983. Intracardiac flow patterns in early embryonic life. A reexamination. Circ. Res. 53, 363-371.

# Chapter 2

# Measuring motion in the amniote heart tube to define the parameters that constitute proper heart development

# Chapter 2: Measuring motion in the amniote heart tube to define the parameters that constitute proper heart development

## 2.1 Abstract

The embryonic vertebrate heart begins as a straight tube. Through a process of cardiac looping, the chambers and valves of the heart are created. By measuring heart contractions at different locations in the developing quail embryo during the looping process, we aim to learn more about the parameters necessary for proper heart development. This was principally accomplished by using laser scanning confocal microscopy (LSCM) in conjunction with a Tie1 transgenic line of quail that expresses H2B::eYFP in endothelial cells. Quail embryos from different stages of development (Hamburger-Hamilton stages 10-13) were imaged under a LSCM microscope using line scans to analyze heart contractions across different regions of the developing heart tube. Our methods follow established protocols in analyzing echocardiograms in humans, and quantify heart development in terms of diameters of myocardial and endocardial tubes, thicknesses of cardiac jelly, changes in diameters and thicknesses observed during contractions, the amount of time spent in relaxation during a heartbeat, and the contractile strength and intensity of relaxation. These were compiled into graphs to create a system for measuring cardiogenesis in the early stages of development.

## 2.2 Introduction

The embryonic vertebrate heart begins as a straight tube of serially aligned primitive chambers that rearranges itself to form fully functioning chambers in parallel (reviewed by Moorman and Christoffels, 2003). Through the process of cardiac looping, the chambers and valves of the heart are created from a single heart tube. This complex process also allows for the formation of abnormalities that may result in congenital heart defects, which affect 1% of the human population (reviewed by Srivastava, 2006). By creating a system to quantify heart contractions in developing quail embryos during the initial phase of cardiac looping, we aim to learn more about the cellular aspects relating to heart morphogenesis, thereby creating a methodology for detecting certain heart abnormalities at an earlier stage of development.

The formation of the heart is a vital and complex process during embryogenesis. Without a proper functioning heart, most embryos will die. It is the heart, after all, that circulates oxygen and nutrient-rich blood to the developing organs. The aim of this project is to learn more about how the heart functionally develops during organogenesis. Using quail as a model system, we aim to find the parameters that can quantify proper heart development. Quail have four-chambered hearts comparable to humans, and are an excellent model for studying heart morphogenesis due to their size and ease of manipulation. Similar heart morphology research has already been completed in humans, except it was done on adult hearts using echo cardiography (Martin *et al.*, 1983). Echocardiograms use

ultrasound techniques to image the heart in two-dimensional optical slices. Martin and his colleagues focused on quantifying the motions seen in the left ventricle of the human heart to find the parameters that define proper heart function.

As ultrasound technology improves, visual access to a developing human embryo inside the womb will become greatly enhanced. With better pixel and temporal resolution, cardiologists will soon be able to image a human heart during the initial stages of development. When this happens, it would be ideal if the parameters of tube formation and contractile motion observed during dextral looping can be quantified to make use of the technology.

Using echocardiograms as a basis for quantifying heart morphogenesis, data was collected on quail hearts at stages from tube formation to early dextral looping (HH10 - HH12) (Hamburger and Hamilton, 1951) (see figure 1). At HH10 (10-12 somites), the heart tube is fully extended and is showing a bulge to signify the beginning of dextral looping. As the embryo grows, the loop forms a “c-“-shape at HH11 (13-15 somites) and the contractions have become stronger. At HH12 (16-18 somites), the c-loop has grown in size and thickness, preparing the heart for chamber formation in future stages (Manner, 2000; Martinsen, 2005).

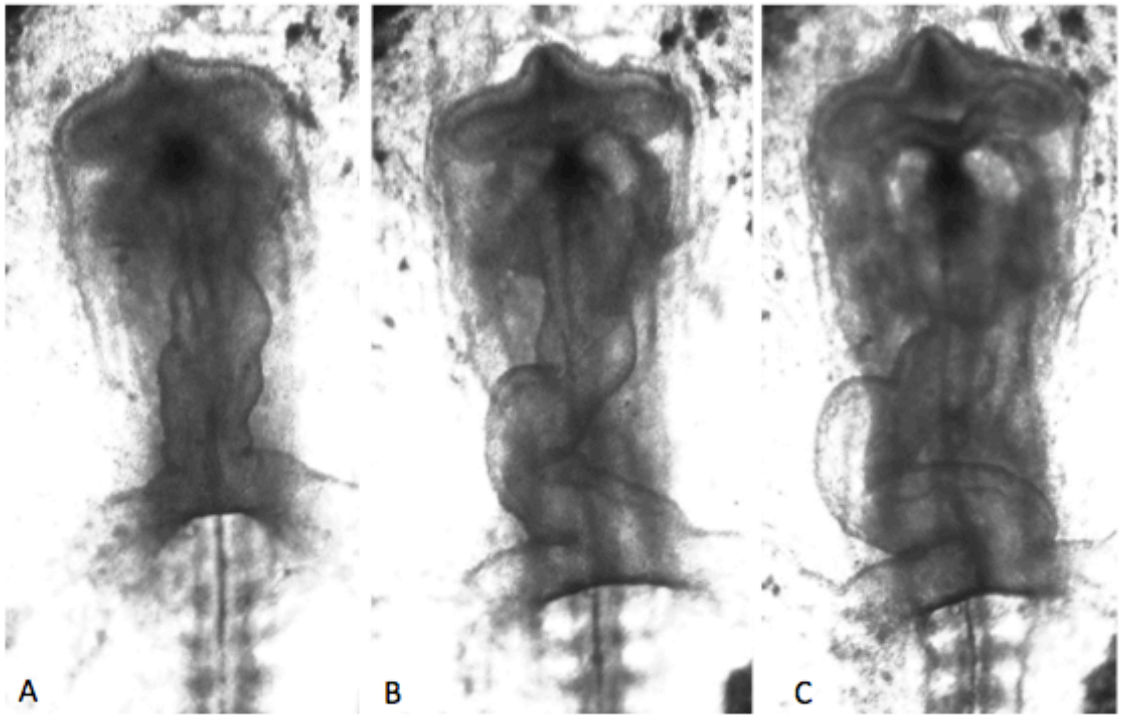


**Figure 1** Heart morphology at the early developmental stages in a quail embryo. A) HH10 shows that the tube has completely formed and is beginning to bulge outwards. B) HH11 the tube has looped to the right and contractions have begun. C) HH12 the tube is a fully formed "c"-shape and the diameter has thickened.

The contractile forces on the heart tube in developing quail embryos were studied using confocal laser scanning microscopes. Our principal tool was a transgenic line of quail that expresses yellow fluorescent protein (YFP) under the Tie1 promoter (Poynter and Lansford, 2008; Sato *et al.*, submitted). This expression pattern is localized to the nuclei of all endothelial cells in the quail embryo. YFP tagged endothelial cells enabled us to image the inner endocardial layer of the heart tube using fluorescent confocal microscopy. The outer myocardial layer was visualized using autofluorescence.

This study focused on the measurement of motion along the heart tube at different locations for comparison and across multiple stages (HH10-12). The two layers of the heart, the myocardium and endocardium, were measured on the left and right sides of the tube for a total of four measurements. These were then taken in five regions along the length of the heart tube: presumptive atria (A), atria-ventricle boundary (AV), lower ventricle (LV), upper ventricle (UV), and conus (C)

Even though the heart is a three-dimensional structure, measurements had to be reduced to one-dimension to achieve the temporal resolution required to capture the contracting and relaxing heart in detail. The early quail embryonic heart beats at approximately 1 Hz at 37 degrees C. To capture the beating heart in two-dimensions, a high-speed microscope can be used but will limit the frame rate to approximately 40 frames per second, meaning an image is taken every 25 msec. To improve on this, one-dimensional line scans were employed, which could image a 512X1 pixel region in three msec. This allows for over 300 line scans per second, giving a much more accurate image of the motions occurring during the heartbeat.

The embryonic quail heartbeat has a very distinct pattern. It begins with 1) a strong contraction, followed by 2) a rapid relaxation, and finally 3) a resting period that brings the heartbeat to its original starting point. This pattern is observed for the entire length of the heart tube at stages HH10-12. Using this as a basis, measurements of the contractile strength, relaxation velocity, and resting period were done to determine the parameters of properly developing hearts in quail

embryos. The hope is to apply this knowledge to human hearts when they are developing in the womb to detect congenital heart defects before they have fully developed. With modern drugs and non-surgical techniques, the heart abnormality may be corrected and the defect prevented.

## 2.3 Results & Discussion

The embryonic quail is composed to two layers, the myocardium (outer muscle layer) and the endocardium (inner lining), which are separated by the cardiac jelly. Using confocal laser scanning microscopy, the two layers of the heart were measured on the left and right side of the heart tube (see figure 2).

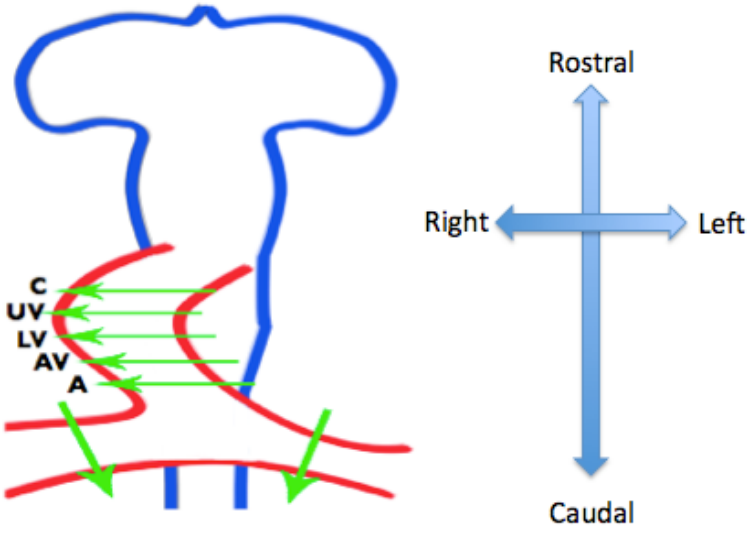


**Figure 2** Cartoon of the heart region of a quail embryo, ventral view. Measurements were taken of the myocardium and endocardium on the left and right sides for a total of four measurements at the five specified regions along the heart tube. A – presumptive atria, AV – atrioventricular boundary, LV – lower ventricle, UV – upper ventricle, and C – conus.

Contractile strength and relaxation velocity was measured, active and resting periods were quantified, diameters of the myocardium and endocardium were measured, and contractile displacement of the tissue layers and cardiac jelly were evaluated. The data was collected as line scans, which used a one-dimensional measurement to maximize temporal resolution during the heartbeat.

To study the anatomy in more detail, measurements of the heart were taken at diastole and systole. Quail embryos differ in size and have different growth rates. The first thing to determine is the range in sizes of quail hearts as they develop. The diameter of the outer myocardial tube and the inner endocardial tube were plotted for the five specified regions: presumptive atria (A), atrioventricular region (AV), lower ventricle (LV), upper ventricle (UV) and conus (C). Thickness of the cardiac jelly, defined as the space between the myocardium and endocardium, was also plotted (see figure 3).

**Figure 3** Graphs showing diameters and thicknesses of the different layers of the heart at relaxation using somite number for stage. The layers are the myocardium, endocardium, and cardiac jelly. The different regions are A) atria, B) atrioventricular region, C) lower ventricle, D) upper ventricle, E) conus. As the heart tube lengthens, horizontal dimensions are not affected.

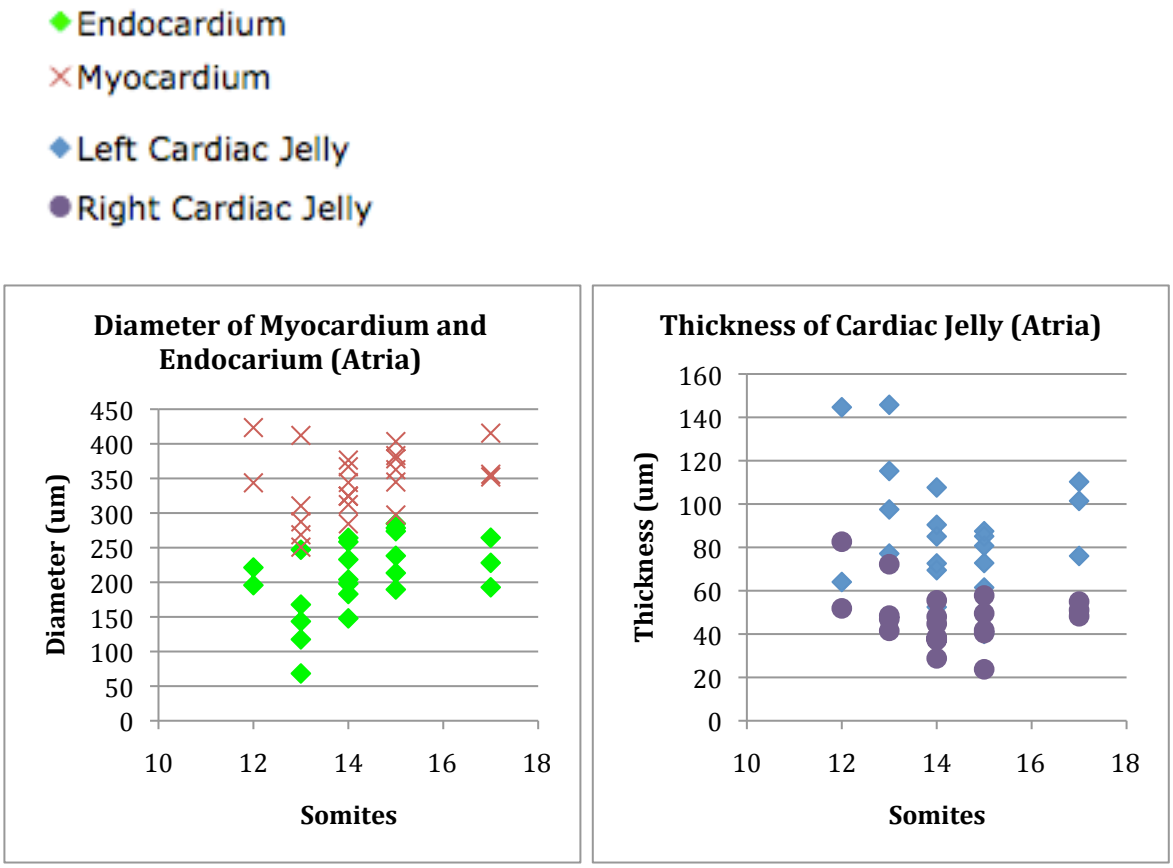

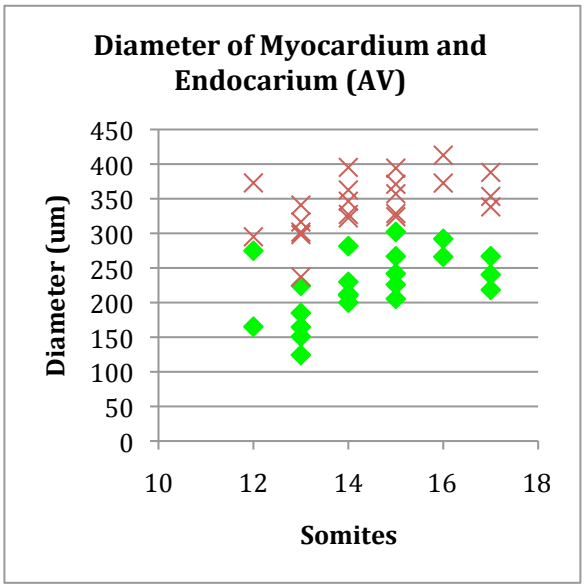
Diameter of Myocardium and Endocarium (AV)
Diameter (um)
450
400
350
300
250
200
150
100
50
0
10
12
14
16
18
Somites

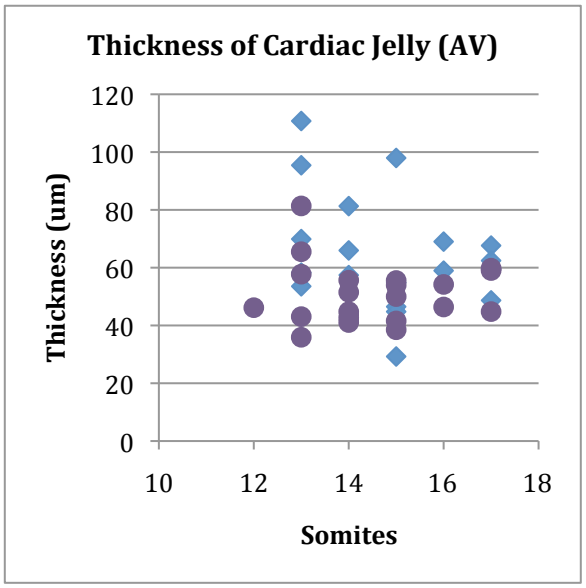
Thickness of Cardiac Jelly (AV)
Thickness (um)
120
100
80
60
40
20
0
10
12
14
16
18
Somites

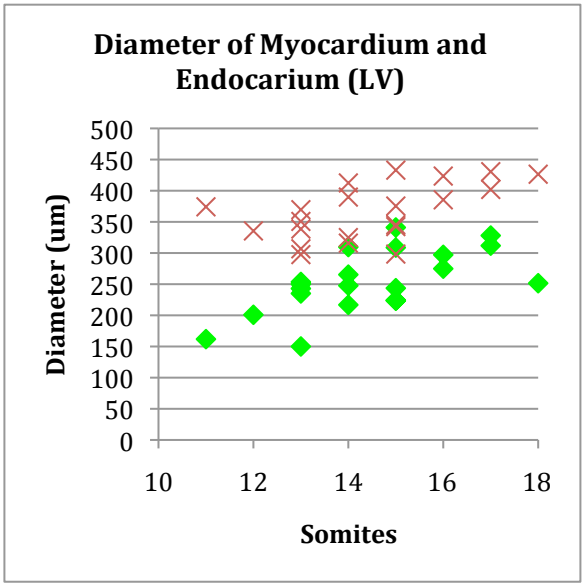
Diameter of Myocardium and Endocarium (LV)
Diameter (um)
500
450
400
350
300
250
200
150
100
50
0
10
12
14
16
18
Somites

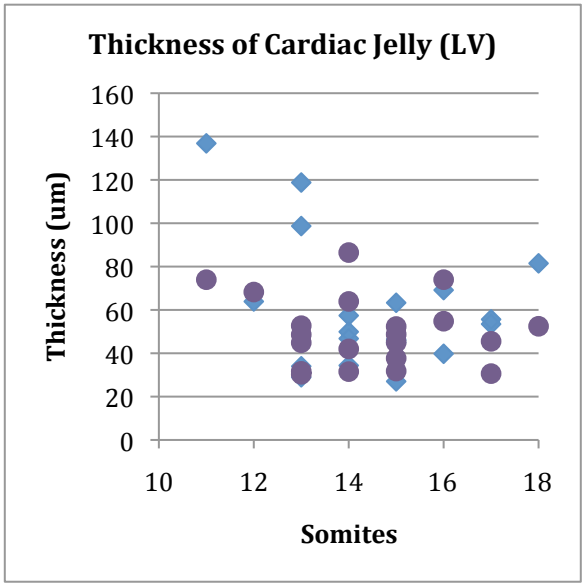
Thickness of Cardiac Jelly (LV)
Thickness (um)
160
140
120
100
80
60
40
20
0
10
12
14
16
18
Somites

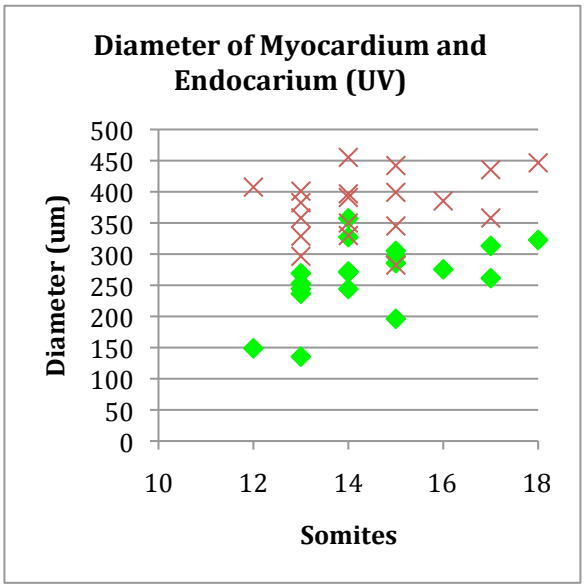
Diameter of Myocardium and Endocarium (UV)
Diameter (um)
500
450
400
350
300
250
200
150
100
50
0
10
12
14
16
18
Somites

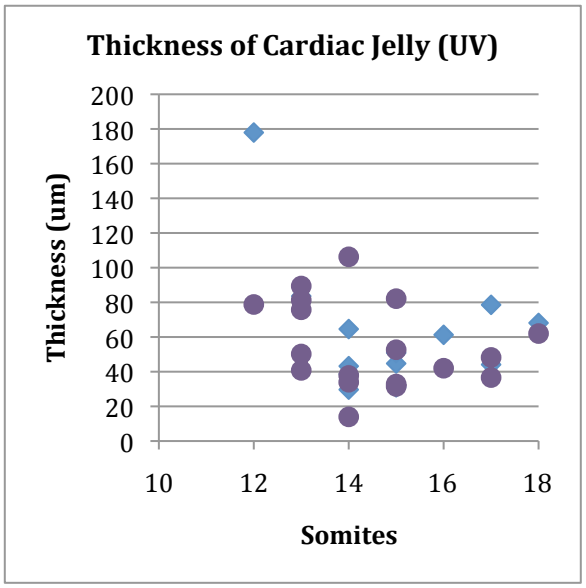
Thickness of Cardiac Jelly (UV)
Thickness (um)
200
180
160
140
120
100
80
60
40
20
0
10
12
14
16
18
Somites

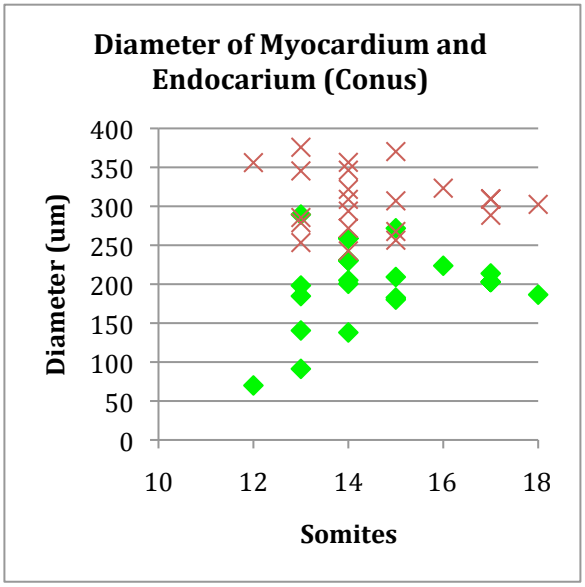
Diameter of Myocardium and Endocarium (Conus)
Diameter (um)
400
350
300
250
200
150
100
50
0
10
12
14
16
18
Somites

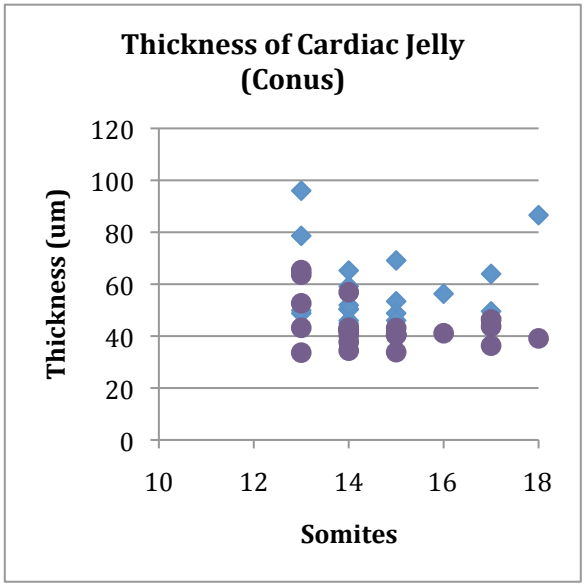
Thickness of Cardiac Jelly (Conus)
Thickness (um)
120
100
80
60
40
20
0
10
12
14
16
18
Somites

For these measurements, the diameter of the myocardial and endocardial tubes were consistently within a certain range across the developmental stages of somites 12-18. The myocardium ranged from 250-450 um for all five regions. For the endocardium, the range observed in the atria and AV is 100-300 um, in the LV and UV is 150-350 um, and in the conus is 100-250 um. Much individual variation is observed for the cardiac jelly in all five regions.

For developmental stages somites 12-18, the thickness range is uniform for each of the five regions measured. The ranges for the right and left cardiac jelly are as follows:

| Region | Thickness of Right Cardiac Jelly (um) | Thickness of Left Cardiac Jelly (um) |
|---|---|---|
| Atria | 20-60 | 60-120 |
| AV | 30-70 | 40-100 |
| LV | 30-80 | 30-80 |
| UV | 20-80 | 20-80 |
| Conus | 30-70 | 40-80 |

At the cranial and caudal ends of the heart tube, the right cardiac jelly consistently measures thinner than the left cardiac jelly while in the central region the range is identical for both left and right sides. The diameter and thickness plots give a range

to show the measurements of proper heart development. The consistency of the measurement ranges during this growth period (somites 12-18) shows that while the heart tube is lengthening and looping, the horizontal dimensions are not affected.

Once the diameters of the heart tube and the thickness of the cardiac jelly were known, the fraction of change in diameter and thickness during contraction was calculated (see Materials and Methods and figure 4). For all five regions, the myocardium increases in ∆diameter from somite 12-15, at which point the contraction reaches maximum value of approximately 0.25. In conjunction with the myocardium, the endocardium increases in ∆diameter in a similar pattern but in a higher range with a maximum value of 0.35. The fraction of change in the cardiac jelly ranges from 0 – 0.5, but does not have any clear patterns. These data match the description of the embryonic heart tube as a 2-layer-fluid-filled elastic tube with a thick gelatinous interior as described by Loumes *et al.* (2008). The cardiac muscle contracts, constricting the viscoelastic cardiac jelly, which then transfers the energy to the endocardium. Due to the nature of the tube, the inner tube shows more fraction of change since it can only contract inwards in a restricted space.

**Figure 4** Graphs showing the fraction of change in diameters and thicknesses of the different layers of the heart during contraction using somite number for stage. The layers are the myocardium, endocardium, and cardiac jelly. The different regions are A) atria, B) atrioventricular region, C) lower ventricle, D) upper ventricle, E) conus. The endocardial inner tube shows more of a fraction of change compared to the myocardial outer tube, reflecting the nature of the heart tube and viscoelastic properties of the cardiac jelly.

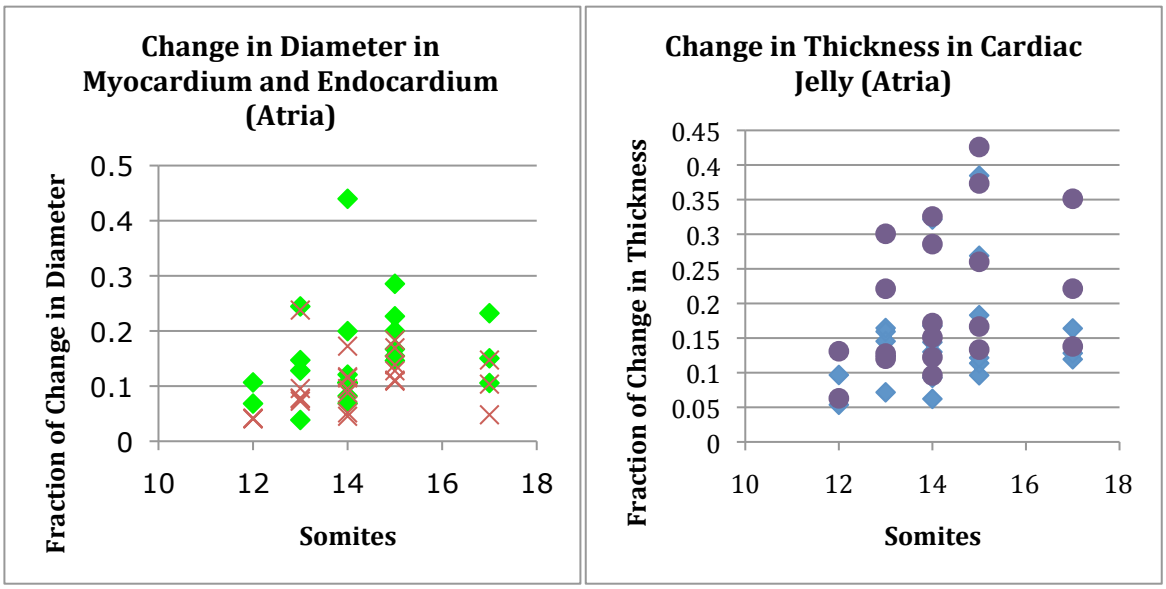

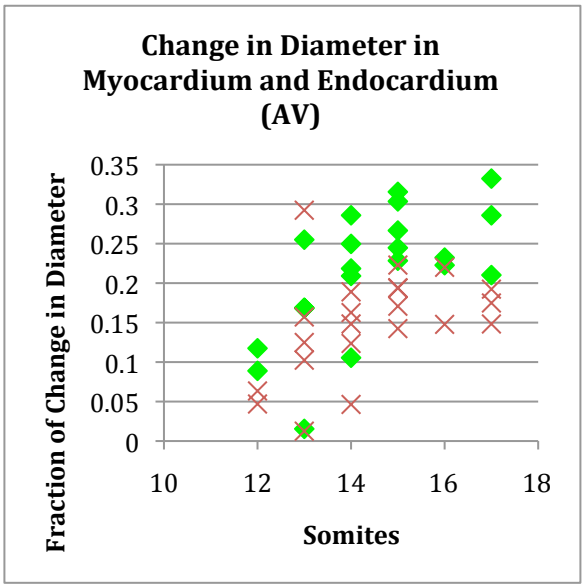
Change in Diameter in Myocardium and Endocardium (AV)
Fraction of Change in Diameter
0.35
0.3
0.25
0.2
0.15
0.1
0.05
0
10
12
14
16
18
Somites

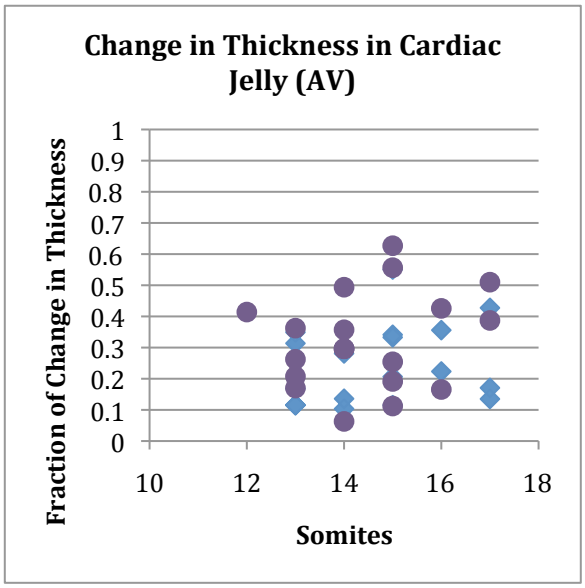
Change in Thickness in Cardiac Jelly (AV)
Fraction of Change in Thickness
1
0.9
0.8
0.7
0.6
0.5
0.4
0.3
0.2
0.1
0
10
12
14
16
18
Somites

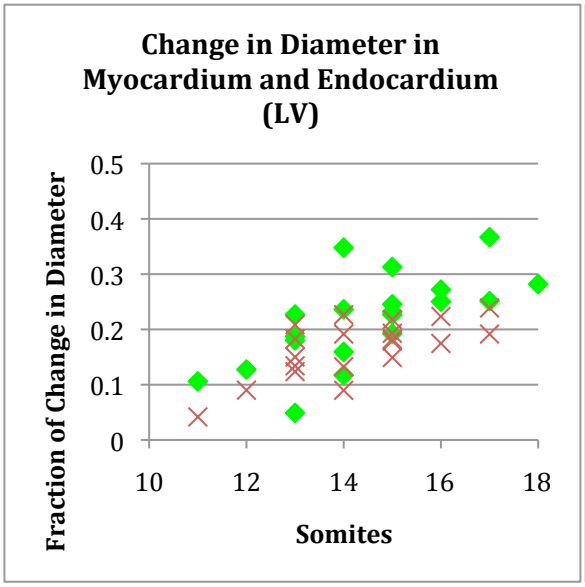
Change in Diameter in Myocardium and Endocardium (LV)
Fraction of Change in Diameter
0.5
0.4
0.3
0.2
0.1
0
10
12
14
16
18
Somites

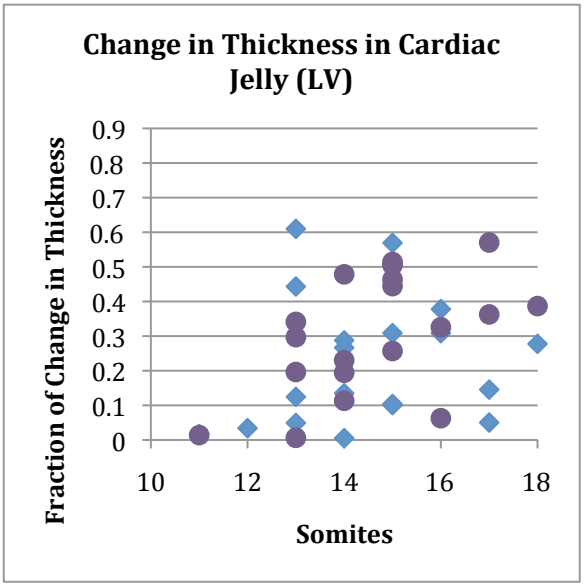
Change in Thickness in Cardiac Jelly (LV)
Fraction of Change in Thickness
0.9
0.8
0.7
0.6
0.5
0.4
0.3
0.2
0.1
0
10
12
14
16
18
Somites

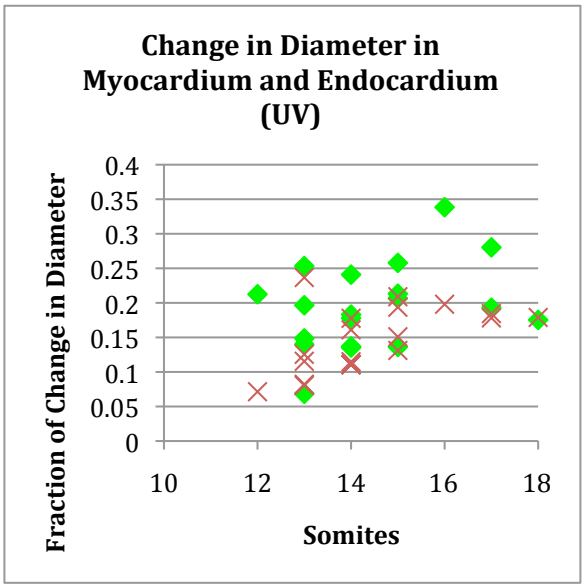
Change in Diameter in Myocardium and Endocardium (UV)
Fraction of Change in Diameter
0.4
0.35
0.3
0.25
0.2
0.15
0.1
0.05
0
10
12
14
16
18
Somites

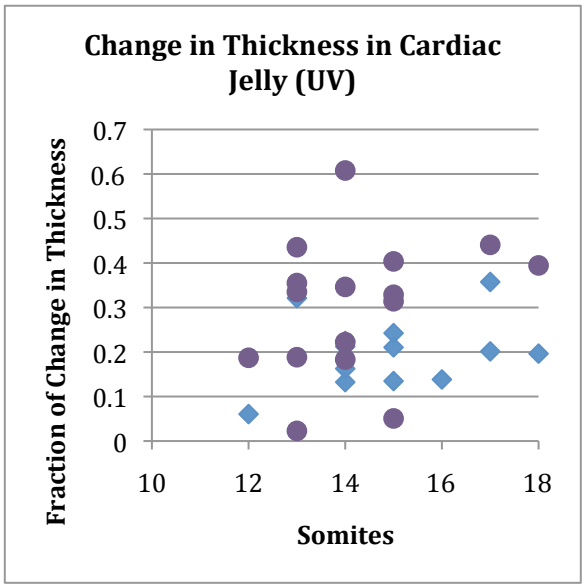
Change in Thickness in Cardiac Jelly (UV)
Fraction of Change in Thickness
0.7
0.6
0.5
0.4
0.3
0.2
0.1
0
10
12
14
16
18
Somites

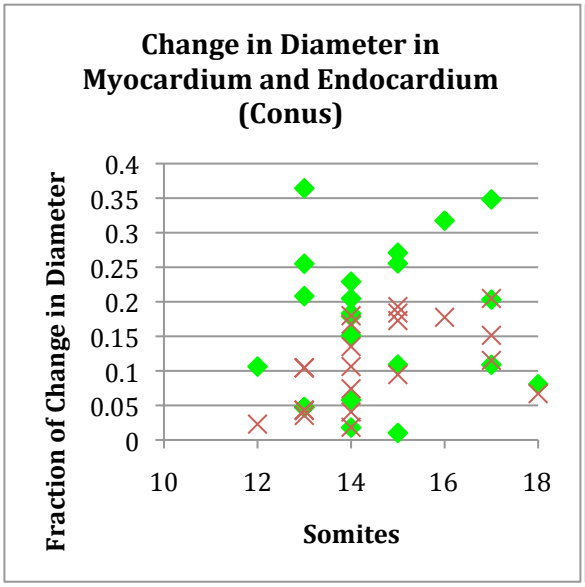
Change in Diameter in Myocardium and Endocardium (Conus)
Fraction of Change in Diameter
0.4
0.35
0.3
0.25
0.2
0.15
0.1
0.05
0
10
12
14
16
18
Somites

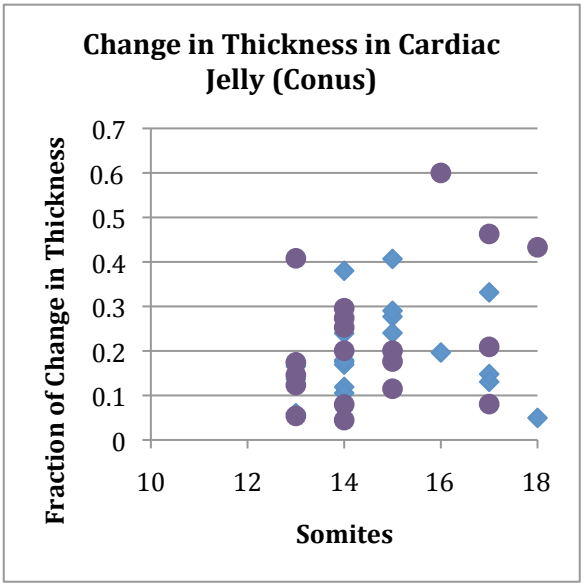
Change in Thickness in Cardiac Jelly (Conus)
Fraction of Change in Thickness
0.7
0.6
0.5
0.4
0.3
0.2
0.1
0
10
12
14
16
18
Somites

In figure 5, the fraction of the heartbeat cycle spent in the resting state was calculated as shown in the Materials and Methods section. For both the myocardium and endocardium at somites 12-14, the resting state is ~50-90% of total cycle time in the atria, 60-80% in the AV and LV, and widens to 40-80% in the UV and conus. As development occurs, the amount of rest time increases to 70-90% of cycle time for the atria, AV, and LV while it changes to 50-80% for the UV and conus. This shows that at younger stages (somites 12-14) in the atria, AV, and LV, the contraction is more controlled and methodical since the amount of resting time is limited to a 20% range while in the UV and conus, which are further along the length of the heart tube, the contractile wave has had time to spread and is less constrained so the resting time has a wider range of 40%. As the embryo develops, the resting time increases as a percentage, implying that the contraction occurs in a smaller range than before. This could be due to an increase in strength of contraction, which was investigated in the next set of measurements.

**Figure 5** Graphs showing the amount of resting time that is present in one heartbeat cycle across multiple embryos organized by cardiac layer and somites. The different regions are A) atria, B) atrioventricular region, C) lower ventricle, D) upper ventricle, E) conus. The fraction of resting time of the endocardium and myocardium tend to stay within the same range and follow the same trends.

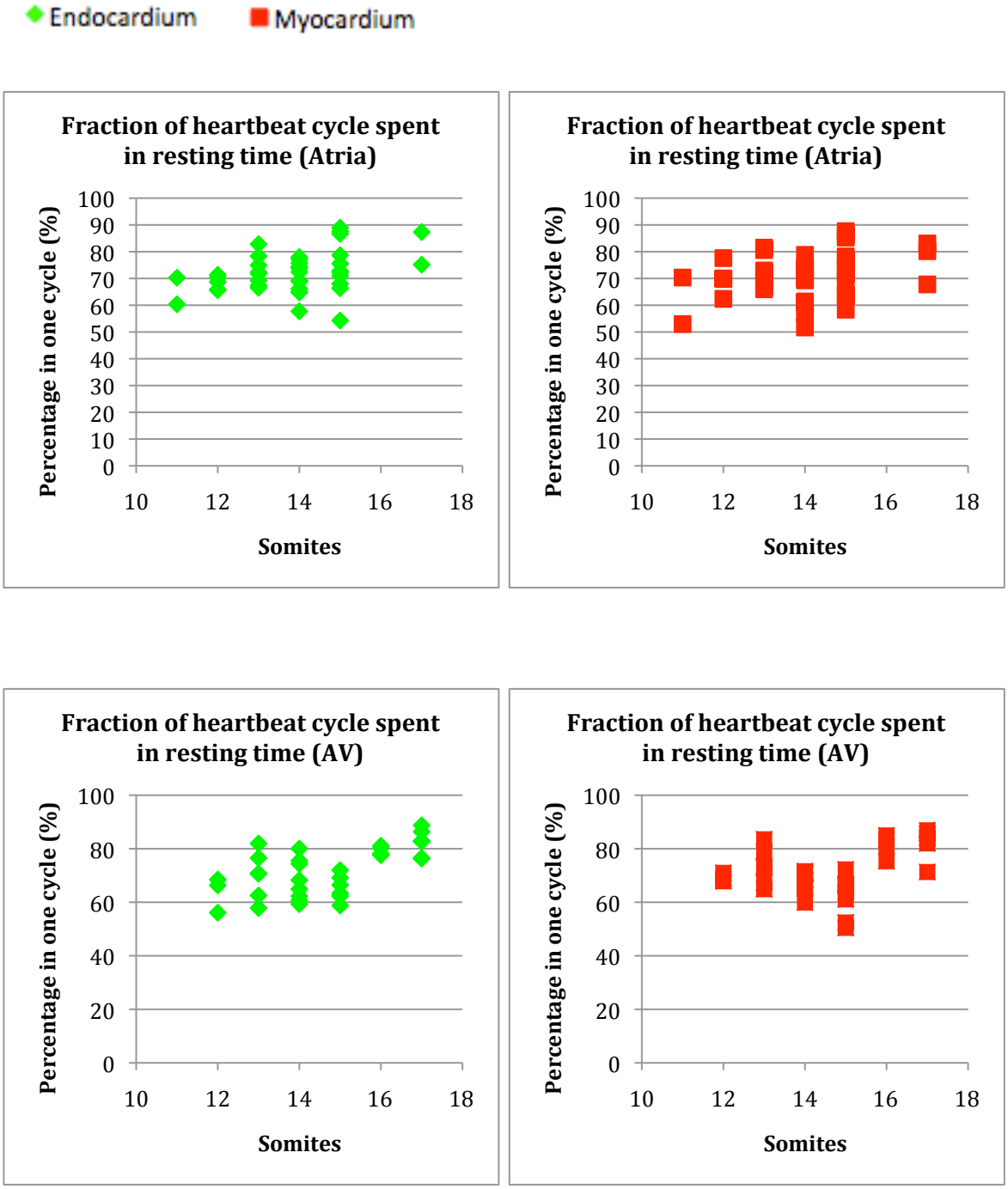

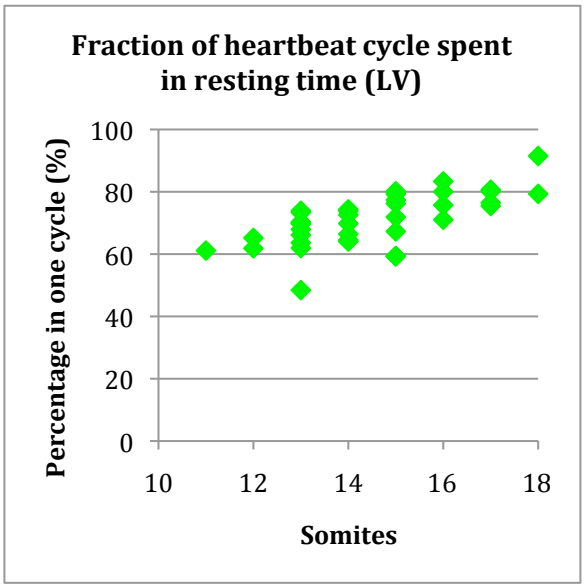
Fraction of heartbeat cycle spent in resting time (LV)
Percentage in one cycle (%)
100
80
60
40
20
0
10
12
14
16
18
Somites

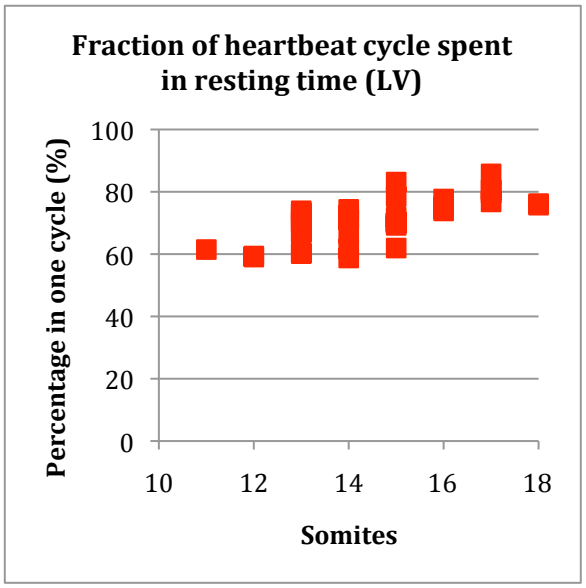
Fraction of heartbeat cycle spent in resting time (LV)
Percentage in one cycle (%)
100
80
60
40
20
0
10
12
14
16
18
Somites

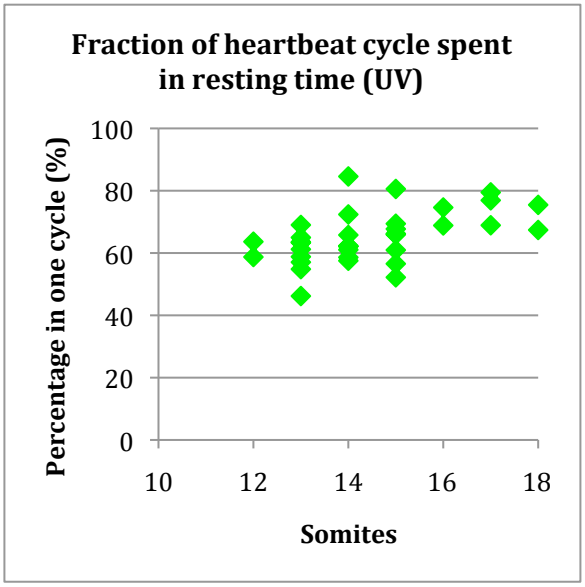
Fraction of heartbeat cycle spent in resting time (UV)
Percentage in one cycle (%)
100
80
60
40
20
0
10
12
14
16
18
Somites

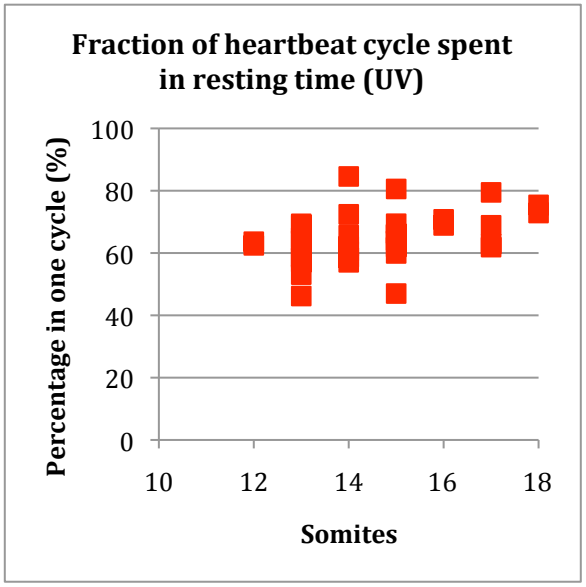
Fraction of heartbeat cycle spent in resting time (UV)
Percentage in one cycle (%)
100
80
60
40
20
0
10
12
14
16
18
Somites

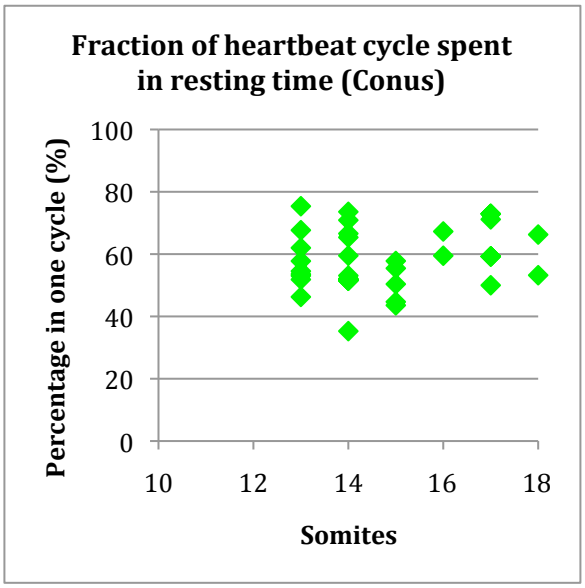
Fraction of heartbeat cycle spent in resting time (Conus)
Percentage in one cycle (%)
100
80
60
40
20
0
10
12
14
16
18
Somites

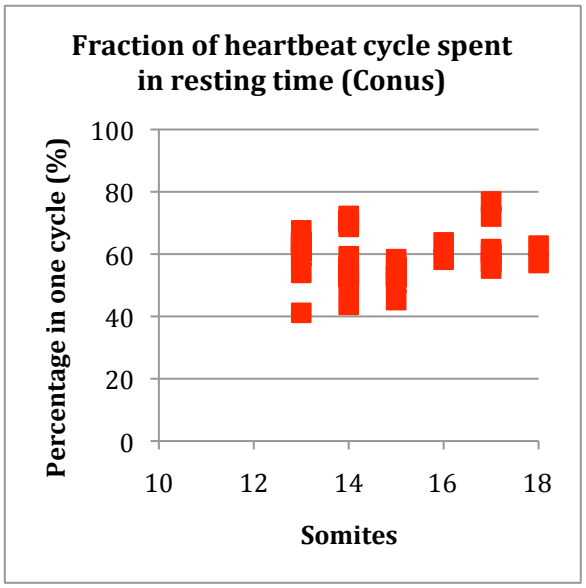
Fraction of heartbeat cycle spent in resting time (Conus)
Percentage in one cycle (%)
100
80
60
40
20
0
10
12
14
16
18
Somites

In figure 6, contractile strength and relaxation intensity were plotted for the myocardium and endocardium by calculating the slope of the line from the data (see figure 9 and Materials and Methods section). For the atria, the contractile wave has a wide range of velocities while the AV and LV regions consist of velocities that increase with developmental stage. The UV has only a slight increase in velocities compared to the AV and LV, and the conus contractile and relaxing velocities remain constant across somites 12-18. These data match the concept presented earlier that as the strength of the contraction increases, the amount of time in the heartbeat it occupies is reduced, allowing the heart to maintain the resting stage for longer periods of time.

**Figure 6** Graphs showing the velocity of contractions to measure contractile strength and intensity of relaxation present in one heartbeat cycle across multiple embryos organized by cardiac layer and somites. The different regions are A) atria, B) atrioventricular region, C) lower ventricle, D) upper ventricle, E) conus. As the strength of the contraction increases, the amount of time it occupies in the heartbeat decreases which allows the heart to maintain a resting stage for longer periods.

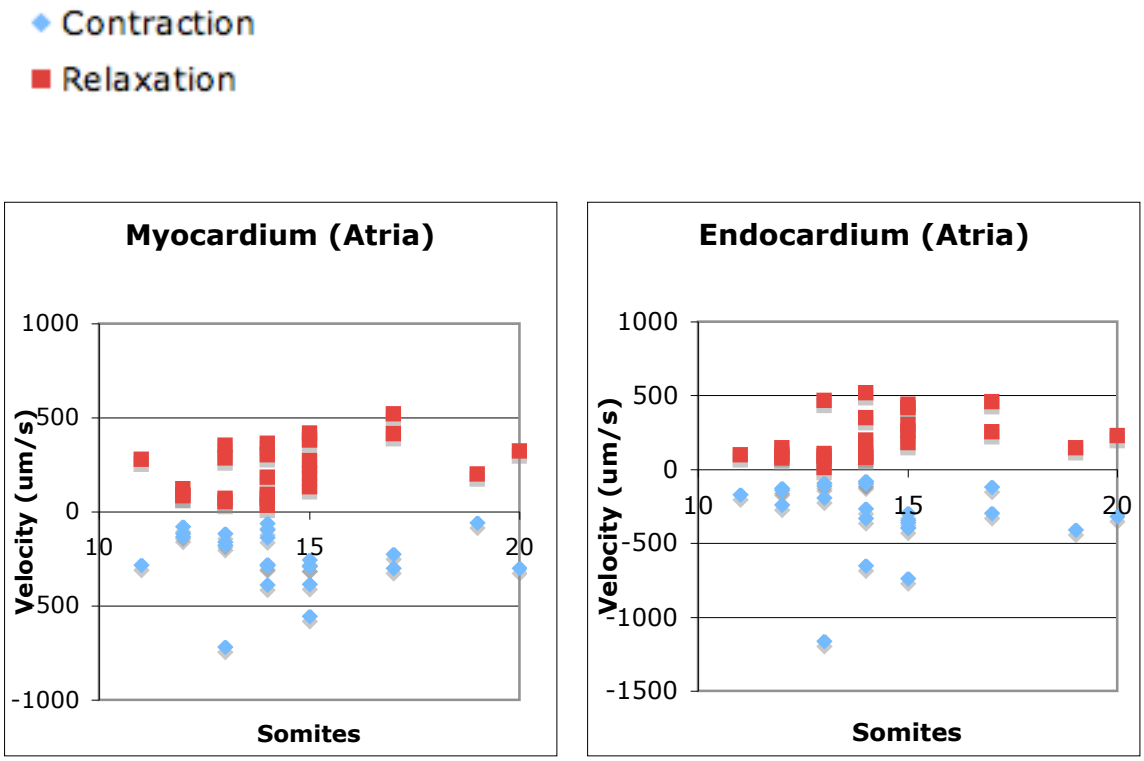

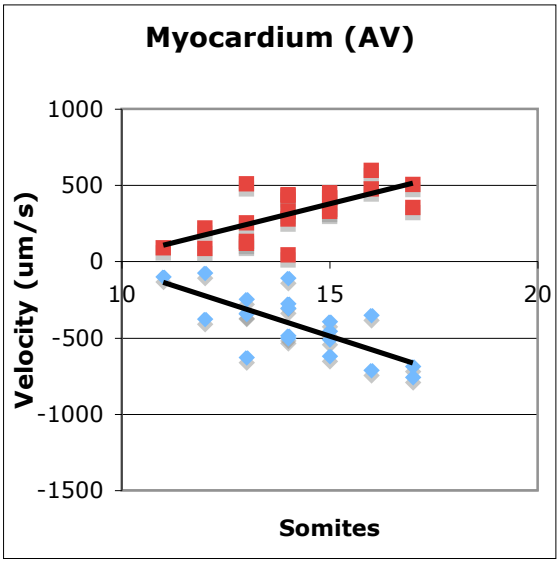
Myocardium (AV)
1000
500
0
-500
-1000
-1500
10
15
20
Velocity (um/s)
Somites

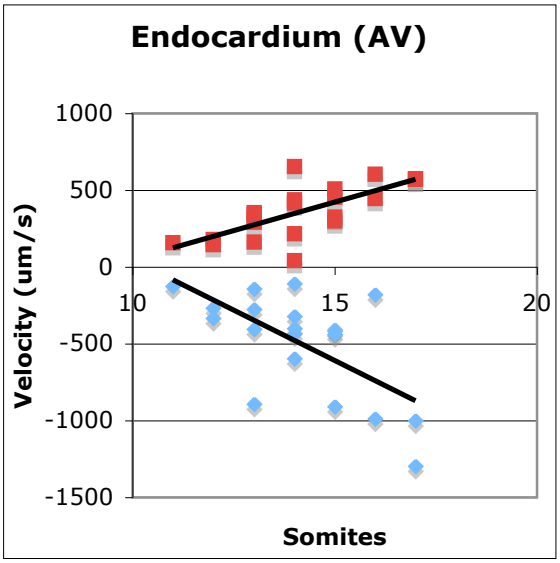
Endocardium (AV)
1000
500
0
-500
-1000
-1500
10
15
20
Velocity (um/s)
Somites

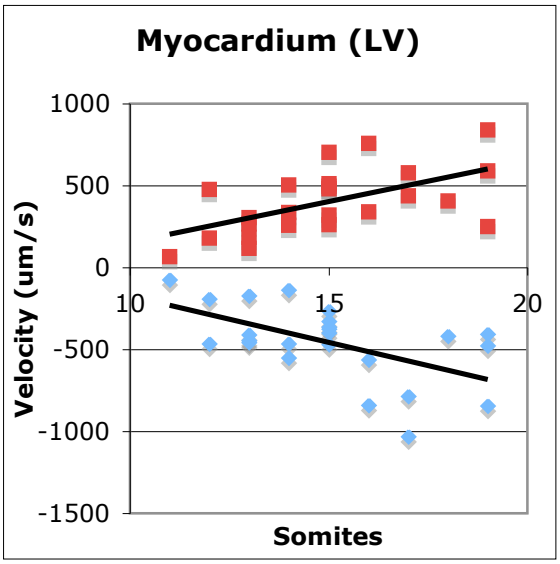
Myocardium (LV)
1000
500
0
-500
-1000
-1500
10
15
20
Velocity (um/s)
Somites

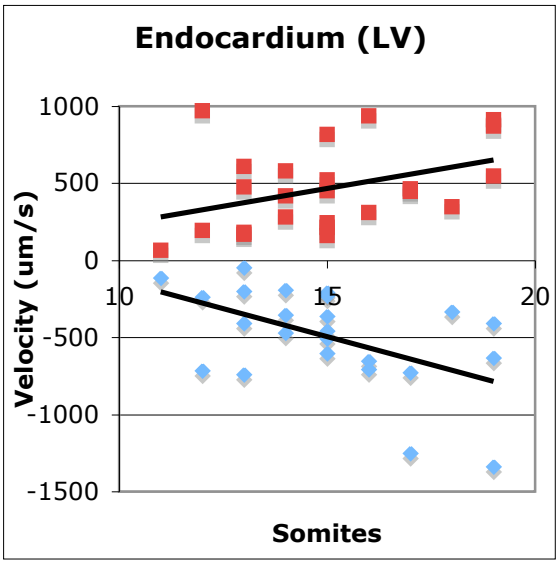
Endocardium (LV)
1000
500
0
-500
-1000
-1500
10
15
20
Velocity (um/s)
Somites

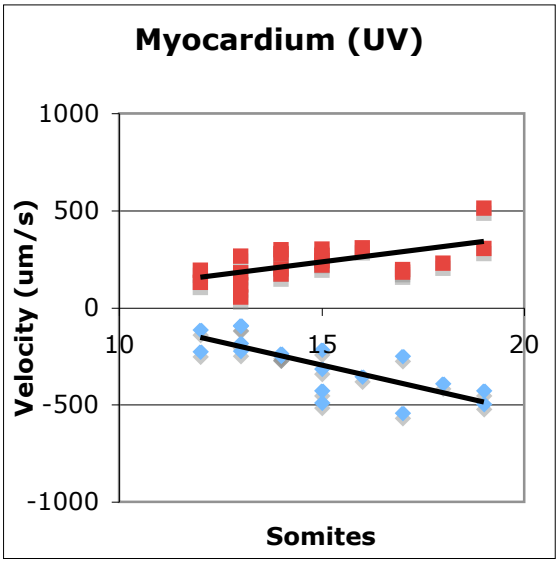
Myocardium (UV)
1000
500
0
-500
-1000
10
15
20
Velocity (um/s)
Somites

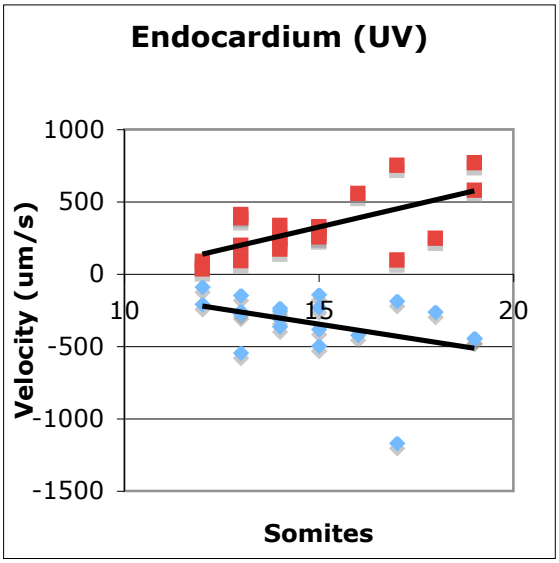
Endocardium (UV)
1000
500
0
-500
-1000
-1500
10
15
20
Velocity (um/s)
Somites

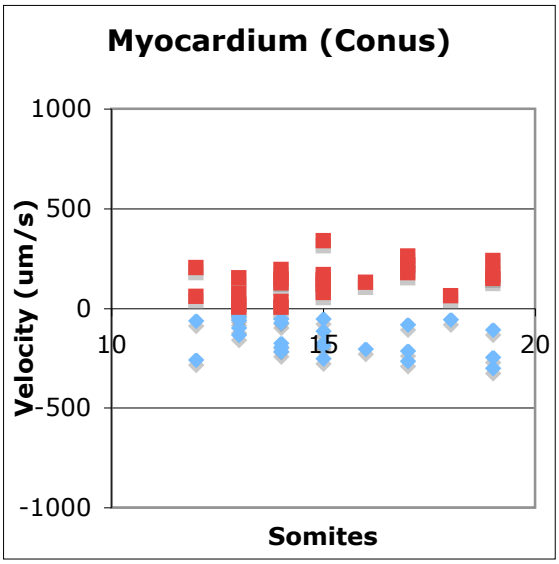
Myocardium (Conus)
1000
500
0
-500
-1000
10
15
20
Velocity (um/s)
Somites

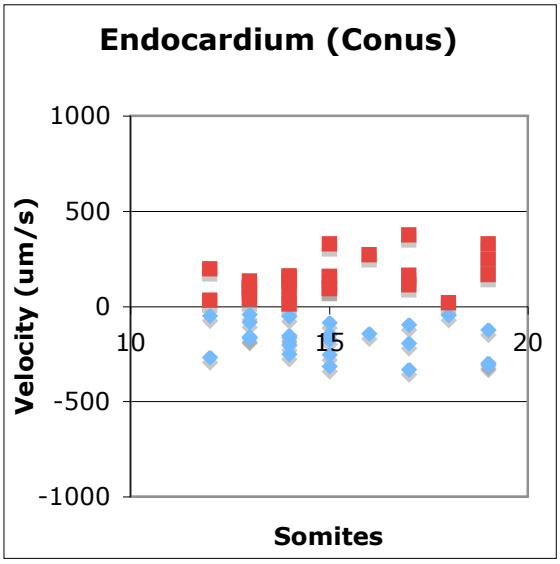
Endocardium (Conus)
1000
500
0
-500
-1000
10
15
20
Velocity (um/s)
Somites

The plots in this study are intended as parameters for determining proper heart development. The next step is to create a transgenic quail with a genetic heart mutation that appears morphologically at a later stage than 18 somites. By repeating all measurements and comparing the abnormal heart to the model, the parameters for that defect can then be quantified. In this way, certain congenital heart defects may be detected early enough and prevented with medical intervention.

## 2.4 Materials and Methods

### 2.4.1 Imaging Technique

Quail eggs were incubated at 37 degrees C for 36-51 hours depending on the desired stage of development. Eggs were then manually opened using surgical scissors. The thick albumen from each egg was removed using a pipette. Next, each embryo was removed from the egg yolk using a square piece of filter paper with a hole punched in the center. Embryos were then transferred into a heated buffer solution of Ringer's. Mounted embryos were inverted and placed ventral side down in glass bottom petri dishes for imaging. Embryos were imaged on an inverted Zeiss 510 laser scanning microscope within a heated enclosure to maintain a 37 degree C environment. Line scans were then taken across the heart tube such that each line scan was perpendicular to the outer edges of the tube. Line scans are defined as an image composed of 512 X 1 pixels. The time-series macro was set up

to take a continuous serious of 1000 line scans, which produced an image of pixel location versus time, similar to the output of a kymograph.

Five measurements were taken: presumptive atria (A), atrioventricular boundary (AV), lower ventricle (LV), upper ventricle (UV), and conus (C) across multiple embryos at the developmental stages of somites 10 through 20. The endocardium, which was labeled with YFP, was imaged using 488 nm laser light. The myocardium is autofluorescent under laser light. For images in which the myocardium could not be imaged using laser light, transmitted light was used to view the myocardium.

### 2.4.2 Fixing Embryos

As a control, embryos were fixed after they were imaged. This involved fixing each embryo in 4% paraformaldehyde (PFA) overnight at 4 degrees C. These embryos were then rinsed 3x with phosphate buffered saline (PBS), then placed in Ringer's solution and stored at 4 degrees C. This control was performed so that heart morphology, as well as somite number could be confirmed.

### 2.4.3 Processing Images

In order to analyze the data from each image, Matlab was used to plot both the movement of both the endocardium and myocardium (see figure 7B). This was accomplished by writing a Matlab code to pinpoint the region of contrast between the

fluorescent endocardium and background or the autofluorescent myocardium and background. For situations in which the contrast was not great enough, Adobe Photoshop CS3 was employed to manually follow the endocardium and myocardium in the beating heart (see figure 7).

**Figure 7** A) Two-dimensional image showing the result of a single line scan taken 1000 times. Two heart contractions are clearly visible. B) Matlab profiling of the myocardium (red) and endocardium (green) of the same image.

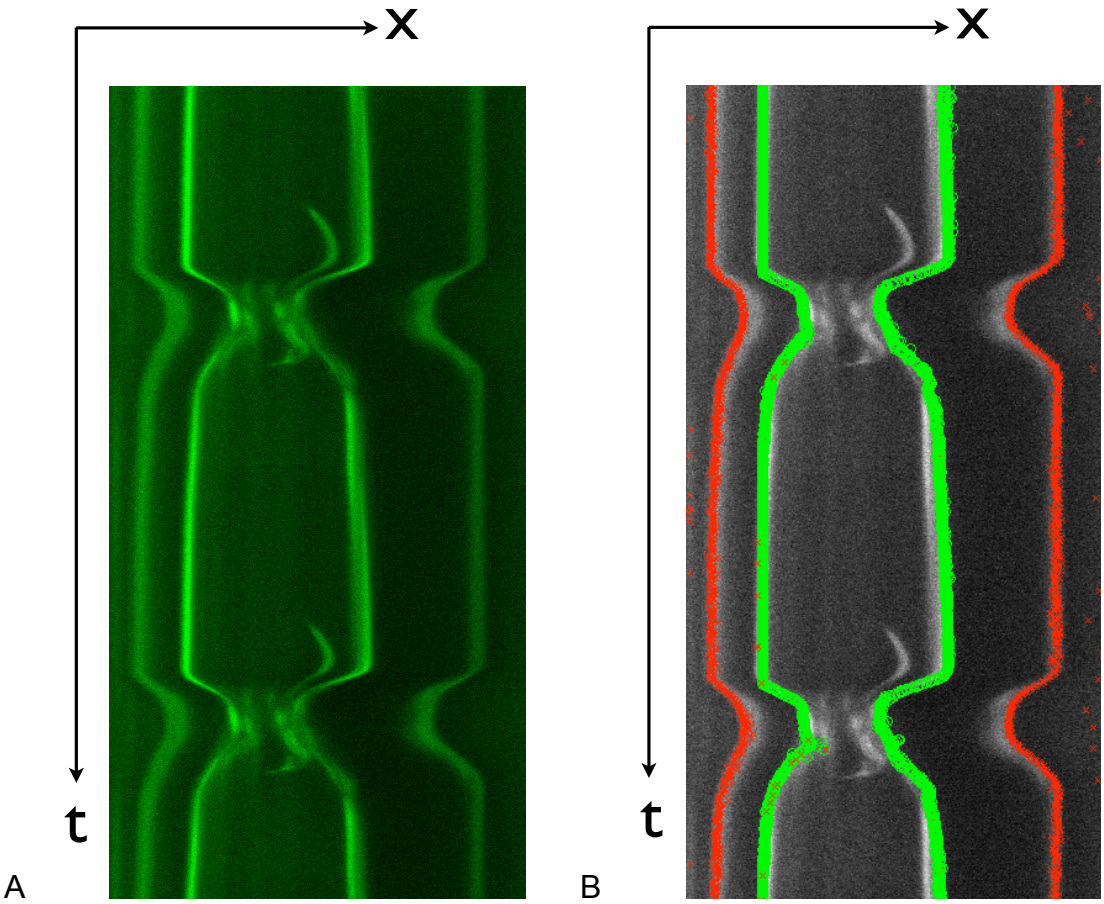


The resulting data produced an image with four lines corresponding to the right myocardium, right endocardium, left endocardium and left myocardium (see figure 8A). To remove outliers, the data were processed through a running median filter to

smooth the lines (see figure 8B). These plots show how the heartbeat can be split into three sections: 1) contraction, 2) relaxation and 3) resting period.

**Figure 8** A) Raw data from the Matlab matrix created from profiling in figure 7. B) The data after it has been processed through a running median filter. It is much cleaner without removing essential aspects of heart contraction.

A

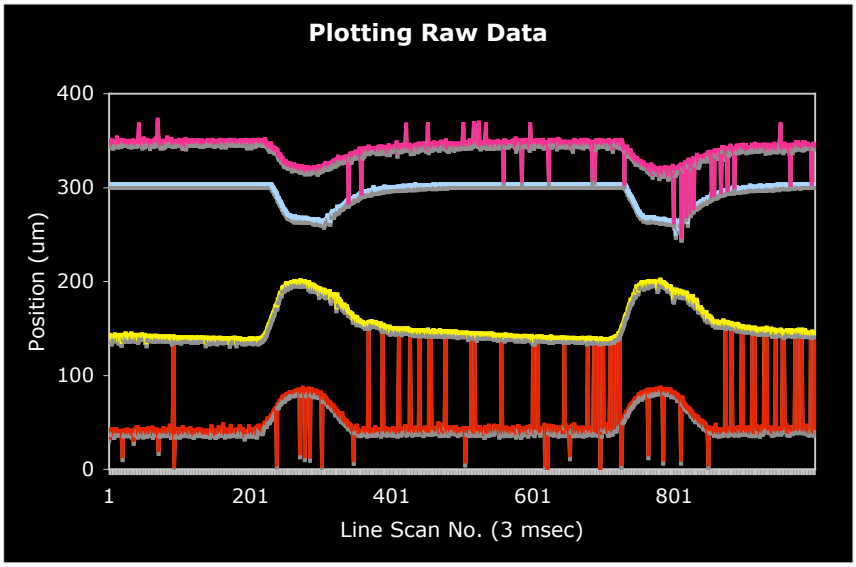


B

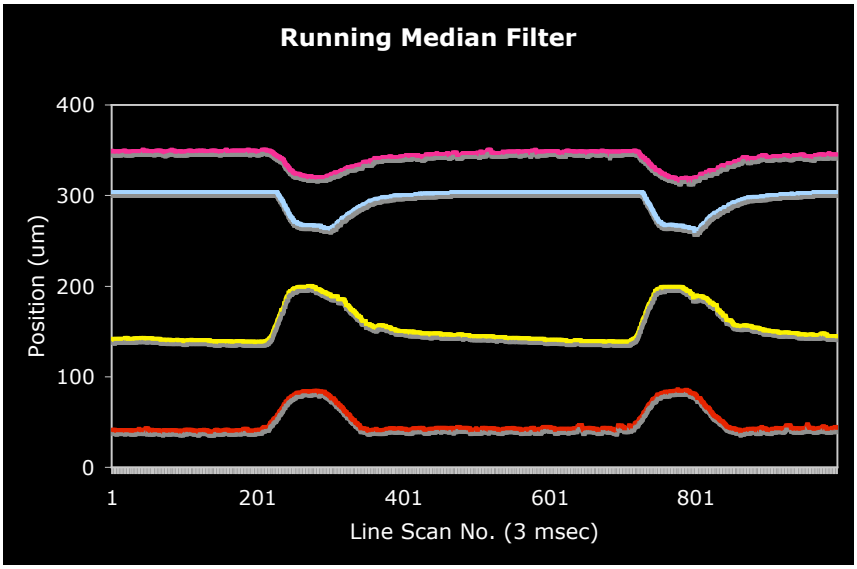

Each data set appeared as a matrix composed of [heart layer X line scan number] with the matrix value signifying pixel placement.

The fraction of the heartbeat cycle spent in the resting state was calculated by the following:

$$\frac{\text{Amount of time during resting}}{\text{Amount of time for 1 heartbeat cycle}} * 100 = \text{percentage}$$

To find the diameter of the myocardial and endocardial layers and the thickness of the cardiac jelly, manipulation of the matrix [number X letter] is as follows:

e.g. Matrix

| | A | B | C | D |
|---|---|---|---|---|
| 1 | 46 | 175 | 250 | 315 |
| 2 | 46 | 178 | 251 | 315 |
| 3 | 46 | 179 | 250 | 314 |
| 4 | 54 | 178 | 241 | 300 |
| 5 | 60 | 185 | 258 | 300 |

where the rows specify line scan number

and A = left myocardium
B = left endocardium
C = right endocardium
D = right myocardium

**Figure 9** Graph showing how the displacement during contraction and relaxation can be calculated for the myocardium, endocardium, and cardiac jelly.

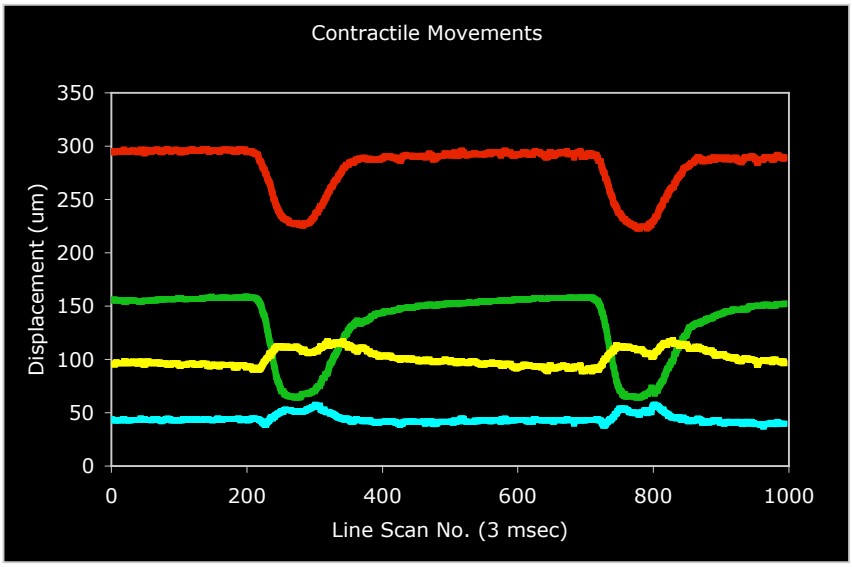


Diameter of the myocardium = D – A at diastole (red line)

Diameter of the endocardium = C – B at diastole (green line)

Thickness of left cardiac jelly = B – A at diastole (yellow line)

Thickness of right cardiac jelly = D – C at diastole (blue line)

The fraction of change in diameter during contraction for the following layers is calculated as follows:

$$\text{Change in myocardium} = \frac{(\text{D} - \text{A at diastole}) - (\text{D} - \text{A at systole})}{(\text{D} - \text{A at diastole})}$$

$$\text{Change in endocardium} = \frac{(\text{C} - \text{B at diastole}) - (\text{C} - \text{B at systole})}{(\text{C} - \text{B at diastole})}$$

$$\text{Change in width of left cardiac jelly} = \frac{(\text{B} - \text{A at diastole}) - (\text{B} - \text{A at systole})}{(\text{B} - \text{A at diastole})}$$

$$\text{Change in width of right cardiac jelly} = \frac{(\text{D} - \text{C at diastole}) - (\text{D} - \text{C at systole})}{(\text{D} - \text{C at diastole})}$$

To measure the contraction, the velocities of the contractile strength and relaxation intensity were calculated by finding the slope of the line (dy/dx) for the myocardial and endocardial layers as observed in figure 9.

## 2.5 References

Fishman, M.C. and Chien, K.R., 1997. Fashioning the vertebrate heart: earliest embryonic decisions. Development 124, 2099-2117.

Forouhar, A. S., Liebling, M., Hickerson, A., Nasiraei-Moghaddam, A., Tsai, H., Hove, J. R., Fraser, S. E., Dickson, M. E., Gharib, M., 2006. The embryonic vertebrate heart tube is a dynamic suction pump. Science 312, 751-753.

Hamburger, V. and Hamilton, H.L., 1951. A series of normal stages in the development of the chick embryo. J. Morph. 88, 49-92.

Liebling, M., Forouhar, A.S., Wooleschensky., R., Zimmermann., B., Ankerhold., R., Fraser., S.E., Gharib., M., Dickinson., M.E., 2006. Rapid three-dimensional imaging and analysis of the beating embryonic heart reveals functional changes during development. Dev. Dyn. 235(11), 2940-2948.

Loumes, L., Avrahami, I., and Gharib, M., 2008. Resonant pumping in a multilayer impedance pump. Physics of Fluids 20, 023103.

Manner, J., 2000. Cardiac looping in the chick embryo: A morphological review with special reference to terminological and biomechanical aspects of the looping process. The Anatomical Record 259(3), 248-262.

Martin., C.J., Weir., J., Ng., K.H., 1983. Use of computer analysis of echocardiograms for assessment of left ventricular function. Clin. Phys. Physiol. Meas. 4(4), 381-394.

Martinsen, B.J., 2005. Reference guide to the stages of chick heart embryology. Dev. Dyn. 233, 1217-1237.

Moorman A.F. and Christoffels, V.M., 2003. Cardiac chamber formation: development, genes and evolution. Physiol. Rev. 83, 1223-1267.

Poynter, G. and Lansford, R., Avian Embryology. Methods in Cell Biology, 2nd edition. San Diego: Academic Press, 2008, pp. 281-293.

Sato, Y., Poynter, G., Huss, D., Filla, M., Czirok, A., Rongish, B., Little, C., Fraser, S., and Lansford, R., Dynamic analysis of vascular morphogenesis using transgenic quail embryos. Submitted.

Srivastava, D., 2006. Making or breaking the heart: from lineage determination to morphogenesis. Cell 126, 1037-1048.

# Chapter 3

## Rapid three-dimensional imaging of the beating embryonic quail heart reveals the mechanistic purpose of cardiac jelly

# Chapter 3: Rapid three-dimensional imaging of the beating embryonic quail heart reveals the mechanistic purpose of cardiac jelly

## 3.1 Summary

Recent technological advances in dynamic confocal microscopy and four-dimensional reconstruction have shown that the embryonic heart tube in the developing zebrafish functions more as a dynamic suction pump than a peristaltic pump, contrary to previous assumptions. With these new technological and biological advances leading to new observations and discoveries, it only makes sense to apply this research to higher order taxa such as bird or mammal. The Japanese quail is an ideal system to study pump mechanics in the four-chambered heart of a warm-blooded vertebrate with easily accessible embryos. All stages of the developing heart during looping and chamber formation are accessible *in ovo* and *ex ovo*, allowing for ease of manipulation of the embryo for dynamic imaging. Using Tie1 transgenic quail embryos, our results show that high-speed imaging and four-dimensional reconstruction of the avian heart reveal detailed motions of heart contractions in avians never seen before. From this data, we were able to track individual cell motion in different regions of the heart tube during contraction, which showed the mechanistic purpose of the cardiac jelly as a buffering agent to remove asynchronicity from myocardial cells to create a smooth contraction in the endocardial lining.

## 3.2 Introduction

The heart is the first functioning organ to form in the developing vertebrate embryo. It begins as a crescent shape that eventually forms a heart tube. Much research has been done on the developing embryonic heart in species ranging from the sea squirt to the zebrafish, chicken, and mouse to study anatomy and genetics.

During amniote cardiogenesis, epiblast cells ingress through the primitive streak to form the mesoderm. The mesodermal cells then move cranio-laterally and separate into the splanchnic mesoderm and the somatic mesoderm. About Hamburger and Hamilton (HH) Stage 6 (Hamburger and Hamilton, 1951), as the quail anterior endoderm folds, heart progenitor cells in the splanchnic mesoderm translocate to the midline and fuse to form a tubular heart. The primitive heart fold forms as the anterior intestinal portal regresses caudally (Moreno-Rodriguez *et al.*, 2006; Stalsberg and DeHaan, 1969). The anterior and posterior portions of the dorsal roof of the trough continue to close, and the tube elongates bidirectionally (Moreno-Rodriguez *et al.*, 2006) forming a linear heart tube between HH stages 9 and 11. The tubular heart contains a single atrium and a single ventricle and soon begins to undergo contractions (Stalsberg and DeHaan, 1969). About HH stage 10, the heart begins to C-loop, which coincides with cranial flexure, but is independent of blood flow (Manner *et al.*, 1993; Patten, 1922). At HH12, the beating heart has formed the c-loop and is comprised of a proximal primitive outlet, which connects to the ventral aortae cephalically, the apical portion of both ventricles, a primitive atrium and a

primitive inlet (de la Cruz et al, 1989).

Looping begins when the myofibrils first appear (Manasek *et al.*, 1978), and the dorsal mesocardium is always located at the inner curvature of the loop (Butler, 1952). In culture, it has been shown that the heart tube bends but does not twist (Butler, 1952; Manning and McLachlan, 1990). Removal of the inflow tract also removes most of the torsional rotation observed in vivo during c-looping. (Voronov *et al.*, 2004; Voronov and Taber, 2002). In the last decade, much detailed work has been done to model the looping aspects of the early embryonic heart tube. Previous data suggest the bending component of looping is intrinsic to the heart tube while the torsional rotation is extrinsic (reviewed by Taber *et al.*, 2006).

The study and modeling of the looping aspects of heart looping is a recent development in the field of cardiac development. Previous research used methods of DiI injected along the ventral mesocardium with images taken during the looping phase, or matching the shape of heart looping in fixed samples to those of pipes bending (Kidokoro *et al.*, 2008; Manner, 2004). Both these methods provide insight into the dextral looping of the heart tube, which has also been shown to contain an element of torsional twisting during the looping process. An aspect of looping that has eluded scientists is the cellular dynamics occurring during each heartbeat during the early phases of heart development. As the heart begins to beat at HH9 and with increasing intensity during development, the contractions occur at a rate that does not allow for imaging by traditional methods. Knowledge of cellular movements from this point onwards is limited due to motion observed during contractions.

A key aspect of heart development that has challenged scientists for decades is that the heart continuously changes shape while it is beating and growing, making it difficult to study in vivo. To access anatomical details of the heart, researchers traditionally have either removed the heart from its host and examined it while it is dying, or used fixed samples to infer function.

Recent research has been able to correct this problem in heart research by creating computer algorithms that can reconstruct a dynamic image of the beating heart in zebrafish (Liebling *et al.*, 2006). From these data, detailed dynamic modeling of the zebrafish heart at various stages of development was performed for the first time. Subsequently, it was concluded that the zebrafish embryonic heart tube actually behaves more similarly to an impedance pump than to a peristaltic pump – a behavior contrary to that originally assumed. (Forouhar *et al.*, 2006; Fishman and Chien, 1997).

Despite recent technological breakthroughs in 2D dynamic imaging, confocal microscopes remain quite slow at capturing optical sections at successive depths and gathering 3D data over time. Nevertheless, when the studied motion is cyclical – such as for a beating heart – a way to circumvent this problem is to acquire, successively, sets of 2D+time slice sequences over multiple depths (and over at least one time period) then computationally reassemble them to recover a 3D+time sequence.

It has been shown, both *in silico* and from *in vivo* measurement of the heart in zebrafish, that when the acquired optical sections at different depth overlap sufficiently, it is possible to accurately reconstruct volumes based solely on pixel information contained in the images (Liebling *et al.*, 2005). The acquisition and reconstruction procedure is illustrated in figure 1.

Acquisition and reconstruction were successfully carried out in the embryonic zebrafish heart at multiple developmental stages. These revealed morphology and function of the beating heart at the tube stage (26-30 hours post fertilization) throughout heart looping, chamber formation and of the mature heart (Forouhar *et al.*, 2006; Liebling et al, 2006). Zebrafish has many advantages for imaging (the heart is optically accessible and many stable transgenic lines are available) yet it is a two-chambered heart. Extensions of these techniques to imaging the quail will permit characterization of a model system with a four-chambered heart.

Quail and humans are amniotes with four-chambered hearts, which are more similar than zebrafish and humans. The quail heart is easily accessible for manipulation *in ovo* and *ex ovo* (Manner, 2000). Knowledge obtained from an avian four-chambered heart can then be applied to the less accessible mammalian and human hearts.

A system was developed to image beating amniote hearts on a high-speed confocal microscope using transgenic quail to view the nuclei of cells and dynamically follow

individual cellular movements. We focused our dynamic imaging on the Hamburger-Hamilton stages 9-12 due to size constraints on the microscope (Hamburger and Hamilton, 1951). The imaging area of the quail heart is approximately 1000 um by 700 um, which can be viewed with a 10X objective. Using Tie1 transgenic quail, we imaged the ventral myocardium and endocardium of the heart and followed the paths of individual cells during one cycle of the heartbeat (Poynter and Lansford, 2008; Sato *et al.*, submitted). Dynamic imaging and four-dimensional reconstruction of these two ventral layers revealed the interaction between the muscle layer (myocardium) and the inner lining of the heart (endocardium) in each contraction over different morphological stages.

## 3.3 Results & Discussion

We were able to track the cells of the ventral myocardium and endocardium in embryos of various stages of development. In figure 2, we show the endocardium and myocardium of the stage HH9 heart. The middle panel shows only one frame of an entire heart beat captured at 37 frames per second. Importing the high-speed movie into the image-visualization software Imaris, we have tracked the movements of individual cells during one cycle of a heartbeat, which is shown in the right panel. From these, we can see that cells of the endocardium move in cyclic trajectories, the planes of which are approximately parallel. The cells of the myocardium, by contrast, move in planes that are angled relative to each other, suggesting a small amount of twist during the heart beat. This can be seen in the far right loops where the trajectory of the most caudal loop is angled down and right, while the more cranial loops begin to angle up. This twist seems to follow the edge of the myocardium.

As the embryo progresses in stage HH10 as shown in figure 3, we observe the initiation of the C-loop forming in the lower bulges of the heart tube. Tracking individual cells during the heart beat shows that cellular movement is similar to that at HH9.

Upon viewing the heart at HH11 in figure 4, we observe strikingly different patterns between the cells of the endocardium and those of the myocardium. The

myocardium seems to have an outward to inward motion while the endocardial cells follow more of a lateral motion. In a heart with a mature loop as seen in HH12 in figure 5, the differences between the myocardial and endocardial cells are even more pronounced.

In figure 6, the cell tracks of myocardial cells are placed next to an image of the tracks of endocardial cells. In this side-by-side comparison, the paths of muscle cells differ from that of the inner lining of the heart. At the most caudal end of the heart tube, the myocardial cells move in a circular pattern in a clockwise motion. As they enter the loop region, the pattern becomes more perpendicular to the plane of the image. At the cranial end of the heart tube, circular patterns that move in a counter-clockwise rotation are observed. This gradual change in motion can only be explained by torsional twisting during dextral looping. Dextral looping of the heart is composed of two components: right-handed bending and torsional twisting (reviewed by Taber *et al.*, 2006). Bending of the heart tube does not allow for the change in cyclical motional that is observed and requires cell motion to remain in the same plane (Manner, 2004). A tube that is fixed at the rostral and caudal ends that is forced to loop contains the requisite torsion that causes the shift in cyclical motion as observed in the data (Voronov *et al.*, 2004). In comparison to the myocardial cells, the endothelial cells have a narrow, circular motion at the caudal end of the heart tube, which quickly opens up to circular patterns in a clockwise motion along the length of the tube.

In figure 7A, the data collected provides an interesting picture of how the myocardium and endocardium interact with each other. Focus was on the heart of an HH11 embryo due to the easily observable strength of contraction and imaging completeness since the heart fits entirely in the viewing area. The myocardial and endocardial cells in cross-sectional areas of the heart tube were manually tracked during the heartbeat cycle. Each cell was confirmed to follow a circular pattern within the plane of the screen, and the amount of rotation during one heartbeat was measured (see figure 7B). The data for each cross-sectional region was then plotted.

From the graphs (see figure 7C), it can be seen that the myocardium and endocardium follow similar rotation cycles. During the heartbeat, there is a period of dormancy followed by the quick movement of the contraction. Focusing on the myocardial cells in the upper region, the movement of the four cells contract as a group with some cells lagging behind. Observing the plot of endocardial cells in the upper region, the cells have managed to contract in a synchronous pattern with the cells at the right most part of the heart beginning the contraction and cells to the left lagging sequentially. As the heartbeat continues, the pattern shifts and the left most cells now lead the contraction while the cells to the right follow sequentially. In the middle region, the cross-section of myocardial cells contract asynchronously, similar to those in the upper region. Comparing these to the endocardial cells of the middle region, the graph is composed of four cells that follow the contraction grouped together very tightly.

The plots of the endocardial cells in the upper and middle regions differ in that the middle region is tightly grouped while the upper region contracts in a wave pattern. Correlating this to figure 6 and the torsional twist observed along the length of the heart tube, this difference in contractile rotation seems logical. The lack of delay from the right to left in the middle region implies a lesser amount of torsion is present than in the upper region.

From figure 7C, the phase lag observed in the plots show how the cardiac muscles contract asynchronously. This implies the electrical signal passing through the muscles to initiate contractions has some variance. At the level of the endocardium, however, the asynchronous nature of the contraction is removed. This suggests that the cardiac jelly imparts a buffering action to the contractile wave as it passes from the muscle to the inner lining of the heart. The smoothing of the contraction may be required to encourage the transverse sections of the tube to beat in a synchronous manner for moving blood through the heart.

These data are the first to capture the beating amniote heart dynamically and provide a method for observing the torsional twist that appears as the heart develops from a straight tube to a c-loop. Previous results from the zebrafish have shown pump dynamics are different than what has been assumed. We can only assume this will also apply to the avian embryo. Future research will develop techniques for imaging through the entire quail heart, not just the ventral side, with cellular

resolution. This is a requirement for the development of a precise and complete model of the avian heart for more in-depth analysis, which can then be compared to the human heart.

## 3.4 Materials and Methods

### 3.4.1 Transgenic Quail

The transgenic quail line was created by injecting lentivirus encoding for tie1:H2B::eYFP into the blastoderm of freshly laid and un-incubated Japanese quail eggs following the protocol of Poynter and Lansford (2008). The G0 birds that successfully hatched were then bred to WT mates to screen for germline transmission. Once the individual transgenic lines were established, Tg(tie1:H2B::eYFP) offspring were crossed with other Tg(tie1:H2B::eYFP) to create homozygous transgenics for brighter imaging conditions.

### 3.4.2 Dynamic Imaging

Transgenic embryos were removed from the egg and placed ventral side down in a coverglass chamber (Chambered #1.0 Borosilicate Coverglass System, Lab-Tek, catalog #155380) for imaging on an inverted microscope. All imaging was done on a Leica TCS SP5 Confocal Microscope with resonant scanner for dynamic imaging at high speed using a 10x.0.4NA objective lens. To achieve a frame rate of approximately 40 fps, the scanned image was set to 512X256 pixels. The pinhole and gain were adjusted for optimal viewing at high frame rate, and collection of Z-depth was manually adjusted for every 5 um to achieve the specified overlap of optical slices for 4D reconstruction (Liebling *et al.*, 2005; Liebling *et al.*, 2006). Each

optical slice contained 5 seconds or approximately 200 frames to capture a minimum of two heartbeats. Total depth penetration was approximately 100 microns, which required about 20 optical sections.

### 3.4.3 Cell Tracking

Tracking was performed manually using the application Imaris (Bitplane).

## 3.5 References

Butler, J.K. An experimental analysis of cardiac loop formation in the chick. M.S. Thesis, University of Texas, 1952.

De la Cruz, M.V., Sanchez-Gomez, C., Palo-Mino, M.A., 1989. The primitive cardiac regions in the straight tube heart (Stage 9-) and their anatomical expression in the mature heart: an experimental study in the chick embryo. J. Anat. 165,121–131.

Fishman, M.C. and Chien, K.R., 1997. Fashioning the vertebrate heart: earliest embryonic decisions. Development 124, 2099-2117.

Forouhar, A. S., Liebling, M., Hickerson, A., Nasiraei-Moghaddam, A., Tsai, H., Hove, J. R., Fraser, S. E., Dickson, M. E., Gharib, M., 2006. The embryonic vertebrate heart tube is a dynamic suction pump. Science 312, 751-753.

Hamburger, V. and Hamilton, H.L., 1951. A series of normal stages in the development of the chick embryo. J. Morph. 88, 49-92.

Kidokoro, H., Masataka, O., Tamura, K., 2008. Time-lapse analysis reveals local asymmetrical changes in C-looping heart tube. Dev. Dyn. 237, 3545-3556.

Liebling, M., Forouhar, A.S., Gharib, M., Fraser, S.E., Dickinson, M.E., 2005. Four-dimensional cardiac imaging in living embryos via postacquisition synchronization of nongated slice sequences. J. Biomed. Opt. 10(5), 054001-10.

Liebling, M., Forouhar, A.S., Wooleschensky., R., Zimmermann., B., Ankerhold., R., Fraser., S.E., Gharib., M., Dickinson., M.E., 2006. Rapid three-dimensional imaging and analysis of the beating embryonic heart reveals functional changes during development. Dev. Dyn. 235(11), 2940-2948.

Manasek, F.J., Kulikowski, R.R., Fitzpatrick, L., 1978. Cytodifferentiation: a causal antecedent of Looping? Birth Defects 14,161-178.

Manner, J., 2000. Cardiac looping in the chick embryo: A morphological review with special reference to terminological and biomechanical aspects of the looping process. The Anatomical Record 259(3), 248-262.

Manner, J., 2004. On rotation, torsion, lateralization, and handedness of the embryonic heart loop: new insights from a simulation model for the heart loop of chick embryos. The Anatomical Record 278A, 481-492.

Manner, J., Seidl, W. and Steding, G., 1993. Correlation between the embryonic head flexures and cardiac development. An experimental study in chick embryos. Anat Embryol (Berl) 188, 269-285.

Manning, A. and McLachlan, J.D., 1990. Looping of chick embryo hearts in vitro. J. Anat. 168, 257-263.

Moreno-Rodriguez, R.A., Krug, E.L., Reyes, L., Villavicencio, L. Mjaatvedt, C.H. and Markwald, R.R., 2006. Bidirectional fusion of the heart-forming fields in the developing chick embryo. Dev. Dyn. 235, 191-202.

Patten, B.M., 1922. The formation of the cardiac loop in the chick. Am. J. Anat. 30, 373-397 .

Poynter, G. and Lansford, R., Avian Embryology. Methods in Cell Biology, 2nd edition. San Diego: Academic Press, 2008, pp. 281-293.

Sato, Y., Poynter, G., Huss, D., Filla, M., Czirok, A., Rongish, B., Little, C., Fraser, S., and Lansford, R., Dynamic analysis of vascular morphogenesis using transgenic quail embryos. Submitted.

Stalsberg, H. and DeHaan, R.L., 1969. The precardiac areas and formation of the tubular heart in the chick embryo. Dev. Biol. 19, 128-59.

Taber, L.A., 2006. Biophyical mechanisms of cardiac looping. Int. J. Dev. Biol. 50, 323-332.

Voronov,D.A., Alford, P.W., Xu, G., Taber, L.A., 2004. The role of mechanical forces in dextral rotation during cardiac looping in the chick embryo. Dev. Biol. 272, 339-350.

Voronov, D.A. and Taber, L.A., 2002. Cardiac looping in experimental conditions: the effects of extraembryonic forces. Dev. Dyn. 224, 413-421.

3.6 Figures

**Figure 1** Four-dimensional imaging: acquisition and reconstruction procedure. a) Sequential acquisition of two-dimensional slices (confocal microscopy) as a time-series at increasing depths of the beating heart. b) Direct reconstruction is not possible from the nongated data. c) Temporal alignment procedure d) Reconstruction.

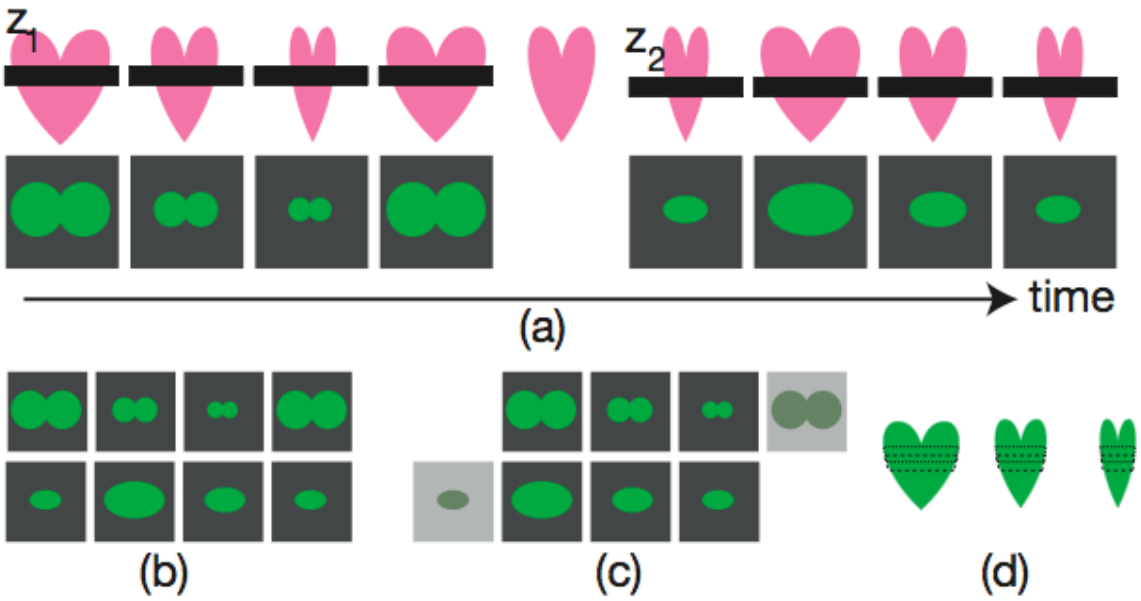

**Figure 2** Left panel shows the stage of the heart at HH9. Middle panel shows one frame of the data collected with the two layers of the heart outlined – red is the myocardium, green is the endocardium. Right panel shows a zoomed in view of the tracks created by Imaris with the data removed to give a clearer picture. Endocardial trajectories are approximately parallel to each other while myocardial trajectories become angled relative to each other along the length of the tube, which suggests a small amount of torsional twist is occurring.

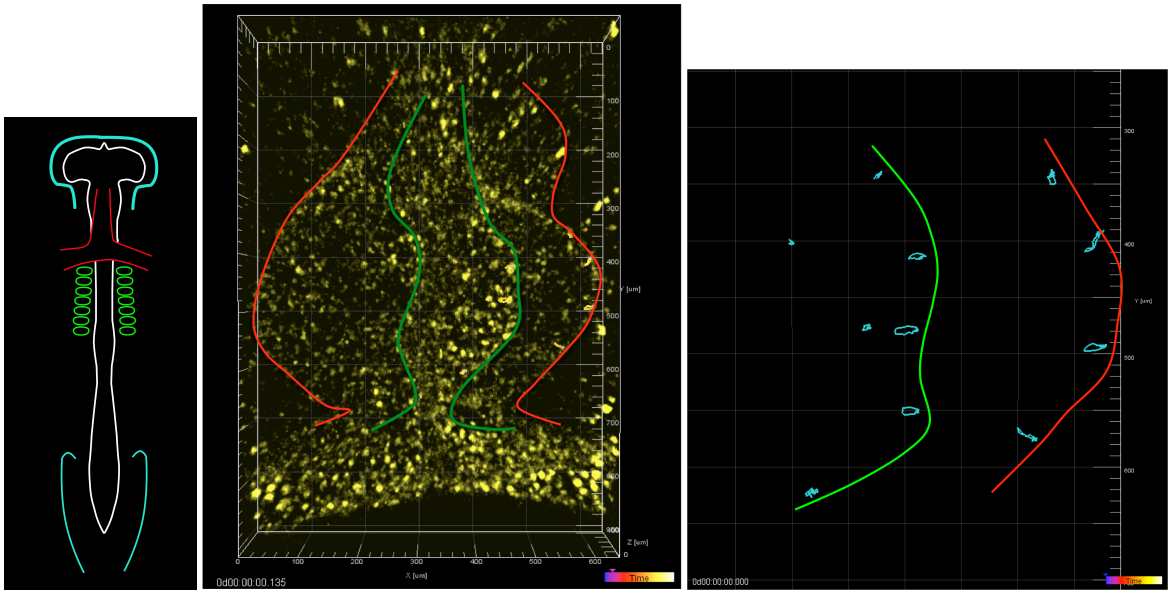

**Figure 3** Left panel shows the stage of the heart at HH10. Middle panel shows one frame of the data collected with the two layers of the heart outlined – red is the myocardium, green is the endocardium. Right panel shows a zoomed in view of the tracks created by Imaris with the data removed to give a clearer picture. Endocardial trajectories are approximately parallel to each other while myocardial trajectories become angled relative to each other along the length of the tube, which suggests a small amount of torsional twist is occurring.

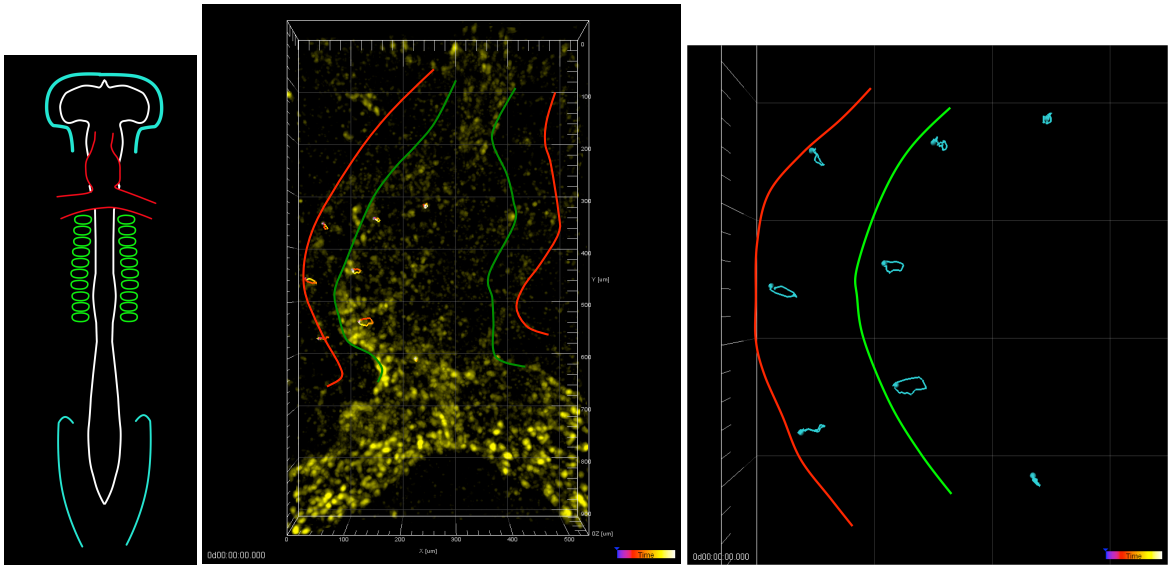

**Figure 4** Left panel shows the stage of the heart at HH11. Middle panel shows one frame of the data collected with the two layers of the heart outlined – red is the myocardium, green is the endocardium. Right panel shows the tracks created by Imaris with the data removed to give a clearer picture. The torsional twist can be observed in the endocardial layer.

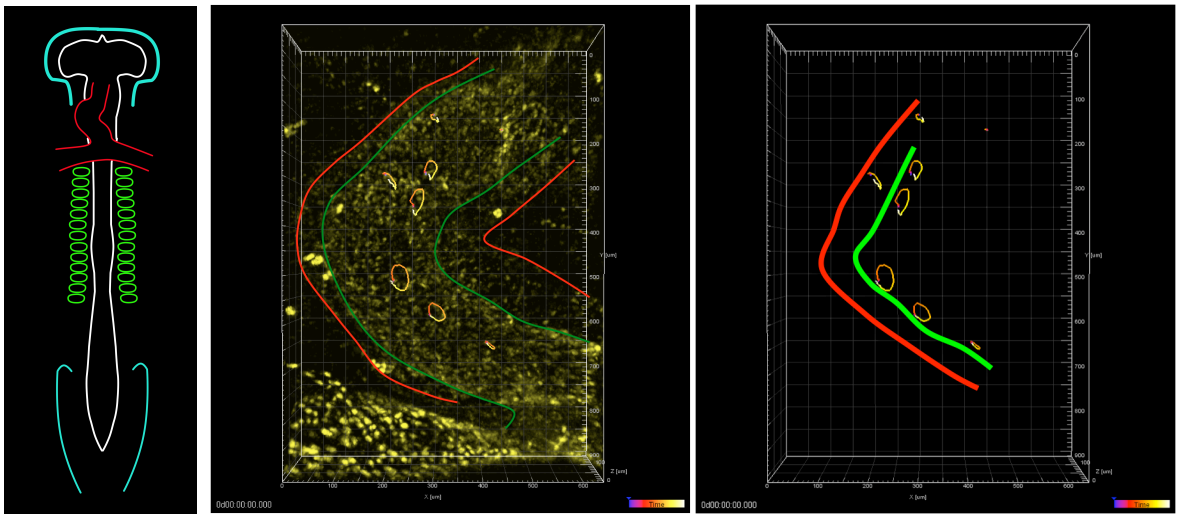

**Figure 5** Left panel shows the stage of the heart at HH12. Middle panel shows one frame of the data collected with the two layers of the heart outlined – red is the myocardium, green is the endocardium. Right panel shows the tracks created by Imaris with the data removed to give a clearer picture. The torsional twist can be observed in the endocardial layer.

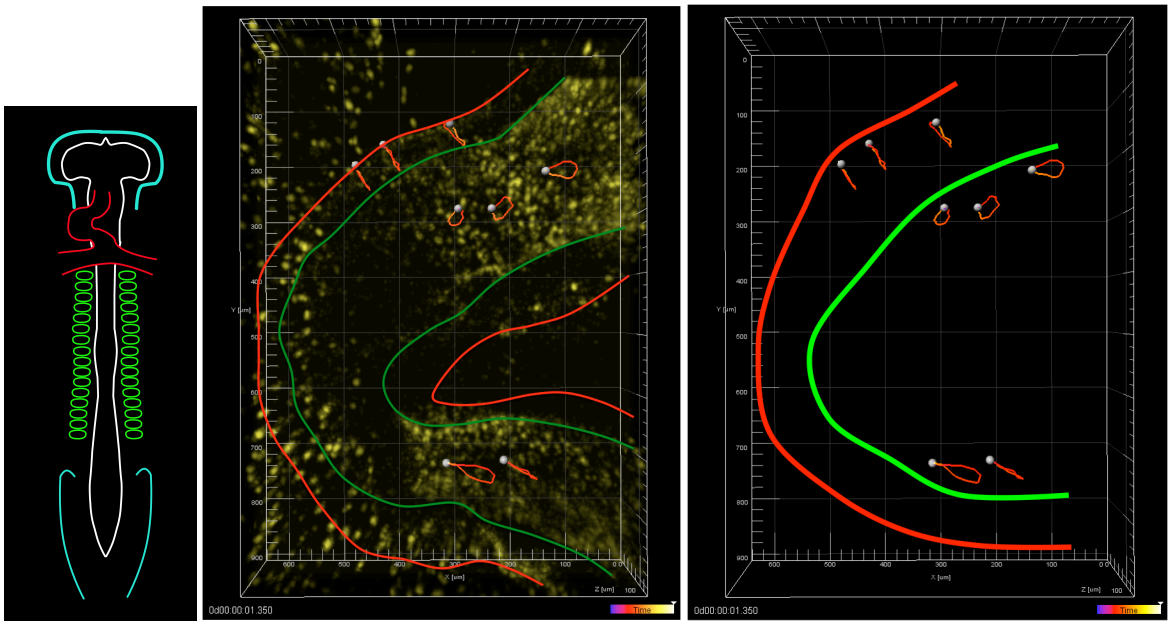

**Figure 6** The individual tracks of the myocardial and endothelial cells from figure 4 (HH11) are placed side by side to compare the amount of torsional twist involved along the length of the heart tube as dextral looping occurs. The two layers of the heart are outlined – red is the myocardium, green is the endocardium. A) Myocardial cells are tracked, B) Endocardial cells are tracked.

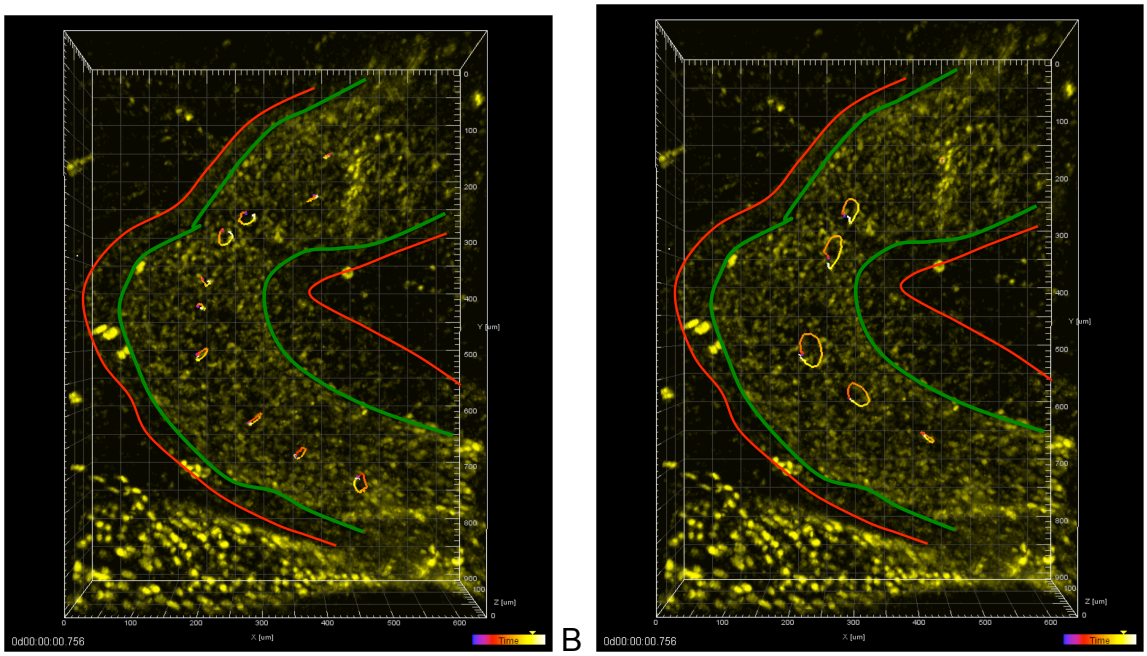

**Figure 7** A) Individual tracks of myocardial and endothelial cells are shown at different cross sectional sites along a stage HH11 heart. Red are myocardial tracks and green are endocardial tracks. The right panel is a zoomed in view of the tracks.

A 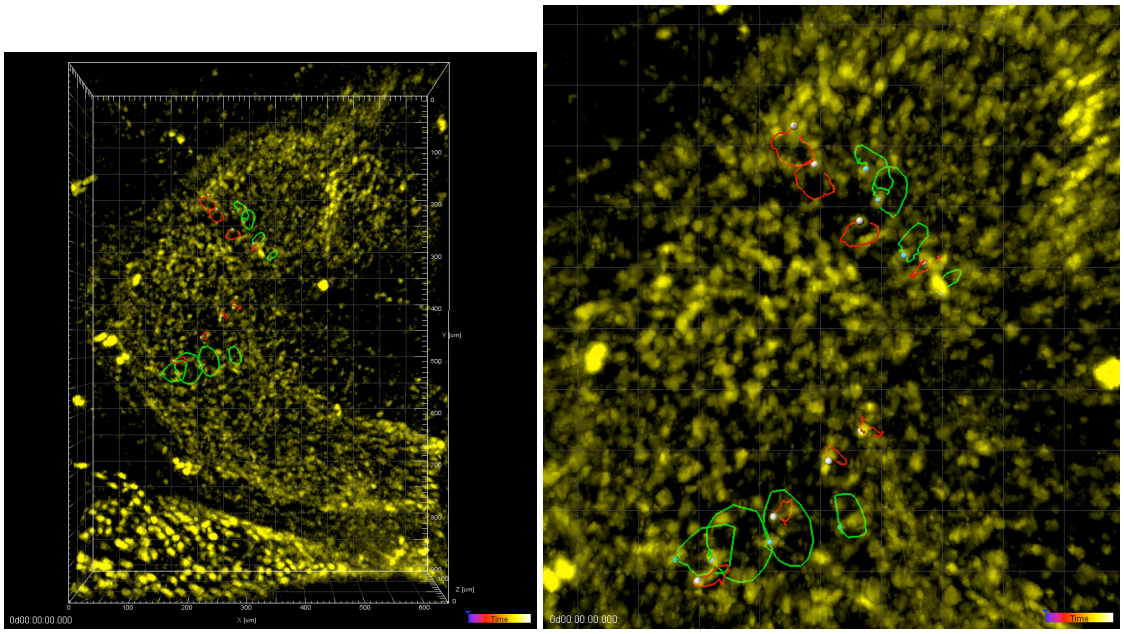

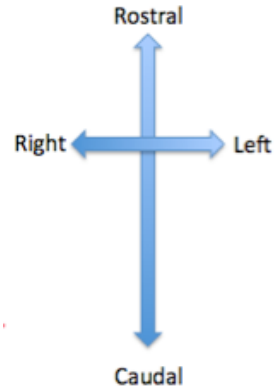

**Figure 7** B) Magnified view of a series of tracks showing the method for measuring the rotation angles. Timepoints were 1 (white), 11 (blue), 21 (purple), 31 (pink) and the rotation angle of the arrow as the cell moved cyclically was measured. Angles were then plotted for visual comparison.

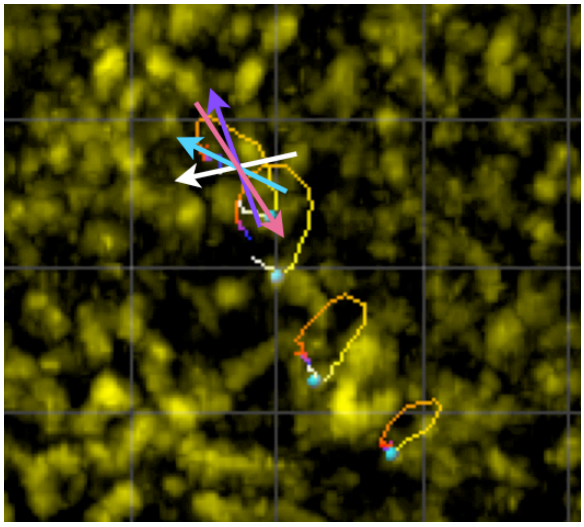

**Figure 7** C) Angles of rotation versus timepoint from individual cells in a beating stage HH11 heart were plotted for myocardial and endocardial cells in two specific regions. We see that the muscles beat asynchronously, implying that the electrical signal initiating contraction has some variation as it moves across cells. At the level of the endocardium, however, the asynchronicity is largely lost. This suggests that the cardiac jelly imparts a buffering action of the contractile wave from the muscle to the inner lining, thereby smoothing out the muscle contraction to make cross sectional regions beat in a synchronous manner.

Cross section of cells are shown by the following colors:


C

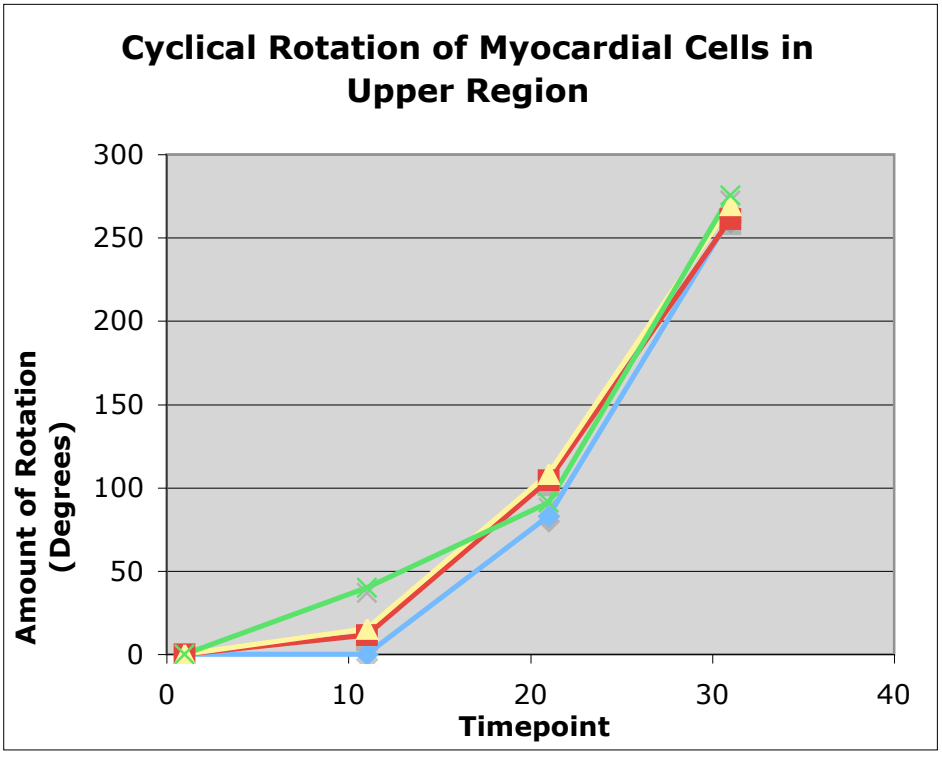

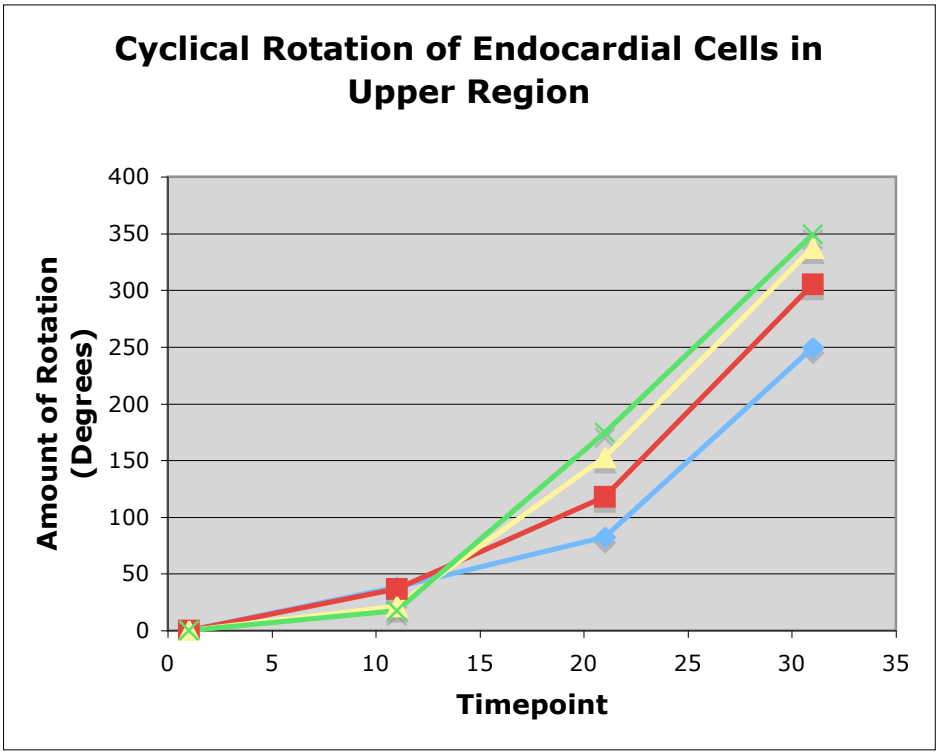
Cyclical Rotation of Endocardial Cells in Upper Region
Amount of Rotation (Degrees)
400
350
300
250
200
150
100
50
0
0
5
10
15
20
25
30
35
Timepoint

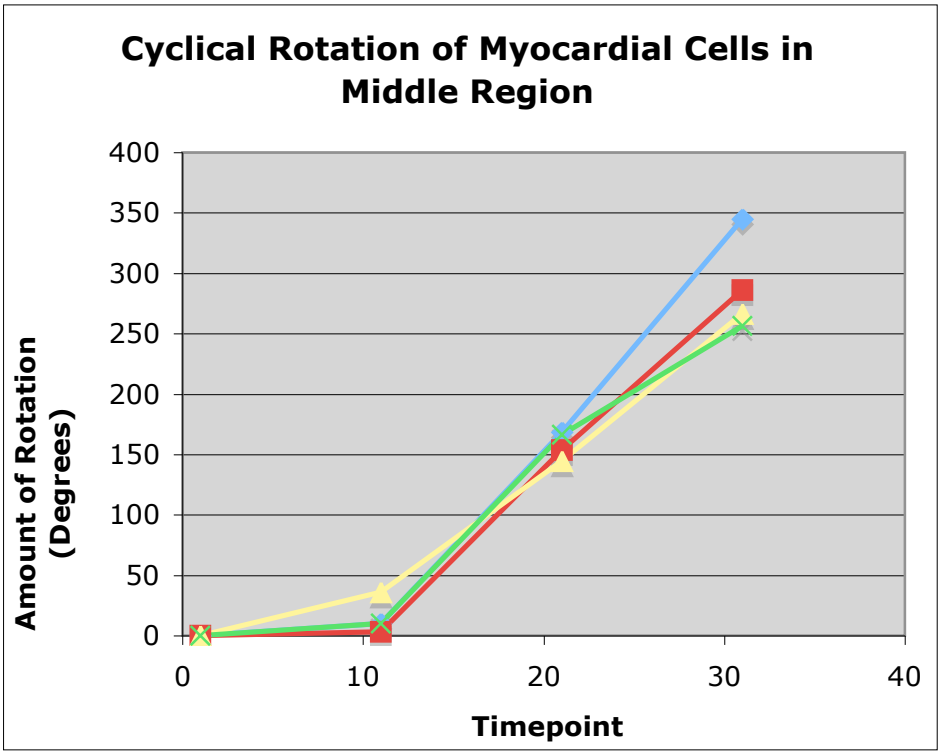
Cyclical Rotation of Myocardial Cells in Middle Region
Amount of Rotation (Degrees)
400
350
300
250
200
150
100
50
0
0
10
20
30
40
Timepoint

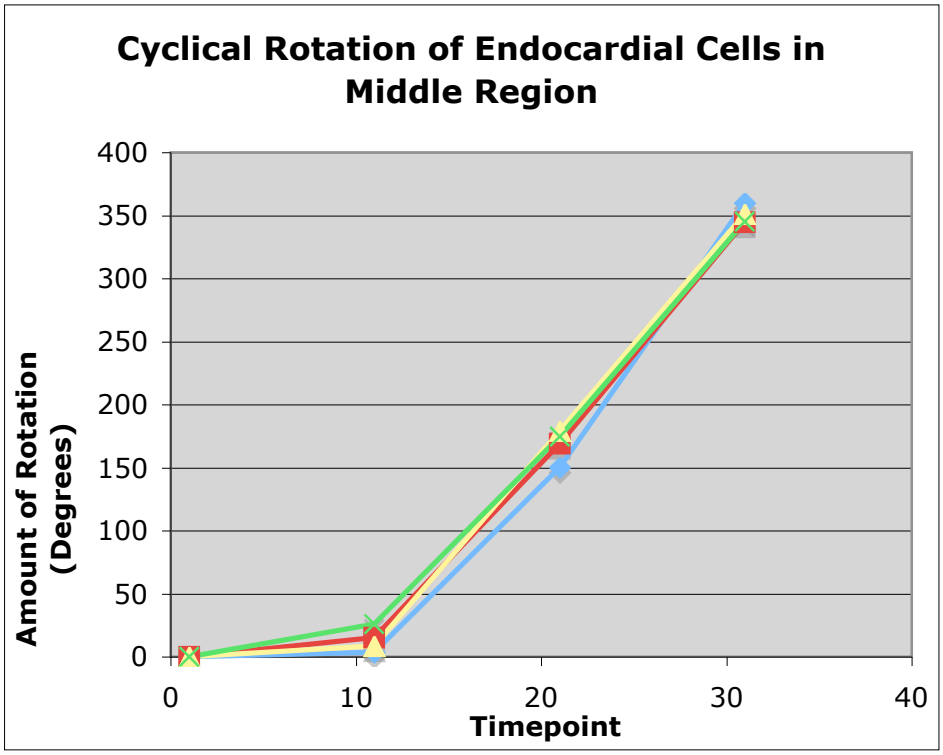
Cyclical Rotation of Endocardial Cells in Middle Region
Amount of Rotation (Degrees)
400
350
300
250
200
150
100
50
0
0
10
20
30
40
Timepoint

# Chapter 4

# Resolving cellular movements during heart tube formation and primitive looping with time-lapse microscopy of fluorescent quail

# Chapter 4: Resolving cellular movements during heart tube formation and primitive looping with time-lapse microscopy of fluorescent quail

## 4.1 Summary

Vertebrate heart morphogenesis is a complex process that integrates different tissues and cell types driven to interact by genetic and epigenetic factors. We have taken an interdisciplinary approach to studying heart formation by combining the power of molecular genetics with advanced optical imaging within living embryos. We have developed multiple transgenic quail lines and novel imaging methods that permit dynamic observation and manipulation of vascular development. Avian embryos are ideal for imaging due to the accessibility at all stages of development outside the vertebrate mother. These embryos also develop hearts with four chambers, allowing for meaningful comparisons to human hearts. Our results give a detailed fate map of heart morphogenesis with increased spatial and temporal resolution compared to current fate maps. We found that the left and right regions of the caudal portion of the heart tube do not intercalate and move by tissue mechanics. The upper portions of the heart tube are formed by cells already present in the primary heart field region during HH8, and form the heart tube by assembling at the midline. Cells migrating from the sinoatrial regions to the caudal portion of the heart tube complete the elongation of the tube. The myocardial cells then fuse around the outside of the endocardial cells to form a tube within a tube.

## 4.2 Introduction

Congenital heart defects affect ~1% of live births (reviewed by Srivastava, 2006). Yet the morphogenetic anomalies that occur during embryonic growth when the heart is still developing are poorly understood. To better understand the causes of congenital heart defects, it is crucial to understand how a healthy heart forms. Most of our current knowledge of cardiogenesis is achieved through fixed samples or still images. Previous research gives a clear anatomical view of the embryonic chick heart, which is similar to the human heart in that it loops to create four functional chambers with valves (Manner, 2000; Martinsen, 2005). This gives an inadequate picture as to the true nature of the live, beating heart as it pumps blood through the vasculature. The latest research is a time-lapse movie showing the progression of genetic markers involved in cardiogenesis from Hamburger-Hamilton stages 3 to 10 (Hamburger and Hamilton, 1951; Cui *et al.*, 2009).

Yet with all these recent discoveries, we still do not know the details of morphogenetic movements with any type of cellular resolution. The cardiac precursor cells of the mesoderm are derived during gastrulation from the cells that migrate through the primitive streak at HH4 (Garcia-Martinez and Schoenwolf, 1993). The paired heart-forming regions are located anteriorly in the lateral plate mesoderm at HH5-6 (Rawles, 1936). The plates then split into somatic and splanchnic epithelial layers to form the coelom (Linask, 1992). At HH8, the first physical appearance of the heart emerges when the bilateral areas of splanchnic

mesoderm merge in front of the developing foregut to form the cardiac crescent (Brand, 2003; Moorman and Christoffels, 2003). As the foregut extends, the primary heart fields begin to elongate to form the heart tube seen at HH9 (Stalsberg and DeHaan, 1969). The exact process of how the paired primary heart fields fuse during formation of the heart tube and the origin of these cells remains unknown.

The elongating heart tube is attached to the embryo through the ventral and dorsal mesocardium. As the heart tube loops dextrally to form the c-loop, both mesocardia rupture and the heart remains connected to the embryo only at the anterior and posterior limits (Noden, 1991). Dextral looping is the first physical manifestation of the breaking of left-right symmetry in the embryo. As the embryo develops further, looping extends farther to the right to continue the “c” shape and the heartbeat becomes stronger and more consistent. Beyond HH12, the chick embryo becomes much harder to image due to the increasing complexity of the heart as it continues looping and grows in size. The inclusion of secondary heart fields after initial tube formation remains a point of contention.

Recent advances in molecular biology and imaging have allowed us to develop new methods for modeling the early stages of cardiogenesis. A double transgenic quail was produced in which two types of cells were fluorescently labeled: the nuclei of the inner lining of the vasculature with YFP and the nuclei of cells with a ubiquitous PGK promoter with mCherry. This created a new line of birds in which the inner and outer layers of the heart are easily visualized in yellow and red, respectively.

## 4.3 Results

In figure 1, wholemount immunostainings show the location of cardiac muscle in relation to the developing embryonic heart from HH 8 to 11. This is used to correlate the location of muscle cells in figure 2. Figure 1A clearly show a crescent formation of cardiomyocytes developing just above the anterior intestinal portal (AIP). We can see that tissue differentiation has already begun by HH8, even though the endothelial cells have not formed a distinct vasculature. By HH9, figure 1B depicts a forming heart tube composed clearly of cardiomyocytes on the outside. The forming endocardium is merging just above the AIP region to extend out the inflow tracts of the heart. In figure 1C, the embryonic heart at HH10 has begun to loop slightly to the right, and here we can actually see the endocardium has formed on the inside of the heart tube, while the cardiomyocytes have entirely enclosed this region of the endocardium. The sinoatrial regions have formed distinct vessels now as the heart prepares to circulate blood cells through the embryo. Figure 1D gives a detailed image of the looped heart at HH11. We can see folds in the cardiac myocyte layer caused by dextral looping. Also, we see that the conus region of the heart has an extra outer layer of endothelial cells, probably to connect the heart to the connecting vessels of the vasculature.

Using figure 1 as a reference, the specific location of endothelial and cardiomyocytes can be located in reference to the developing heart (see figure 2). Four timelapse movies were collected of double transgenic quail embryos

Tg(tie1:H2B::eYFP) X Tg(pgk:H2B::mCherry) and analyzed (see Materials and Methods). Panels from one of the movies were lined up in sequential manner to show the development of the heart from crescent to c-loop (see figures 2A - 2E and 2K – 2O). By aligning these images with figure 1, the position of cardiomyocytes (red) and endothelial cells (green) was extrapolated (see figures 2F – 2J and 2P – 2T). This allows for visualization of the location of muscle cells during heart tube formation for cell tracking, which is shown in figures 4 and 5.

In figure 3, we have separated the stages of the heart to look at the movement patterns of the Tie1 and PGK cells during HH9, HH10, and HH11. In figure 3A and 3D, we see that both the endothelial cells and cardiomyocytes of the forming heart tube actually move in the cranial and medial direction. The cells in the sinoatrial regions, by contrast, move to the junction where the AIP meets the notochord. At the junction between the heart tube and inflow tracts, we see a separation in the direction of vectors, which shows the two regions are moving in different directions. In figures 3B and 3E, we see that there is still rapid movement of the endothelial cells in both the sinoatrial regions and the heart tube while it is looping. This contrasts to the image of the corresponding PGK cells where the sinoatrial regions have essentially stopped moving, while the cells in the heart tube region are following the same movements as the Tie1-labeled cells. Figures 3C and 3F, which correlate to HH11, show the extreme dextral motion of both the endothelial and cardiomyocytes of the looping heart as they move completely perpendicular to the notochord. Again, the difference appears in the sinoatrial regions where the

endothelial cells have directed motion to the junction between the heart tube and inflow tracts while the PGK cells move more randomly. These vectors show the behavior of populations of cells, and we wanted to follow up with showing the behavior of single cells residing in the presumptive upper ventricle and those that move from the inflow tracts to the presumptive lower ventricle.

In figure 4, as the heart tube is forming at HH9, the cells that comprise the presumptive upper ventricle migrate very little. The cells that become the endothelial and myocardial layers of the upper ventricle move from the lateral part to the midline to form the heart tube. As the tube coalesces and begins the c-loop, the cells stay grouped together very closely.

On the other hand, the presumptive lower ventricle begins in a very different position compared to the upper ventricle, while both end up in neighboring regions. The cells forming both the myocardium and endocardium of the presumptive lower ventricle actually begin their migration extending from the far regions of the sinoatrial regions (see figure 4A). As these cells move medially (see figure 4B), they continue on a path that brings them into inner endocardial regions of the heart tube at HH9, then they continue upwards and outwards into the C-loop at HH10 (see figure 4C). In the looped heart, we see that these cells stay tightly packed with their neighbors as they begin to form the lower ventricle of the heart tube (see figure 4D).

Individual cells in the far right and left sinoatrial regions are marked with blue and orange spots, respectively (see figure 5A). They begin migrating medially to just above the anterior intestinal portal and below the fully formed heart tube at late stage HH9 (see figure 5B). As the embryo progresses into stage HH10, we see these cells form two distinct sheets at the midline while they migrate together into the presumptive lower ventricle (see figure 5C). Hours later, as these cells continue to migrate upwards and inwards into the looping heart tube, the individual cells of the left and right sides of the original sinoatrial regions still have not crossed paths even after extension of the heart tube (see figure 5D).

Developmentally, the myocardial and endocardial cells originate in the cardiac crescent and move medially as the heart tube forms during HH9. The myocardial cells (pink and yellow) remain on the outside regions of the tube while the endocardial cells (purple and white) enter the inner tube. The process of tube formation occurs as the endothelial cells in the sinoatrial regions progress to the midline. They move cranially, passing the base of the heart tube, while becoming enclosed by the myocardial walls. This is the first time that the cellular dynamics of heart tube formation have been observed in an amniote.

## 4.4 Discussion

The mechanism underlying the developing embryonic heart has eluded scientists for centuries. As data emerged, it was determined that the heart progenitor cells begin at bilateral positions to the midline and in most species, will form the cardiogenic crescent (Stalsberg and DeHaan, 1969).

From these timelapse images taken using the double transgenic quail, we have produced a detailed fate map of heart development in an avian embryo for the stages of development from HH8-12, which can be used to determine the mechanism underlying tube formation and the source of cells during the early stages of heart looping.

The data presented show clearly that the upper portions of the heart tube are formed by cells already present in the primary heart field region during HH8, and they assemble at the midline, coalescing to form the heart tube. The lower region of the heart tube is formed during HH9 by cells migrating from the sinoatrial regions to the bottom portion of the heart tube while the myocardial cells fuse on the outside to form a tube within a tube. As the embryo progresses from HH10 to HH11, more cells migrate medially and cranially adding cells to the tube as it lengthens to begin the looping process.

Following the cells in the time-lapse experiment, we can actually see that cell cycle time is approximately 14 hours and that there is not an abundance of cell divisions during this period of rapid development in the heart region. This is consistent with the conclusion that cells in the heart migrate there from other regions of the embryo and do not divide at accelerated rates to form the heart tube, as was observed by Stalsberg (1969, 1970).

From these time-lapse images of our experiments, we observed how closely cells follow their neighbors as they move from the sinoatrial regions into the heart tube. At the same time, the left and right regions of the caudal portion of the heart tube do not intercalate at all and maintain neighbor relations, suggesting sheet-like behavior and not individual cell migration is the driving force behind tube formation.

The movement patterns of the cardiac cells show that myocardial and endocardial cells have predestined fates by HH8. Unfortunately, the fluorescence of Tie1 transgenics can not yet be viewed before this stage due to low levels of protein production. With better optics in the near future, the developmental timing of cardiac cell differentiation may be possible.

The formation of the heart tube progresses in an orderly manner. The cells closest to the midline move the farthest cranially in the heart tube (upper ventricle) while the cells located more laterally contribute to later developing structures (lower ventricle and presumptive atria). Fusion of the endocardium and myocardium occurs at the

base of the tube first when the endothelial cells begin involuting into the tube and become enclosed by myocardial cells.

The aforementioned cellular dynamics involve just the primary heart fields. The secondary heart fields begin their contribution from the conus region at the outflow tract, continuing the extension and development of the heart tube in a caudal direction. Extending the timelapse imaging to stages HH14 and beyond while focused in the conus region will give a detailed, dynamic fate map of the contributions of the secondary heart fields.

Much has already been revealed by these detailed time-lapse movies and immunostainings, but more analysis can be done. Much of the tracking was done manually using software designed for cell tracking. Unfortunately, it was not optimized for multispectral 4-dimensional data sets with an abundance of cells. With more sophisticated tracking algorithms and new software, more can be concluded from these datasets.

## 4.5 Materials and Methods

### 4.5.1 Transgenic Quail Embryos

Two lines of transgenic quail were created by injecting lentivirus encoding for tie1:H2B::eYFP and pgk:H2B::mCherry into the blastoderm of freshly laid and un-

incubated Japanese quail eggs following the protocol of Poynter and Lansford (2008). The G0 birds that successfully hatched were then bred to WT mates to screen for germline transmission. Once the individual transgenic lines were established, a Tg(tie1:H2B::eYFP) was crossed to a Tg(pgk:H2B::mCherry) to produce offspring with a 25% chance of being a double transgenic, e.g. Tg(tie1:H2B::eYFP) x Tg(pgk:H2B::mCherry).

### 4.5.2 Ex ovo Culturing

Embryos were removed from the egg using a square piece of filter paper with a hole punched out of the middle. This was placed over the embryo and the edges of the filter paper were cut to clamp the membranes to the filter paper. The filter ring and embryo was then slowly lifted off the yolk with forceps and placed in Ringer's solution (Appendix) to remove excess yolk. The embryo was then moved to a coverglass chamber (Chambered #1.0 Borosilicate Coverglass System, Lab-Tek, catalog #155380) coated with semi-solid agarose (Chapman *et al.*, 2001) modified with the addition of 3% glucose.

### 4.5.3 Live Embryo Microscopy

Images were taken using a Zeiss 510 Confocal Laser Scanning Microscope with a 20x Plan-Apochromat 0.8 NA objective lens. The microscope stage was enclosed in plexiglass with a heater to create a thermostable environment of 37 degrees Celsius

for the explanted embryo. The MultiTime macro on the AIM software of Zeiss was used to collect an image composed of 6 tiles arranged in a 3X2 pattern with no overlap. The optical slice was 12 um. Tiled images were collected to create a full image approximately every 8 minutes.

Z-stacks were taken with an interval of 6.0 um, with a total stack size of 120.0 um. YFP fluorescence was excited at 488 nm (12% laser power of a 25 mW Argon laser) and detected through a 505-550 nm bandpass emission filter. Red fluorescence was excited at 561 nm (15% power of a 15 mW laser) and detected through a 575 nm longpass emission filter.

Confocal data were concatenated using Zeiss LSM Image Examiner and post-processed using the application Imaris (Bitplane).

4.5.4 Wholemount Immunostaining

Embryos at the proper HH stage were fixed in 4% paraformaldehyde for 2-3 hours at room temperature. Embryos were rinsed 3 times in PBST (phosphate buffered saline with 0.5% Triton X-100) for 10 minutes each. During these rinses, embryos were removed from the filter rings. After blocking in 5% goat serum in PBST for 1 hour, embryos were incubated in a solution of MF20 (1:10 dilution) and QH1 (1:1000 dilution) antibodies overnight at 4 degrees C, both obtained from the Developmental Studies Hybridoma Bank of the University of Iowa (Moreno-Rodriguez *et al.*, 2006;

Finkelstein and Poole, 2003). Embryos were rinsed again 3 times for 15 minutes each in PBST and blocked for 15 minutes at room temperature. The embryos were then soaked in a cocktail of blocking solution and anti-mouse IgG1-Alexa 488 goat antibody and anti-mouse IgG2b-Alexa 568 for 2 hours at room temperature and rinsed with large amounts of PBST at least 3 times for 15 minutes each.

4.5.5 Fixed Embryo Imaging

Images were taken using a Zeiss 510 Confocal Laser Scanning Microscope with a 20x Plan-Apochromat 0.8 NA objective lens. The optical slice was 6 um.

Z-stacks were taken with an interval of 3.0 um, with a total stack size of 100.0 um. Alexa Fluor 488 (Invitrogen) was excited at 488 nm (15% laser power of a 25 mW Ar laser) and detected through a 505-550 nm bandpass emission filter. Alexa Fluor 568 (Invitrogen) was excited at 543 nm (50% power of a 1 mW He/Ne laser) and detected through a 560 nm longpass emission filter.

Confocal data were concatenated using Zeiss LSM Image Examiner and post-processed using the visualization software Imaris (Bitplane).

## 4.6 References

Brand, T., 2003. Heart development: molecular insights into cardiac specification and early morphogenesis. Dev. Biol. 258, 1-19.

Chapman, S.C., Collignon, J., Schoenwolf, G.C., Lumsden, A., 2001. Improved method for chick whole-embryo culture using a filter paper carrier. Dev. Dyn. 220, 284-289.

Cui, C., Cheuvront, T.J., Lansford, R.L., Moreno-Rodriguez, R.A., Schultheiss, T.M. and Rongish, B.J., 2009. Dev. Biol. 332, 212-222.

Developmental Studies Hybridoma Bank

Finkelstein, E.B. and Poole, T.J., 2003. Vascular endothelial growth factor: a regulator of vascular morphogenesis in the Japanese quail embryo. The Anatomical Record 272A, 403-414.

Garcia-Martinez, V. and Schoenwolf, G.C., 1993. Primitive streak origin of the cardiovascular system in avian embryos. Dev. Biol. 159, 706-719.

Hamburger, V. and Hamilton, H.L., 1951. A series of normal stages in the development of the chick embryo. J. Morph. 88, 49-92.

Linask, K.K., 1992. N-cadherin localization in early heart development and polar expression of Na+, K(+)-ATPase, and integrin during pericardial coelom formation and epithelialization of the differentiating myocardium. Devl. Biol. 151, 213-224.

Manner, J., 2000. Cardiac looping in the chick embryo: A morphological review with special reference to terminological and biomechanical aspects of the looping process. The Anatomical Record 259(3), 248-262.

Martinsen, B.J., 2005. Reference guide to the stages of chick heart embryology. Dev. Dyn. 233, 1217-1237.

Moorman A.F. and Christoffels, V.M., 2003. Cardiac chamber formation: development, genes and evolution. Physiol Rev. 83, 1223-1267.

Moreno-Rodriguez, R.A., Krug, E.L., Reyes, L., Villavicencio, L. Mjaatvedt, C.H., Markwald, R.R., 2006. Bidirectional fusion of the heart-forming fields in the developing chick embryo. Dev. Dyn. 235, 191-202.

Noden, D.M., 1991. Origins and patterning of avian outflow tract endocardium. Development 111, 857-861.

Poynter, G. and Lansford, R., Avian Embryology. Methods in Cell Biology, 2nd edition. San Diego: Academic Press, 2008, pp. 281-293.

Rawles, M. A., 1936. A study in the localization of organ forming areas of the chick blastoderm of the head process stage. J. Exp. Zool. 72, 559-568.

Sato, Y., Poynter, G., Huss, D., Filla, M., Czirok, A., Rongish, B., Little, C., Fraser, S., and Lansford, R., Dynamic analysis of vascular morphogenesis using transgenic quail embryos. Submitted.

Srivastava, D., 2006. Making or breaking the heart: from lineage determination to morphogenesis. Cell 26, 1037-1048.

Stalsberg, H., 1969. Regional mitotic activity in the precardiac mesoderm and differentiating heart tube in the chick embryo. Dev. Biol. 20, 18-45.

Stalsberg, H. and DeHaan, R.L., 1969. The precardiac areas and formation of the tubular heart in the chick embryo. Dev. Biol. 19, 128-59.

Stalsberg, H., 1970. Mechanisms of dextral looping of the embryonic heart. Am. J. Cardiol. 25, 265-271.

4.7 Figures

**Figure 1** Wholemount immunostainings showing the heart at different stages of development. The red is the antibody MF20 that binds to the sarcomeres of the myosin heavy chain in the cardiac muscle. The green is the antibody QH1 that binds to endothelial cells. A) HH8, B) HH9, C) HH10, D) HH11. Scale bar in the lower right corner is 100 um for all images. The anatomy of the heart muscles and inner lining are very clear for the four stages as tube formation occurs.

Figure 1A:

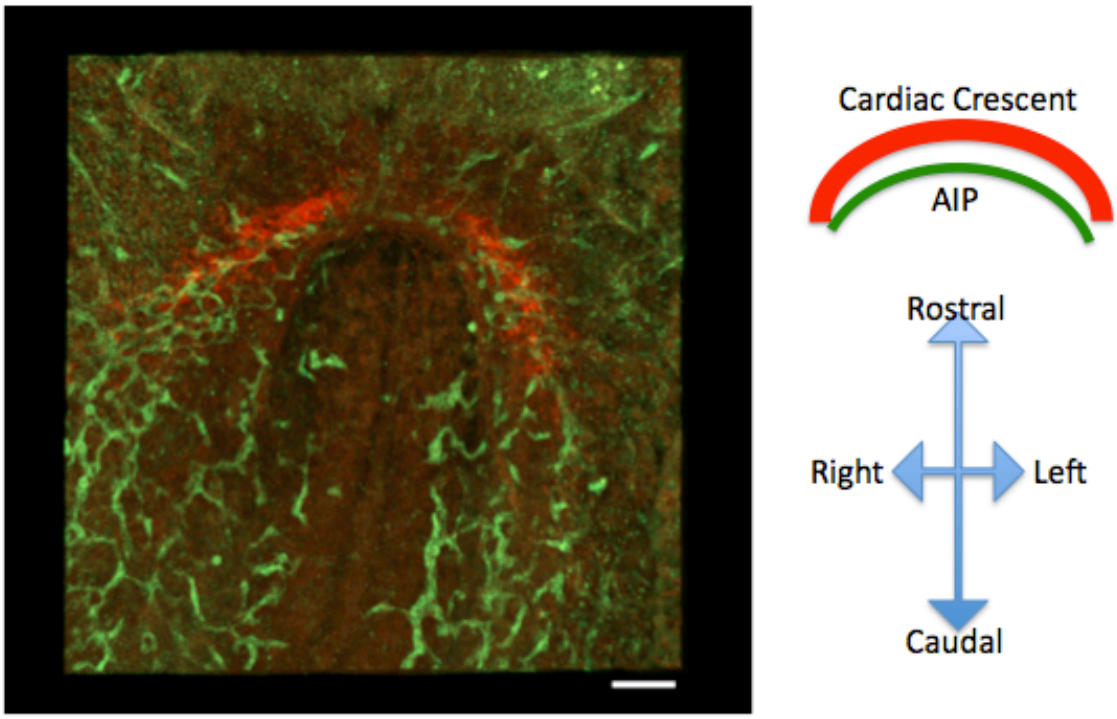

Figure 1B:

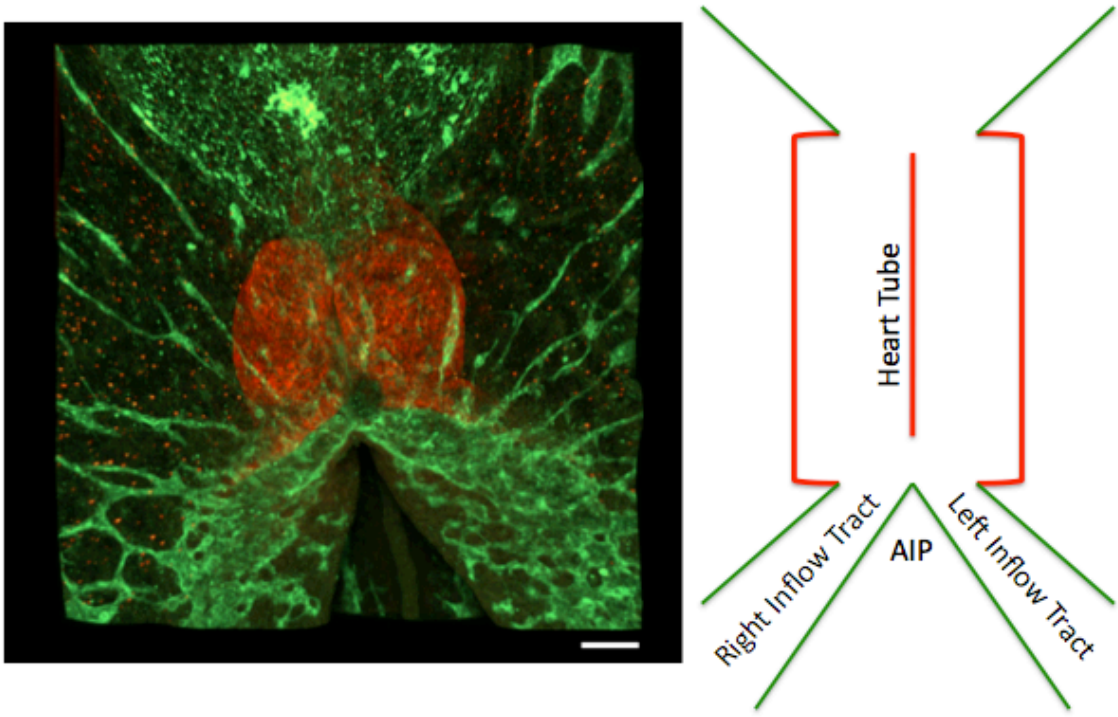

Figure 1C:

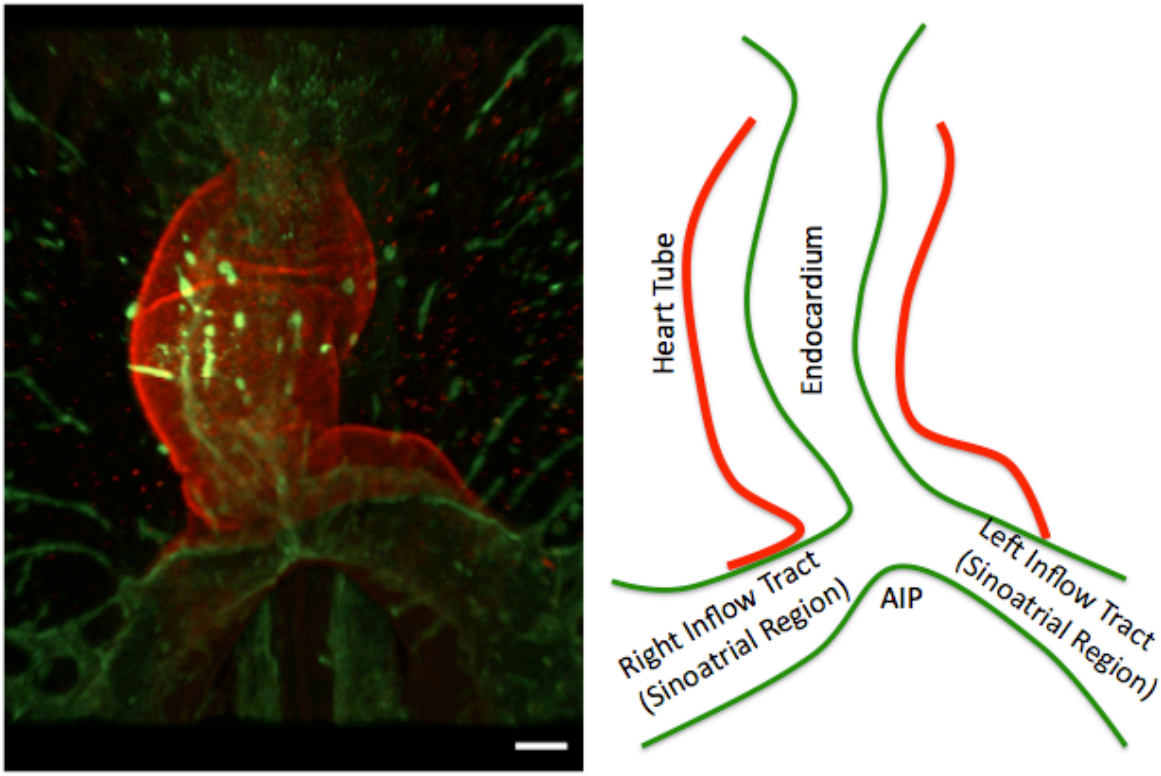
Heart Tube
Endocardium
Right Inflow Tract
(Sinoatrial Region)
AIP
Left Inflow Tract
(Sinoatrial Region)

Figure 1D:

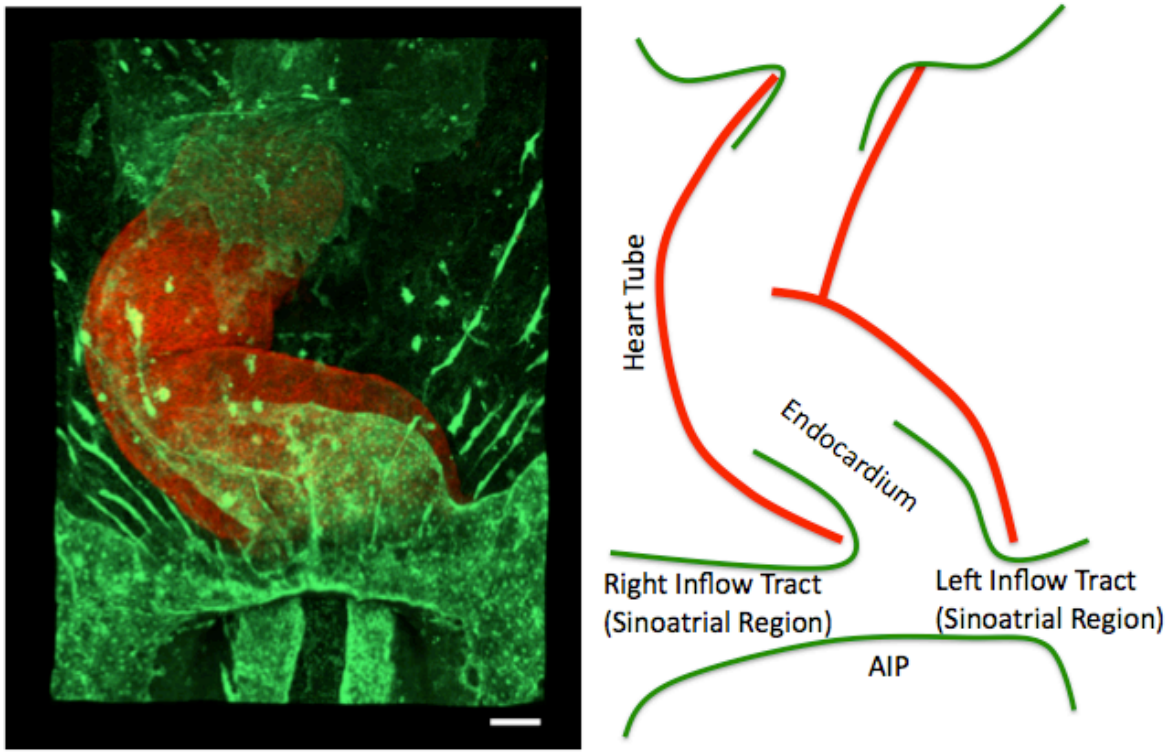
Heart Tube
Endocardium
Right Inflow Tract
(Sinoatrial Region)
Left Inflow Tract
(Sinoatrial Region)
AIP

**Figure 2** The specific location of endothelial and cardiomyocytes can be located in reference to the developing heart. Panels A-E and K-O are from a timelapse movie of the developing heart of a double transgenic embryo from HH8 – HH11 [Tg(tie1:H2B::eYFP) X Tg(pgk:H2B::mCherry)]. By aligning these images with those of figure 1, the position of cardiomyocytes (red) and endothelial cells (green) was extrapolated to create panels F-J and P-T. This allows for visualization of the location of muscle cells during heart tube formation for cell tracking.

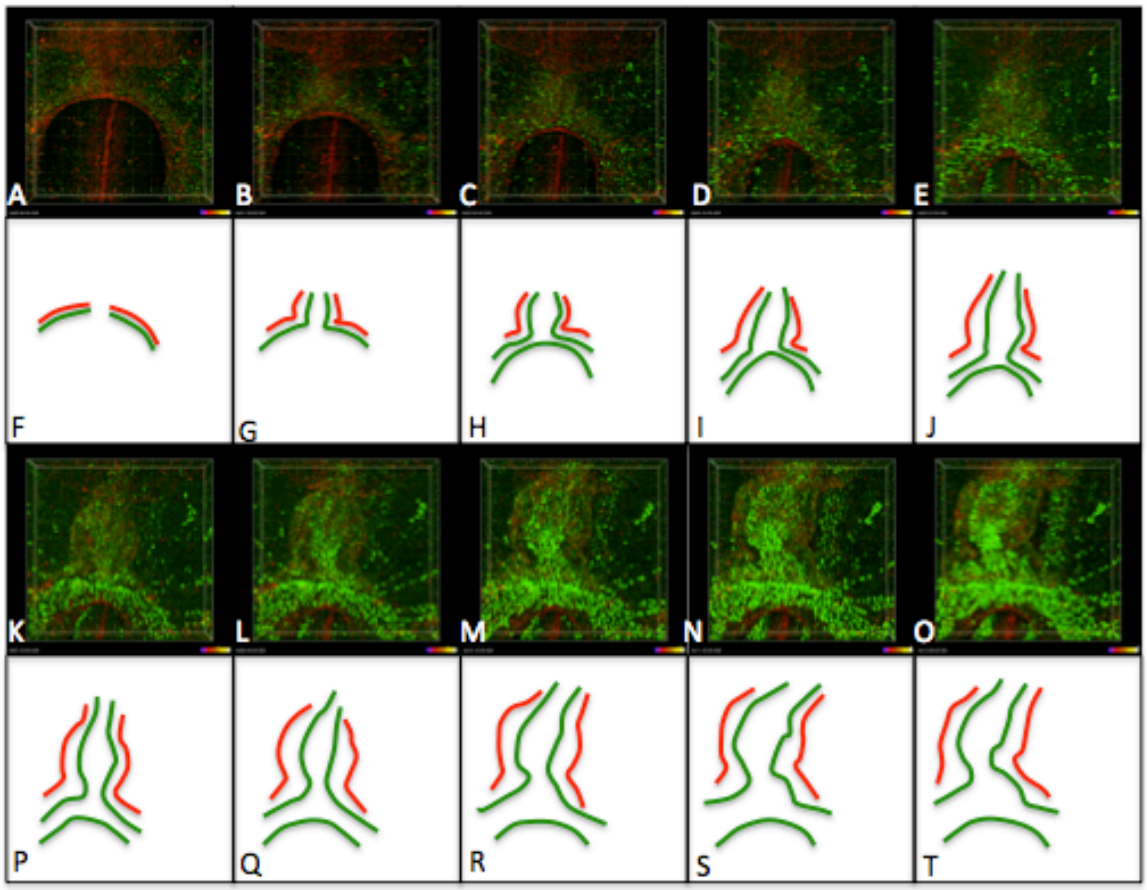

**Figure 3** Vectors showing the group movement of cells for different stages of development. Yellow arrows show the movement of endocardial cells, blue arrows show the movement of myocardial cells. A, D) HH9 – movement happens medially for both layers, B, E) HH10 – directed movement for different regions, C, F) HH11 – movement is focused on looping.

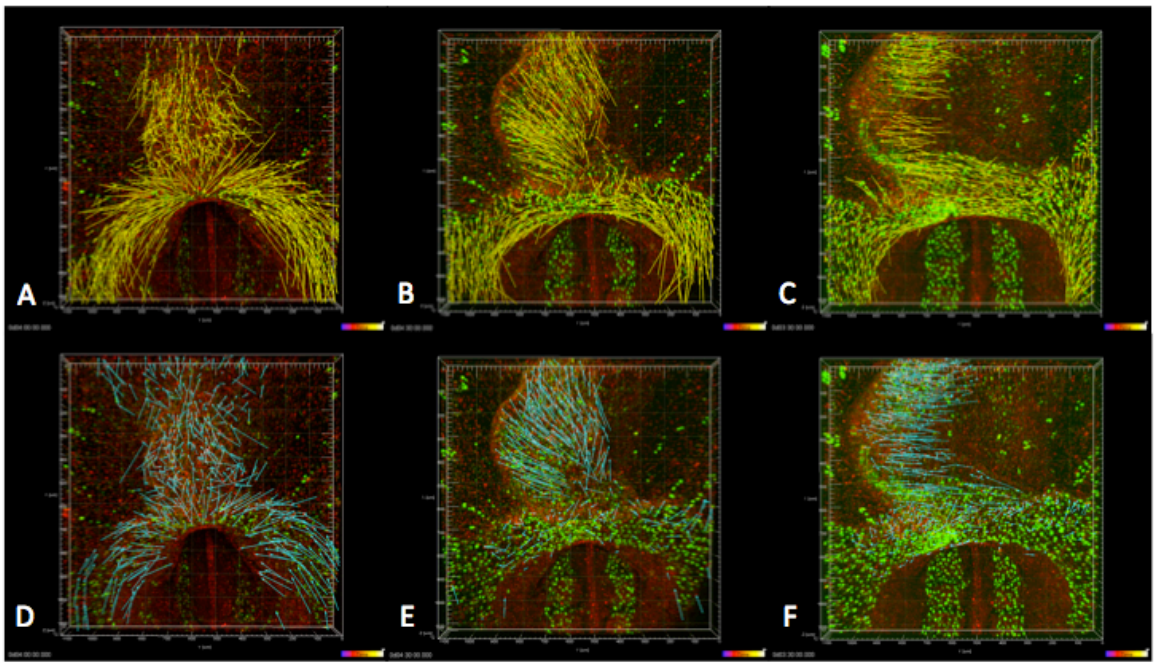

**Figure 4** Cell tracking using Imaris to follow individual movement and create a fate map of the upper and lower ventricles. Pink is the presumptive upper ventricle myocardium, purple is the presumptive upper ventricle endocardium, yellow is the presumptive lower ventricle myocardium, and white is the presumptive lower ventricle endocardium. A) HH8, B) HH9, C) HH10, D) HH11. Lower ventricular cells come from the sinoatrial regions during heart tube formation.

A

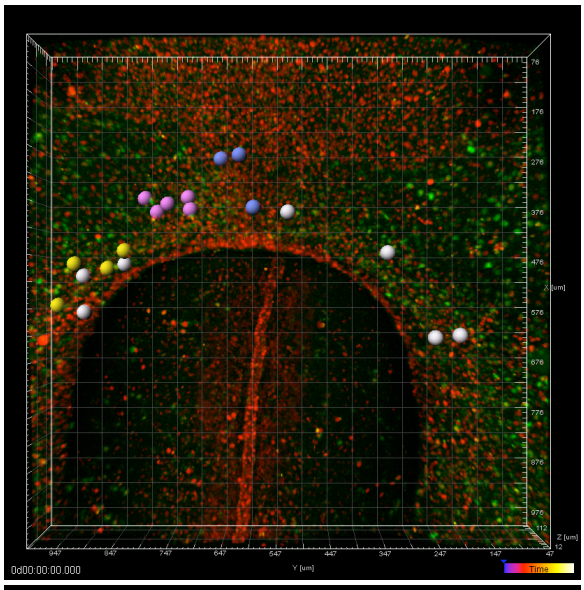


B

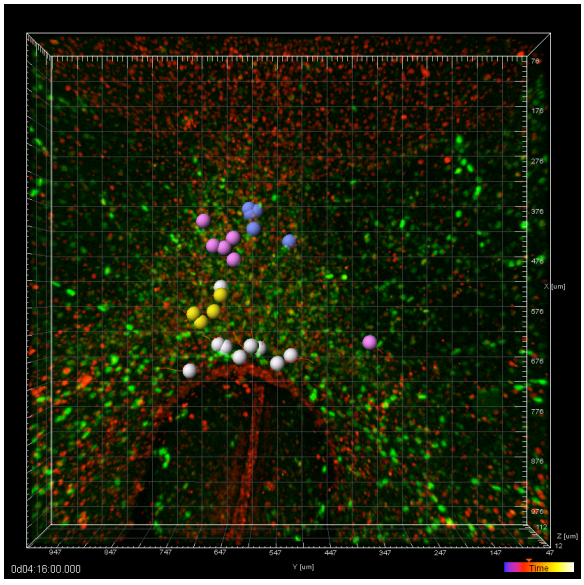

C 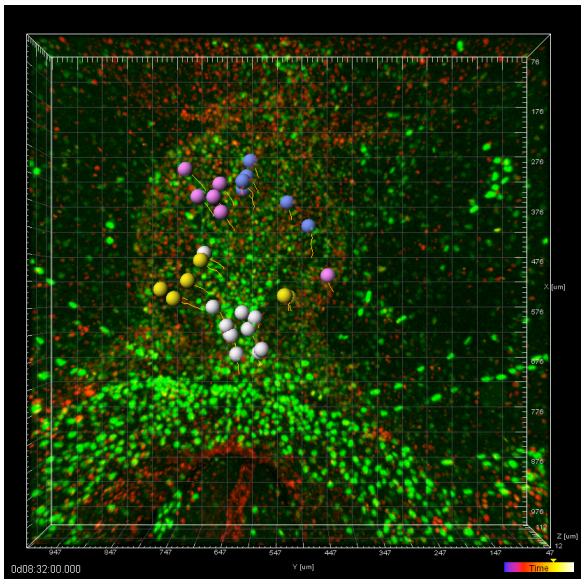


D 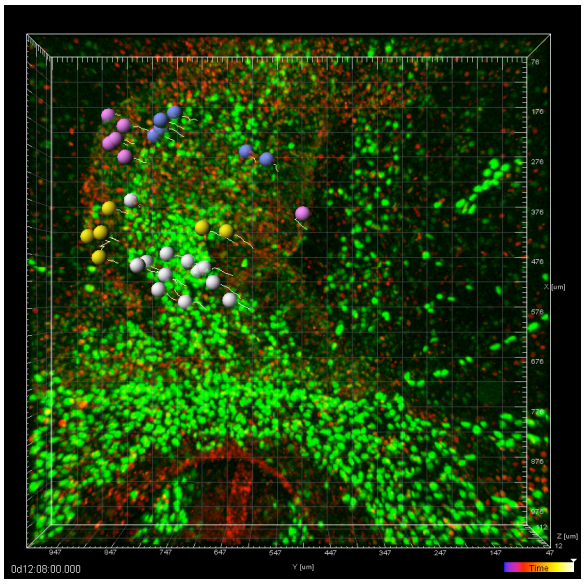

**Figure 5** Cell tracking using Imaris to follow individual movement and create a fate map of the cells migrating from the sinoatrial regions to the midline. Blue is the right sinoatrial region and orange is the left sinoatrial region. A) HH8, B) HH9, C) HH10, D) HH11. Cells from the different sides to not mix and maintain their neighbor relations, suggesting sheet-like behavior during heart tube formation.

A

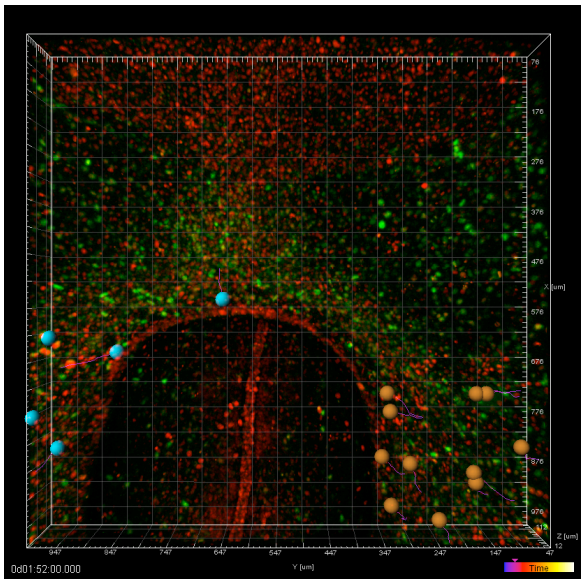


B

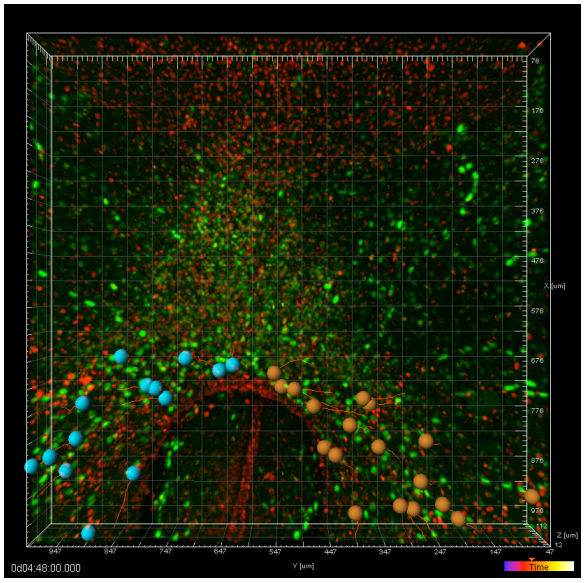

C

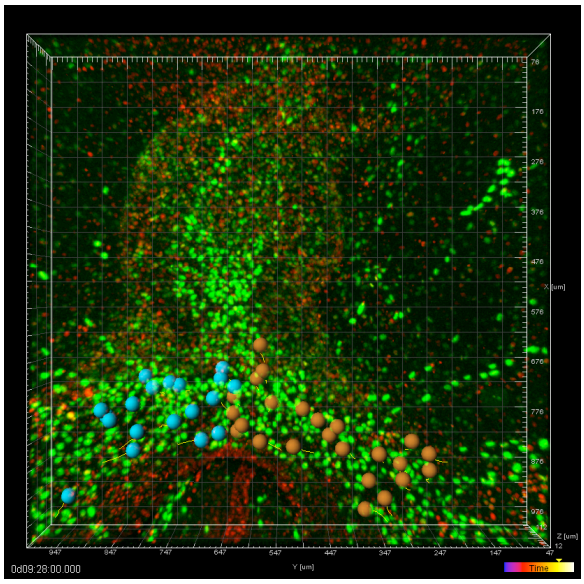


D

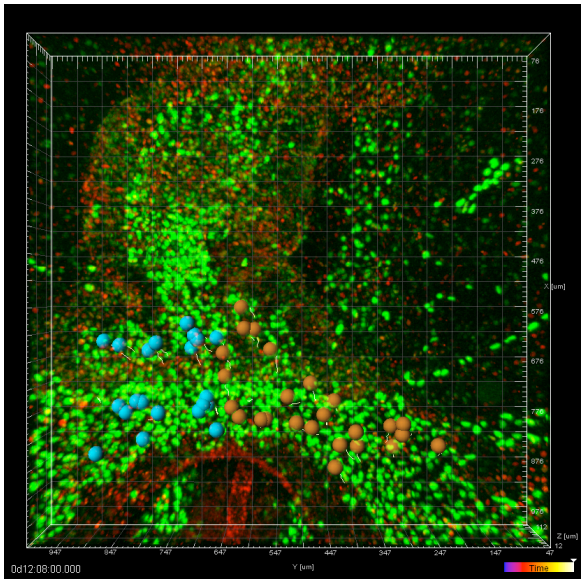

# Chapter 5

# Conclusion

# Chapter 5: Conclusion

We have shown that it is possible to quantify the biological process of cardiogenesis in amniotes and to create a detailed fate map with cellular resolution, both of which will help in the identification of congenital heart defects at an earlier stage in humans. These processes require many of the latest biological, imaging, and computational tools that were not previously available to scientists. The transgenic quail have been especially essential because they allow us to make use of the developmental advantages of the avian system while also giving us the genetic tools prized in other non-avian vertebrates.

Analyses of heart wall motion during contraction and relaxation during heart tube formation and primitive looping provide quantifiable parameters for determining proper heart development at early stages. The data confirm the material composition of the heart tube as described by Loumes *et al.* (2008) as a 2-layer-fluid-filled elastic tube with a thick gelatinous interior.

The high-speed capture of heart contractions and four-dimensional reconstructions at different morphological developmental stages provide a novel view of an amniote heart. The variations in tube formation and cell motions are easily mapped during each contraction. The only comparable research was performed by Liebling *et al.* (2006) in zebrafish, which identified pump mechanics in the two-chambered fish heart. This research, in collaboration with Liebling, determined that the mechanistic

purpose of cardiac jelly is to buffer the mechanical signal from the myocardium to the endocardium.

Lastly, a positional fate map of the cells from the cardiogenic crescent that contribute to heart tube formation and primitive dextral looping was generated by following the nuclei of myocardial and endocardial cells over time. Previous research had used localized injections of carbofluorescein dye with images taken every few hours to study cell migration (Moreno-Rodriguez *et al.*, 2006). The dye experiments did show medial movement of cells during tube formation but mistakenly recorded cellular movement as both cranial and caudal during tube elongation. Unfortunately, the dye labeled multiple tissue layers, making identification of individual cell movement impossible.

Recently, fixed sections of the elongating heart tube were scanned and reconstructed computationally (Abu-Issa and Kirby, 2008), but these also lacked cellular resolution and depended on extrapolation of movement based on changes in anatomical structure. These reconstructions were supplemented with timelapse images of embryos injected with DiO. Though the computer-animated reconstructions were very elaborate, the DiO labeled the majority of the embryo and did not provide extra information. Based on these reconstructions, the authors claimed tube elongation occurred through simple medial fusion due to caudal extension of the foregut.

The most recent study was done at higher resolution, electroporating fluorescent protein into early stage embryos and tracking the spots using time-lapse imaging (Cui *et al.*, 2009). In these images, the authors claim tissue convection and not cell migration is the mechanism of tube formation as the mesoderm “rolls-up.”

All these proposed theories of the motion occurring during heart tube formation and elongation during stages HH9-10 do not tell the whole story. The data presented in this thesis looked at all cells on the ventral surface of the embryo. With a temporal resolution of eight minutes, the timelapse movie of tube formation presented a view of cellular movement that has not been seen before. The results show that at the rostral end of the heart tube, the cells are stationary while cranial tissue movement lengthens the tube at the caudal end. In addition, individual cell migration in sinoatrial regions contributes cells to the tissue that forms the presumptive left ventricle of the heart tube.

These studies required an extensive and multi-faceted research approach due to the interdisciplinary aspects of the experiments, computation, and analysis. They required expertise in developmental and molecular biology, imaging and physics, and computer science. We have laid the groundwork for the quantification of cardiogenesis, but more still needs to be done. This will require the collaboration of many highly skilled research laboratories amongst different scientific disciplines. Combining genetics with developmental analysis in a model system is key to understanding heart development and will assist in preventing pathologies such as

congenital heart defects at birth. With this research as a foundation, we hope that the medical field will develop new drugs to prevent malformations from occurring and bioengineers can develop the tools to fix any cardiac abnormalities that do appear.

References:

Loumes, L., Avrahami, I., and Gharib, M., 2008. Resonant pumping in a multilayer impedance pump. Physics of Fluids 20, 023103.

Moreno-Rodriguez, R.A., Krug, E.L., Reyes, L., Villavicencio, L. Mjaatvedt, C.H. and Markwald, R.R., 2006. Bidirectional fusion of the heart-forming fields in the developing chick embryo. Dev. Dyn. 235, 191-202.

Abu-Issa, R. and Kirby, M.L., 2008. Patterning of the heart field in the chick. Dev. Biol. 319(2), 223-233.

Cui, C., Cheuvront, T.J., Lansford, R.L., Moreno-Rodriguez, R.A., Schultheiss, T.M. and Rongish, B.J., 2009. Dev. Biol. 332, 212-222.

Liebling, M., Forouhar, A.S., Wooleschensky, R., Zimmermann, B., Ankerhold, R., Fraser, S.E., Gharib, M. and Dickinson, M.E., 2006. Rapid three-dimensional imaging and analysis of the beating embryonic heart reveals functional changes during development. Dev. Dyn. 235(11), 2940-2948.

# Chapter 6

# Appendix

# Chapter 6: Appendix

## 6.1 Protocol for Ringer's Solution

7.2g NaCl

0.23g CaCl-2H2O

0.37g KCl

0.946g Na2HPO4 in 100mL H2O (dibasic)

0.907g KH2PO4 in 100mL H20 (monobasic)

Measure salts and add to 1L container

Add a half volume of water and dissolve by mixing with stirbar

Then add monobasic and dibasic stocks as follows

Add 10.5 mls of Na2HPO4 to solution

Add 2.6 mls of KH2PO4 to solution

Fill to 9/10 of full

Adjust pH to 7.4

Fill to 1L

Filter sterilize

## 6.2 Protocol for Semi-solid Agarose EC Culture

(Modified from Chapman, S.C., Collignon, J., Schoenwolf, G.C. and Lumsden, A., 2001. Improved method for chick whole-embryo culture using a filter paper carrier. Dev. Dyn. 220, 284-289)

### 6.2.1 Items

1. 35 mm Petri dishes (Falcon, 3001).

2. 50 ml Falcon tubes (Falcon, 2098).

3. 10 ml pipettes

4. 120 ml of thin albumen, collected from 2 dozen un-incubated eggs.

5. 120 ml of simple saline, autoclaved (7.19g NaCl/ 1L distilled water).

6. 0.72 g Bacto-Agar (Difco).

7. Penicillin/Streptomycin (Sigma, P0906).

8. 3% glucose (Sigma) to saline solution

6.2.2 Protocol

1. Heat a water bath to 49°C.

2. Add the saline to a sterile 500 ml flask and bring it to boiling, using a hot plate/stirrer. Add the agar and stir until it is dissolved.

3. While the agar is dissolving, collect the thin albumen in a sterile Falcon tube (50ml) or similar container. Place the tubes into the water bath at 49°C.

4. Once the agar is dissolved, put the flask into the water bath. Allow the liquid to equilibrate at 49°C.

5. On a flat surface, lay out 80 35-mm sterile Petri dishes with their lids removed.

6. Add the albumen to the flask containing the dissolved agar, and mix by swirling for 30 – 60 sec. Also add the penicillin/streptomycin to this mixture, 5 U/ml.

7. Using a sterile 10 ml pipette and pipette-aid (e.g., Drummond, Bibby Jet) or similar device, aliquot 2.5 ml of the mixture per Petri dish. Do this reasonably quickly, without introducing bubbles into the dishes. If more than 2.5 ml agar-albumen mixture is pipetted, the substrate will be too thick, subsequently degrading the imaging of embryos with transillumination.

8. Once the aliquoting is complete, replace the lids of the Petri dishes and leave the dishes for several hours or overnight at room temperature to dry.

Place dishes upright in an airtight container at 4°C and use them as required. The dishes can be stored at 4°C for 1–2 weeks, provided that sterile conditions are maintained.